Department of Civil Engineering
School of Engineering

Moment Redistribution in Reinforced Concrete Beams and One-Way Slabs using 500 MPa Steel

Mohammad Mafizul Islam

This thesis is presented as part of the requirements for
the award of the Degree of Master of Engineering
of the Curtin University of Technology

June 2002

ABSTRACT

In the Australian Standard, AS 3600-2001 the neutral axis parameter κ_u is used as a convenient, but approximate, parameter to design for moment redistribution in building frames. The research work reported herein was conducted to obtain complete information regarding moment redistribution of beams and one-way slabs using 500 MPa steel reinforcement.

A computer based iterative numerical method was developed to analyse reinforced two-span continuous concrete beams and one-way slabs. The method takes into account the material and geometrical non-linearities in the calculations. The deflected shape of the beam and one-way slab was calculated by dividing the span length into a number of rigid segments. The program also calculates the failure load and extent of moment redistribution. The analytical method was verified against the test results reported in the literature. The analytical results for load-deflection graphs and moment redistribution showed a good agreement with the test results.

A parametric study was conducted using analytical method. The results of this study showed that moment redistribution depends not only on the neutral axis parameter (κ_u) but also on the ratio of neutral axis parameter (κ_{u-}/κ_{u+}), ultimate steel strain (ε_{su}) and concrete compressive strength (f'_c).

Keywords: Analysis, ductility, moment redistribution, neutral axis parameter, non-linear, reinforced concrete, and steel reinforcement.

ACKNOWLEDGEMENTS

First of all, the author would like to express his sincere appreciation and gratefulness to his supervisor Prof. B.V. Rangan, Head of School of Engineering for his continuous guidance and all out support through out the course study. The author is particularly grateful for his contributions in carrying out this research project through his valuable comments, suggestions and special efforts in reviewing the thesis. Sincere thanks are extended to Dr. Hamid Nikraz for his interest in this work and serving as Associate Supervisor.

Special thanks are extended to Dr. P.K Sarker and Mr. F.E. Faruashany who helped in all possible ways during author's difficulties to carry out the research work. Their encouragement, and advice made author's work easy on a number of occasions.

The author also thanks Mr. Zahurul Islam, PhD student, Department of Spatial Science, Curtin University of Technology, for his consistent encouragement and advice throughout the course of research work.

The financial support provided by the Curtin University of Technology and the School of Engineering is sincerely acknowledged.

Finally, the author thanks his wife and parents for their continuous encouragement and support during the period of study.

TABLE OF CONTENTS

NOTATION

α	=	ratio of mean stress in equivalent compressive rectangular stress block of concrete to f'_c
γ	=	ratio of the depth of the assumed rectangular compressive stress block to $\kappa_u d$
β	=	percentage moment redistribution at support
σ_t	=	tensile strength of concrete
Δ_x	=	length of the rigid segment
θ_j	=	slope at any node j of the beam
ε_{su}	=	ultimate steel strain
ε_{co}	=	strain at peak compressive stress
ε_c	=	strain at extreme compressive fibre of beam cross-section
ε_{ci}	=	compressive strain at any level-i of beam cross-section
ε_t	=	strain in tensile zone
ε_{ct}	=	strain at peak tensile stress
ε_s	=	strain in steel
ε_{sy}	=	yield strain of steel
ε_{sj}	=	strain in reinforcement at j-th level
κ_u	=	neutral axis parameter, the ratio of depth of neutral axis (measured from the compression zone) to effective depth
κ_{u-}	=	neutral axis parameter at support
κ_{u+}	=	neutral axis parameter at mid-span region
$(\kappa_{u-})_{min}$	=	minimum neutral axis parameter over support
$(\kappa_{u+})_{min}$	=	minimum neutral axis parameter at mid-span
κ_j	=	curvature at any node j of the beam
A_{sj}	=	total steel area at level j
$A_{st\,min}$	=	minimum area of reinforcement in a tensile zone of flexural member
$(A_{st\,min})_-$	=	minimum area of reinforcement in a tensile zone over support
$(A_{st\,min})_+$	=	minimum area of reinforcement in a tensile zone at mid-span

b_i	=	width of beam cross-section at strip *i*
D	=	total depth of beam cross-section
d	=	effective depth of beam cross-section
d_{ci}	=	depth of *i-th* concrete strip in the compression zone from the compressive face
d_{cti}	=	depth of the *i-th* concrete strip in the tension zone from the compressive face
d_i	=	depth of i-th concrete strip from the compression face
d_n	=	depth of neutral axis from the compression face of beam cross-section
d_{sj}	=	depth of the *j-th* layer of steel form the compressive face
d_{sj}	=	distance of reinforcement at *j*-th level
d_y	=	depth of strip of beam cross-section
E_c	=	modulus of elasticity of concrete
E_s	=	modulus of elasticity of steel
F_c	=	total compressive force in concrete compression zone
F_{ct}	=	total tension force in concrete tension zone
F_s	=	steel force
f_{ci}	=	compressive stress at strip *i* of beam cross-section
f_{cti}	=	tension stress at strip *i* of beam cross-section
f_s	=	stress in steel
f_{sj}	=	steel stress at level *j*
f_t	=	ultimate strength of steel
f_y	=	yield strength of steel
$f_{y.L}$	=	lower characteristic yield stress of reinforcement
$f_{y.U}$	=	upper characteristic yield stress of reinforcement
f'_c	=	characteristic compressive cylinder strength of concrete at 28 days
I_g	=	moment of inertia of the gross concrete section
l	=	centre-to-centre distance between the supports of beam
k_3	=	reduction factor to relate in-situ concrete in the beams or slabs to f'_c
M_{cr}	=	cracking moment
M_{EL}	=	support moment calculated by elastic analysis for the failure load
M_i	=	internal moment about the neutral axis depth of the beam cross-section

M_{u-} = ultimate support moment at failure

M_{u+} = ultimate mid-span moment at failure

$(M_{sup})_1$ = bending moment at node 1 due to κ_1

n = number of rigid segments of beam

Q_{FL} = actual failure load

Q_{PL} = idealized plastic failure load

v_{max} = maximum deflection of beam

v_j = deflection at node j

x_j = distance of node j from support of the beam

y_t = centroid of the gross concrete section from the tension face

LIST OF TABLES

LIST OF FIGURES

CHAPTER 1

INTRODUCTION

1.1 Ductility and the Importance of Steel Ductility

Ductility is the property, which has been valued in reinforced concrete design from an early stage in the development of the material. In the design of every concrete structure, the ductility has to be considered carefully.

Ductility is the ability of a material, or a member, or a structural system, to undergo large deformations at high overload (Patrick, Turner & Warner, 2001). The large deformations that occur in a ductile, indeterminate structure at high overload allow significant redistribution of the internal actions to occur, so that the full potential load-carrying capacity can be achieved, without premature failure. Good ductility also allows the structure to accept the large deformations without loss of strength or undue distress, which frequently occur as the result of external effects such as foundation movement, and internal effects such as shrinkage and temperature gradients. Thus, a ductile structure can accommodate not only simplifying and sometimes inadequate assumptions of the design engineer, but also unforseen adverse events during its working life.

The ductility demand in a critical high-moment region of structure depends on the degree of moment redistribution that will take place as the collapse load is approached, and in turn depends on a range of factors including the moment capacity of critical regions, the load patterns and the support conditions (Patrick, Turner& Warner).

1.2 Australian 500 MPa Reinforcing Steels and AS 3600

Steel reinforcement with characteristic yield stress of 500 MPa is now in the Australian market place. Although this steel has higher strength than 400 MPa hot-rolled reinforcement traditionally used in reinforced concrete structures, it is significantly less ductile (Gilbert, 2001).

The Australian Standard classifies 500 MPa reinforcement according to its ductility, viz, Class L (low ductility) and Class N (normal ductility). Class L steel includes cold worked wires and welded wire mesh. Class N steel includes hot rolled deformed bars.

The ductility requirements in the previous version of the Australian Standard AS 3600 were developed more than a decade ago. It was assumed that the steel reinforcement was sufficiently ductile to allow up to 30 % moment redistribution depending the ratio of depth of neutral axis to effective depth.

Cold-reduced wires used in welded wire fabric are less ductile than hot-rolled bars. To develop new design provisions for the use 500 MPa steel reinforcement in the Concrete Structures Standards AS 3600, Standards Australia Committee BD/2/1 – Ductility undertook experimental and analytical studies of the overload behaviour of concrete beams and slabs. It was observed that the use of low-ductility steel in lightly reinforced flexural members might reduce the load-carrying capacity below that corresponding to a complete plastic hinge mechanism due to premature fracture of the steel reinforcement.

Amendment No. 1 (issued in 1996) to AS 3600 restricted the use of cold reduced bar and mesh in flexural elements to be designed either elastically or plastically assuming moment redistribution in situations where significant amounts of moment redistribution can occur. Amendment 2 to AS 3600 issued in early 2000, contained details of main reinforcement with different ductility classes. In the present Australian concrete design standard, AS 3600-2001, the neutral axis parameter κ_u is used as a convenient, but approximate, measure of available ductility in high moment region of a flexural member.

1.3 Research Significance

Until recently, the Australian Concrete Standard AS 3600, made no distinction between the use of hot-rolled bar and cold-rolled bar or wire in situations where ductility is important. With the introduction of high strength reinforcement (500 MPa) with two ductility levels (Class L and Class N), a review is needed of these ductility requirements. In the present research, therefore, a non-linear analysis is developed to evaluate the strength and ductility of reinforced concrete beams and one-way slabs using 500 MPa steel

1.4 Objectives of the study

The objectives of the proposed research work are as follows:

i) To study the strength and ductility of continuous reinforced concrete beams and one-way slabs using 500 MPa steel.

ii) To develop an analytical method to predict the strength and load-deformation relationships and compare the analytical results with test results reported in the literature.

iii) To study the effect of ductility (or lack of) of 500 MPa steel on the ductility, redistribution of forces and strengths of beams and one-way slabs.

iv) To conduct a parametric study of beams and one-way slabs using the proposed analytical method and to use the results of this study to evaluate the AS 3600 provisions on ductility.

1.5 Scope of the Study

The research examined the strength and ductility of two-span reinforced concrete beams and one-way slabs using 500 MPa steel. Two-span continuous beams and one-way slabs were selected for detailed calculations. The variables were:

- Concrete compressive strength
- Member cross-section and span/depth ratio
- Neutral axis depth parameter, k_u
- Ultimate strain of steel

The analytical work was developed with due consideration to the constitutive laws for concrete and steel.

1.6 Composition of the Thesis

The work began with the searching and reviewing of the previous works related to this research. A considerable volume of information was collected and read from different sources such as books, journals, conference proceedings, research reports, Internet etc. However, only selected literature that relates directly to the objectives of this thesis are reviewed and presented in Chapter 2.

Based on the literature review and objectives of this thesis, the analytical work presented in Chapter 3 was developed to predict the strength, moment redistribution and deformation of continuous beams and one-way slabs.

Chapter 4 contains the correlation of the analytical results with test results reported in the literature.

Chapter 5 describes a parametric study of two-span continuous reinforced concrete beams and one-way slabs. Parameters included in the study were concrete strength, neutral axis depth parameter, cross section dimensions, span/depth ratio, and ultimate strain of steel. Using the results of parametric study, the moment redistribution given

by Australian Standard AS 3600 is evaluated and suitable recommendations for design are proposed in this Chapter.

The results of the research are summarised in Chapter 6 and conclusions and recommendations for further work are made.

The thesis ends with a reference list and appendices.

CHAPTER 2

LTERATURE REVIEW

2.1 Introduction

The literature on the behaviour of reinforced concrete beams and slabs is extensive. Although numerous papers were read by the author for purpose of understanding, the literature review presented in this Chapter is limited to scope of the thesis. Accordingly, only the literature that deals with the effect of steel properties on moment redistribution, ductility and relevant details are reviewed in this Chapter.

2.2 High strength steel

In 1973, steel with yield stress in excess of 414 MPa (60 ksi) was considered as High Strength Steel (ACI Committee 439, 1973). Almost a decade ago, Europe introduced steel with yield stress in excess of 500 MPa. Steel reinforcement with characteristic yield stress of 500 MPa, now available in Australia, is classified according its ductility, viz, Class L (low ductility) and Class N (normal ductility). Class L includes cold worked wires and welded wire mesh. Class N steel includes hot rolled deformed bars. The properties of Class L and Class N steels are summarised in Table 2.1.

The advantages of using high-strength steel may be reduced congestion of reinforcement, weight of structure, reduced transport cost, reduced environmental impact through lower transport demand, and reduced overall material cost. However, the effect of reduced ultimate strain of the steel on ductility and moment redistribution needs attention. Hence the purpose of the research reported in this thesis.

Table 2.1 Characteristic Mechanical Properties of 500 MPa Reinforcement

Property		500L	500N
Nominal diameters (mm)		5-16	10-40
Characteristic yield stress (MPa):	$f_{y.L}$	500	500
	$f_{y.U}$	750	650
Ultimate strength to yield stress ratio:	f_t/f_y	1.03	1.08
Ultimate strain:	ε_{su}	0.015	0.05

Note: The yield stress is f_y, with $f_{y.L}$ and $f_{y.U}$ being the lower and upper characteristic values; f_t is the ultimate strength, and ε_{su} is the ultimate strain corresponding to maximum stress.

2.3 Review of Past Research

Pulmano and Shin (1987) proposed a simple finite element method for predicting the instantaneous and long-term deflections of statically determinate /indeterminate reinforced beams. The analysis took into account the parabolically varying bending stiffness along its length, the non-linearity effects of due to cracking and tension stiffening, and the time-dependant effects due to creep and shrinkage. Predicted values of instantaneous and long-term deflections were in very good agreement with available measured values. The method was also used to predict the redistribution of internal forces in the case of statically indeterminate beams.

Cosenza et al (1991) proposed a non-linear method to calculate the required plastic rotations for the reinforced concrete continuous beams in accordance with Euro Code 2. Parameters such as ratio of neutral axis depth to the effective depth (termed as neutral axis parameter), slenderness ratio, reinforcement ductility and tension stiffening were included. Based on a parametric study, the researchers reported the following:

- The depth of neutral axis at failure is an important parameter in the evaluation of plastic rotations.
- The required plastic rotation is proportional to the slenderness ratio of

the beam and the allowable rotation is independent of this parameter.

- The influence of the tension stiffening on the required plastic rotation is important only for beams designed with values of neutral axis parameter less than 0.20.
- With reference to the normal ductile steel, the redistribution formulas proposed by Euro Code 2 did not seem to be safe. With reference to the plastic analysis, an adequate limitation seemed to be that the neutral axis parameter be less than 0.20.
- Redistribution should not be considered for design in the case of low ductility steel.

Calvi et al (1993) reported the test results on reinforced concrete slabs reinforced with welded wire mashes. Thirty-six slabs were tested and slabs were simply supported at both ends. The test parameters were the type of reinforcing mesh, wire diameter (6 mm or 10 mm), bonding properties (smooth or high bond) and the steel quality (type A and type B). For type A steel, the ultimate strain was 5.71 %, and for type B steel, the ultimate strain was 2.88 % for high bond steel bars and 3.29 % for smooth bars. The percentage of reinforcement varied from 0.229 to 0.638. All slabs failed by steel fracture. It was concluded that the bonding properties influenced available rotation capacity in case of small diameter bars and low reinforcement percentages of steel. From the experimental results it appeared that the use of smooth bars was advantageous if a mechanical bond was guaranteed by the presence of the transversal welded wires. It was found that the minimum values of reinforcement and minimum bar diameters were important particularly in the case of deformed bars, when some plastic rotation was required, even if the ultimate strain of the steel was large.

Eligehausen and Fabritius (1993) tested seven continuous slabs to investigate the rotation capacity of plastic hinges and possible degree of moment redistribution. The test variables were yield stress, ultimate to yield strength ratio and ultimate strain of reinforcing steel in both support and span regions. In all tests the reinforcement percentage was 0.3% in the span as well as over the support. Two ductility classes of steel reinforcement were used in the experiments, viz, class A (f_t/f_y = 1.08 and $\varepsilon_u \geq$ 50%) and class B (f_t/f_y = 1.08 and $\varepsilon_u \geq$ 50%). Two slabs failed by rupture of the steel over the support and others failed by rupture of the steel in the span. In all tests the

moment capacities over the support and in the spans were reached and the assumed design moment redistribution of 28.5 % was obtained.

Pisanty and Regan (1993) carried out an experimental study to investigate the behaviour of reinforced concrete beams designed under various redistribution of moments conditions. Four continuous beams were tested. The beams were designed for the redistribution ratios of +15%, +5%, -15% and –35% from the linear elastic moment at the central support. The test parameters were amount of reinforcement and bar diameters at support and span regions. The reinforcement properties were as follows: yield stress, f_y = 460; tensile strength to yield stress ratio, f_t/f_y = 1.10; and ultimate strain, $\varepsilon_u \geq 0.06$. The experimental work investigated the load-deflection behaviour of the beams and ductility demand of the system so that redistribution of moments could effectively take place in the recommended ranges by the concrete codes. A computer analysis was also carried out using the concept of discrete beam elements and non-linear constitutive laws for the concrete and steel. Good correlation of analytical results with test data was reported.

Russwurm (1993) reported tests on five single span slabs (Eibl, Karlsruhe, 1993) to measure the rotation capacity, and seven tests on two span slabs (Eligehausen, Stattgart, 1993) to measure either rotation capacity or available degree of moment redistribution The test variables were ultimate strain of longitudinal reinforcement, percentage of longitudinal reinforcement, bar size, span-to-depth ratio and strength of concrete. It was concluded that no correlation between steel characteristics and moment redistribution exists. Slabs with low reinforcement ratios failed by steel rupture.

Patrick et al (1997) carried out three tests on two-span continuous reinforced concrete beams to investigate the conditions under which failure can occur. The beams varied in overall depth and in the amount of moment redistribution assumed in their design. The reinforcement used was cold-reduced, ribbed wire with a mean yield stress of approximately 650 MPa, a tensile-strength-to-yield-stress ratio of 1.06 indicating low strain-hardening, and an ultimate strain of only 0.016. The experimental work also investigated the moment redistribution of beams. Beams were subjected to two point

loads in each span. All the beams failed by fracture of the tensile reinforcement. The experimental moment redistribution of first two beams almost reached the design moment redistribution of 30% and the experimental moment redistribution of third beam was 18 % although the beam was designed for zero percent moment redistribution. A computer program was developed using the concept of small finite beam elements. A deflection-control procedure was used to follow the progressive behaviour of the beams. Good correlation was obtained between the computer results and experimental load-deflection curves. The researchers recommended an urgent need for further study of the factors affecting strength and ductility of concrete structures using 500 MPa steels currently available in Australia so that reliable ductility requirements can be established.

Alvarez et al (2000) tested three two-span continuous concrete slab strips to investigate the influence of lower ductility properties of the reinforcing steel on the behaviour of typical structural members. The test variables were reinforcement properties (i.e. steel yield stress, ultimate to yield strength ratio and ultimate strain of reinforcing steel), reinforcement percentage and bar diameter. The experimental work investigated the failure mode, failure load, deflection, plastic rotation capacity of support, and moment redistribution. Slabs were subjected to two point loads per span. All specimen failed by rupture of the top reinforcement at the interior support. It was concluded that the reduced ductility properties of cold-deformed and coiled small-diameter reinforcing bars and wires might result in dangerous strain localizations, impairing rotation capacity, permissible moment redistribution, and ultimate strength. The test results were compared with calculations according to linear, non-linear, and limit analysis approaches. A computer program was developed for the non-linear analysis using the concept of tension chord model and idealised stress-strain diagrams for steel and concrete. The calculation was based on the experimentally observed crack spacings and material properties. Good correlation was obtained between the computer results and experimental load-deflection curves.

2.4 Design considerations

Beeby (1997) presented the reasons for requiring ductility of reinforced concrete sections and the factors influencing the ductility. He reported that owing to rupture of the reinforcement, the ultimate rotation reduces with reduction in relative neutral axis depth for low percentages of reinforcement. The research also presented that the factors influencing the ultimate rotation capacity of reinforced concrete sections were the ultimate strain of the reinforcement, the ratio of the ultimate tensile strength to yield strength, the bonding properties of reinforcing bars, span/depth ratio, and the effective depth. Two modes of failure were observed: a relatively brittle failure where only one crack forms in the hinge region and a more ductile failure where multiple cracks form over a considerable length of beam. It was observed that in the tests, both low ductility and normal ductility reinforcement did not necessarily give the plastic rotations required by Eurocode 2.

Chick et al (1999) reported on the ductility of reinforced concrete beams and slabs in relation to AS 3600 design requirements. It was observed that the use of low-ductility steel in lightly reinforced flexural members might reduce the load-carrying capacity below that corresponding to a complete plastic hinge mechanism due to premature fracture of the steel reinforcement. Accordingly, it was recommended that the use of moment redistribution in design, and plastic analysis should not be used for low-ductility steel.

Patrick et al (2001) reported the utilisation of ductility of 500 MPa steel reinforcement in reinforced concrete structures designed to AS 3600:2001. The findings of the research work undertaken by the Ductility Working Group and the changes to AS 3600 were summarised. Tests on three continuous beams and computer simulations were used to investigate the effect of limited steel ductility on the load carrying capacity of various reinforced concrete members. The results showed that for –15 % and –30 % moment redistribution, the maximum value of steel strain required to form a full plastic hinge mechanism was 0.025 and 0.035 respectively. For 30 % negative moment redistribution, a 15 % reduction in load-carrying capacity was recorded when ultimate steel strain was 0.015.

Gilbert (2001) presented the impact of 500 MPa steel reinforcement on the design of concrete structures. The researcher discussed that the relatively low ultimate strain of the new steel (particularly Class L reinforcement) has significant implication in design. It was stated that the amount of moment redistribution permitted in AS3600 might no longer be appropriate and the reduced steel quantities will result in less stiffness after cracking, and consequently greater deflection, and higher steel stresses, and larger crack widths.

Gravina and Warner (2001) proposed a computer model to predict the local flexural deformations in a reinforced concrete beam from the progressive formation of individual cracks up to failure, either by steel fracture or concrete softening. The model used a bilinear stress-strain relation for the steel with strain hardening, a polynomial expression for the stress-strain relation for concrete, and local bond-slip properties of the steel-concrete interface. The extent of moment redistribution and mode of collapse of indeterminate beams and slabs constructed with 500 MPa Class L and Class N reinforcing steel were investigated Analytical results showed good correlation with experimental results reported by Elghausan and Fabritius (1993) for fixed-end beams. A case study was undertaken to show influence of ductility on possible moment redistribution and mode of collapse for fixed-end slabs. It was concluded that AS 3600 was non-conservative for the steel reinforcement used in analysis.

To allow for the usage of Class L and Class N reinforcing steel, AS 3600 provides the following recommendations:

"7.6.8 Moment redistribution in reinforced concrete members for strength design

7.6.8.1 General requirements

In design calculations for strength of statically indeterminate reinforced concrete members, the elastically determined bending moments at interior support may be reduced or increased by redistribution, provided an analysis is undertaken to show

that there is adequate rotation capacity in critical moment regions to allow the assumed distribution of bending moments to be achieved.

The analysis shall take into account –

(a) the stress-strain curve of the steel reinforcement as defined in Clause 6.2.3 assuming for analysis purposes that fracture of the reinforcement occurs at ε_{su};
(b) static equilibrium of the structure after redistribution of the moments; and
(c) the properties of the concrete as defined in Clause 6.1.

Special consideration shall be given to the detrimental effects that significant relative foundation movements can have on the strength of continuous beams and slabs incorporating Ductility Class L (low ductility) reinforcing steel as the main reinforcement.

7.6.8.2 Simplified approach for Class N reinforcement

The requirements of Clause 7.6.8.1 shall be deemed to be met provided the following requirements are satisfied:

(a) All of the main reinforcement in the member is Ductility Class N.
(b) The elastic bending moment distribution before redistribution shall be determined in accordance with Clause 7.6.5 (a) assuming uncracked cross-sections.
(c) The positive bending moments shall be adjusted to maintain equilibrium.
(d) Where the neutral axis parameter (k_u) is less than or equal to 0.2 in all peak moment regions, the redistribution does not exceed 30 %.
(e) Where k_u exceeds 0.2 in one or more peak moment regions, but does not exceed 0.4, the redistribution does not exceed 75 $(0.4 - k_u)$ %.
(f) Where k_u exceeds 0.4 in any peak moment region, no redistribution is made.

NOTES:

The values of k_u are calculated for cross-sections that have been designed on the basis of the redistributed moment diagram.

The amount of redistribution is measured by the percentage of the bending moment before redistribution.

7.6.8.3 Approval for Class L reinforcement

Where Ductility Class L reinforcement is used, moment redistribution shall not be permitted unless an analysis, as specified in Clause 7.6.8.1, is undertaken".

A primary objective of this thesis is to examine the validity of the above recommendations in the light of the results presented herein.

2.5 Summary

The volume of literature available on topics relevant to the work in this investigation is large. Whilst every effort was made to identifying relevant previous work, it is possible, however, that some work of significance may not have been located. Nevertheless, after reviewing the literature, it was concluded that although extensive experimental and analytical works have been conducted on simply supported beams and slabs, very little experimental and analytical analyses have been carried out on indeterminate beams and slabs. Also, there is no parametric study carried out to show the full pleasant effect of ductility of steel on the behaviour and strength of indeterminate beams.

Steel reinforcement with characteristic yield stress 500 MPa is now in Australian market place. There is a need to study of the factors affecting strength and ductility of concrete structures using 500 MPa reinforcing steel so that reliable ductility requirements can be established. The research reported in this thesis was carried out to address some of these aspects. A non-linear analysis was developed to evaluate the strength and ductility of two-span reinforced concrete beams and one-way slabs using 500 MPa steel. The analytical method is then used to perform a parametric study to evaluate the effect of various factors on the degree of redistribution of forces in indeterminate beams.

CHAPTER 3

NON-LINEAR ANALYSIS OF CONTINUOUS BEAMS AND ONE-WAY SLABS

3.1 Introduction

This chapter describes a non-linear method to calculate the load-deflection relationship and failure load of reinforced concrete continuous T-beams and one-way slabs. The method can also be used to investigate the modes of collapse either by steel fracture or by concrete crushing and moment redistribution.

3.2 Moment-Curvature Relationship

A prerequisite for the analysis presented in this chapter is the moment-curvature relationship of the cross-section of the beams or slabs under any given load. To calculate the moment-curvature relationship a linear strain distribution over the depth of the cross-section is assumed. We need suitable stress-strain relationships for concrete and steel in order to proceed with the calculations.

3.2.1 Stress-Strain Relationship of Concrete

The stress-strain relationship for concrete in compression varies with concrete strength. An expression for the complete stress-strain response of concrete cylinders was proposed by Popovics (1973), which was subsequently modified by Collins et al (1993) to include high strength concretes. The modified relationship is given by

$$f_c = k_3 f'_c \cdot \left(\frac{\varepsilon_c}{\varepsilon_{co}} \right) \cdot \frac{n}{\left[n - 1 + \left(\frac{\varepsilon_c}{\varepsilon_{co}} \right)^{nk} \right]} \qquad (3.1)$$

where,

k_3 = Reduction factor to relate in-situ concrete in the beams or slabs to f'_c.

$$= (0.6 + \frac{10}{f'_c}) \leq 0.85 \qquad (3.1a)$$

f'_c = Maximum compressive cylinder strength

ε_{co} = Strain at peak stress

$$= \frac{f_c}{E_c} \cdot \frac{n}{n-1} \qquad (3.1b)$$

E_c = Modulus of Elasticity of concrete

$$= 3320\sqrt{f'_c} + 6900 \qquad (3.1c)$$

n = Curve fitting factor

$$= 0.8 + \frac{f'_c}{17} \qquad (3.1d)$$

$k =$ 1.0 when $\varepsilon_c \leq \varepsilon_{co}$

$= 0.67 + \frac{f'_c}{62}$ when $\varepsilon_c > \varepsilon_{co}$ (3.1e)

Equation 3.1 applies to all grade of concrete (Figure 3.1).

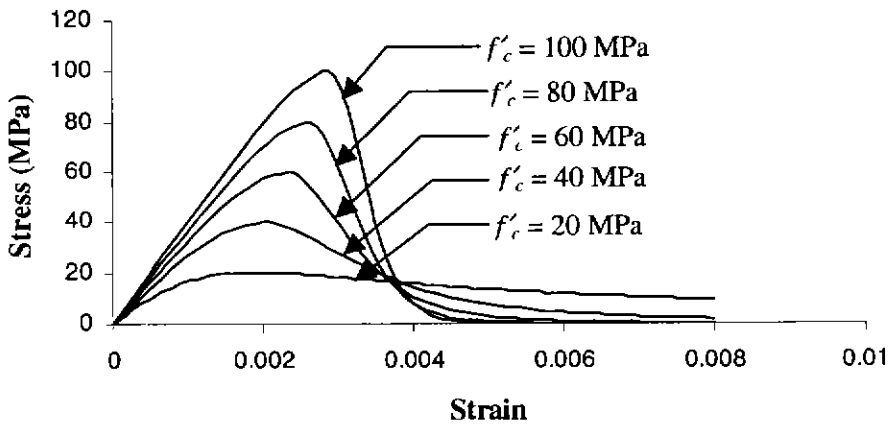

Fig. 3.1 Stress-Strain Relationship for Concrete

Note that the stress-strain relationship does not show an ultimate value for ε_c (i.e. crushing strain ε_u). In the analysis, concrete crushing is assumed to occur at that value

of ε_c when the moment-curvature curve shows unloading as indicated by a fall in the moment as well as the curvature.

3.2.2 Concrete in Tension

The stress-strain relationship of concrete in tension is assumed to be as follows (Figure 3.2).

$$\sigma_t = E_c.\varepsilon_t \qquad \text{when } 0 \le \varepsilon_t \le \varepsilon_{ct} \qquad (3.2)$$

$$\sigma_t = 0 \qquad \text{when } \varepsilon_t > \varepsilon_{ct} \qquad (3.3)$$

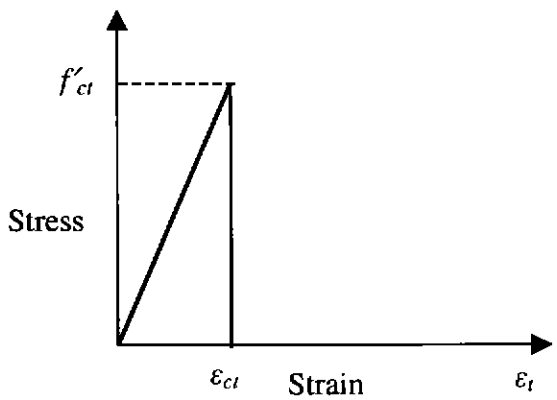

Fig. 3.2 Concrete in Tension

3.2.3 Reinforcing Steel

The stress-strain relationship of the reinforcing steel is assumed to be bilinear (Figure 3.3) as given by the following

$$f_s = E_s\varepsilon_s \qquad \text{when } \varepsilon_s < \varepsilon_{sy} \qquad (3.4)$$

$$f_s = f_y + \frac{(\varepsilon_s - \varepsilon_{sy})(f_t - f_y)}{\varepsilon_{su} - \varepsilon_{sy}} \qquad \text{when } \varepsilon_{sy} \le \varepsilon_s < \varepsilon_{su} \qquad (3.5)$$

$$f_s = 0 \qquad \text{when } \varepsilon_s \ge \varepsilon_{su} \qquad (3.6)$$

where,

f_s = Stress in steel

E_s = Modulus of elasticity of steel

ε_s = Strain in steel

ε_{sy} = Yield strain of steel, equal to $\frac{f_y}{E_s}$

ε_{su} = Ultimate strain of steel

f_y = Yield strength of steel

f_t = Ultimate strength of steel.

It is assumed that steel fractures when ε_s reaches ε_{su}.

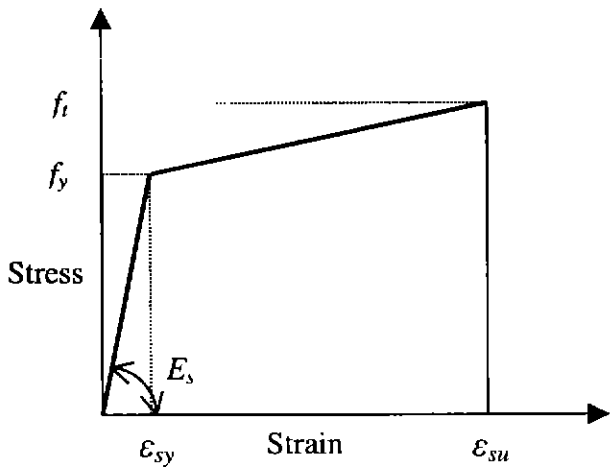

Fig. 3.3 Stress-Strain Relationship for Steel

3.2.4 Calculation Procedure

The moment-curvature relationship of a beam cross-section (Figure 3.4) is calculated using the following steps:

Step 1: Input test specimen data, viz dimensions of the beam cross-section, reinforcement details, location of reinforcement as distance from the compression face, and material properties.

Step 2: Assume a value of strain ε_c at extreme compressive fibre. A minimum value of ε_c was taken as 0.00005. This value was incremented by 0.00005 until either

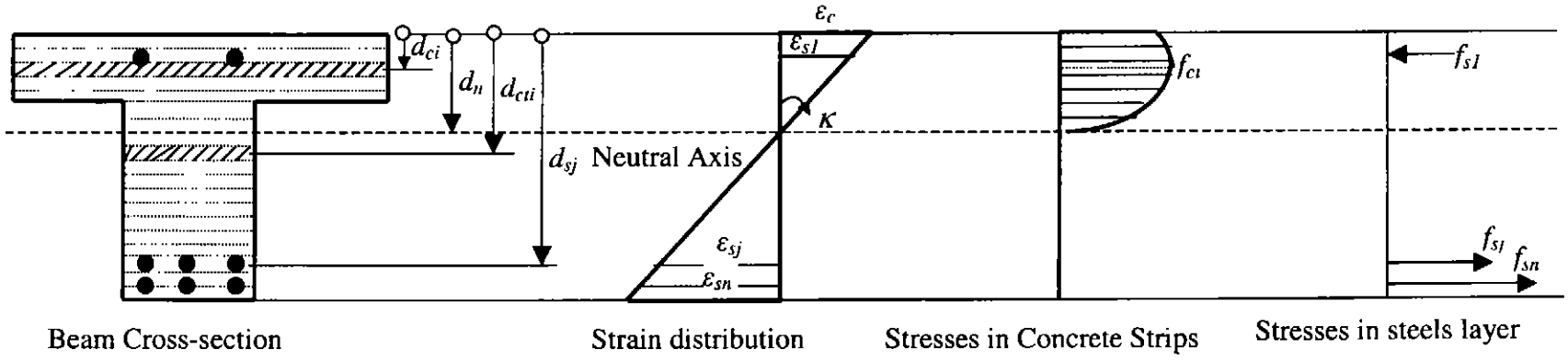

Fig. 3.4 Calculation of Moment-Curvature Relationship (cracked section)

the steel strain reached the ultimate value or the moment-curvature curve unloaded.

Step 3: Assume a trial value of neutral axis depth, d_n for the assumed value of ε_c with an initial trial value of 0.025 times of the depth of the section incremented by 0.0005 times of the depth.

Step 4: Assume a linear strain distribution across the depth of the beam section. With known depth of neutral axis, the strain at any level-i, at a depth of d_i from the extreme compressive fibre is given by

$$\varepsilon_{ci} = \frac{(d_n - d_i)}{d_n}\varepsilon_c \tag{3.7}$$

Step 5: The section is subdivided into a number of strips according to the section depth. From the strain distribution established in Step 4, calculate stresses in concrete strips and steel layers from the appropriate stress-strain relations. The stress at the centroid of a strip is assumed to be constant through its depth. Calculate the total compressive force in concrete using Simpson's one-third rule as

$$F_c = \sum_{i=1}^{m} b_i f_{ci} d_y \tag{3.8}$$

where,

F_c = Concrete force in compression zone

f_{ci} = Compressive stress at strip i

b_i = width of the section at strip i

d_y = depth of the strip

Step 6: Calculate the tension forces in concrete using same procedure as Step 5.

$$F_{ct} = \sum_{i=1}^{m} b_i f_{cti} d_y \tag{3.9}$$

where,

F_{ct} = Concrete force in tension zone

b_i = width of the section at strip i

f_{cti} = Tension stress at strip i

Step 7: Calculate the forces carried by the reinforcement as

$$F_s = \sum_{j=1}^{n} A_{sj} f_{sj} \tag{3.10}$$

where,

F_s = Steel force

A_{sj} = Total steel area at level j

f_{sj} = Steel stress at level j

Step 8: For equilibrium, the algebraic sum of all internal forces should be zero i.e.

$$F_c + F_s + F_{ct} = 0 \tag{3.11}$$

The depth of neutral axis is established when Equation 3.11 is satisfied, within a tolerance of ±1% of F_s.

Note that $F_{ct} = 0$ when the bending moment at a section reaches the cracking moment M_{cr} given by

$$M_{cr} = 0.6\sqrt{f_c'}\frac{I_g}{y_t} \tag{3.12}$$

where,

I_g = Moment of inertia of the gross concrete section

y_t = Centroid of the gross concrete section from the tension face

Step 9: Calculate the sum of the moments due to forces in the concrete and steel about the neutral axis.

$$M_t = \sum_{i=1}^{m} f_{ci} A_{ci} (d_n - d_{ci}) + \sum_{j}^{n} f_{sj} A_{sj} (d_n - d_{sj}) + \sum_{i=1}^{m} f_{ct} A_{ci} (d_n - d_{ct}) \tag{3.13}$$

where,

d_{ci} = Depth of *i-th* concrete strip in the compression zone from the compressive face

d_{sj} = Depth of the *j-th* layer of steel form the compressive face

d_{cti} = Depth of the *i-th* concrete strip in the tension zone from the compressive face

Step 10: Compute curvature by dividing the strain at the extreme compressive fibre by the depth of neutral axis as

$$\kappa = \frac{\varepsilon_c}{d_n} \tag{3.14}$$

Step 11: Increment ε_c as mentioned Step 2, and follow Step 3 to Step 10 to obtain the complete moment-curvature diagram for a given section.

3.2.5 Example

Calculate the moment-curvature relationships for maximum positive and maximum negative moment sections of a continuous beam by the procedure outlined in the previous section.

Development of a moment-curvature relationship for positive moment section

The cross-section of the beam at the maximum positive moment section is shown in Figure 3.5. The material properties are given as follows

Material properties

Compressive strength of concrete cylinder, $f'_c = 40$ MPa

Yield strength of steel, $f_y = 500$ MPa

Ultimate tensile strength of steel, $f_t = 540$ MPa

Modulus of elasticity of steel, $E_s = 200{,}000$ MPa

Ultimate strain of steel, $\varepsilon_{su} = 0.05$

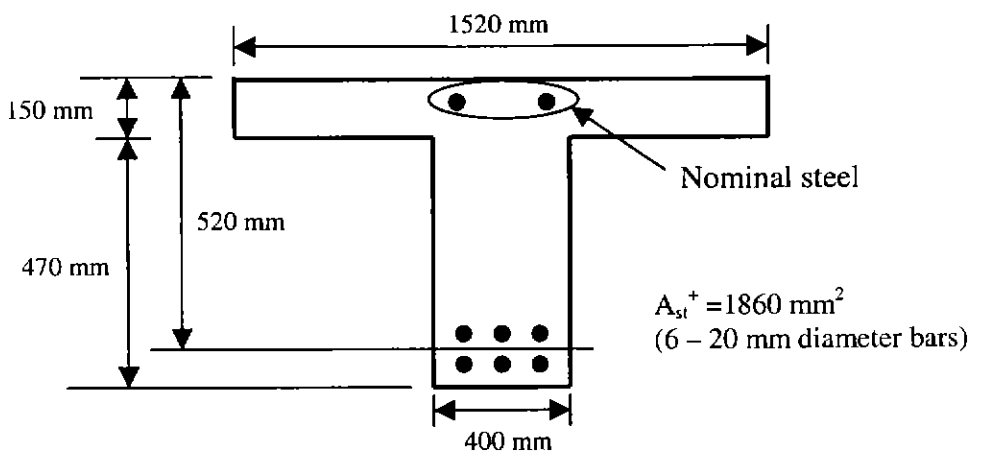

Fig. 3.5 Beam Cross-Section at Maximum Positive Moment Region

Calculations are given in Table 3.1. Note that ε_s reaches 0.05 and steel fractures when ε_c = 0.0038. For this stage, moment M_i = 526.54 kNm and curvature $\kappa = 9.97 \times 10^{-5}$ rad/mm. The results are plotted in Figure 3.6.

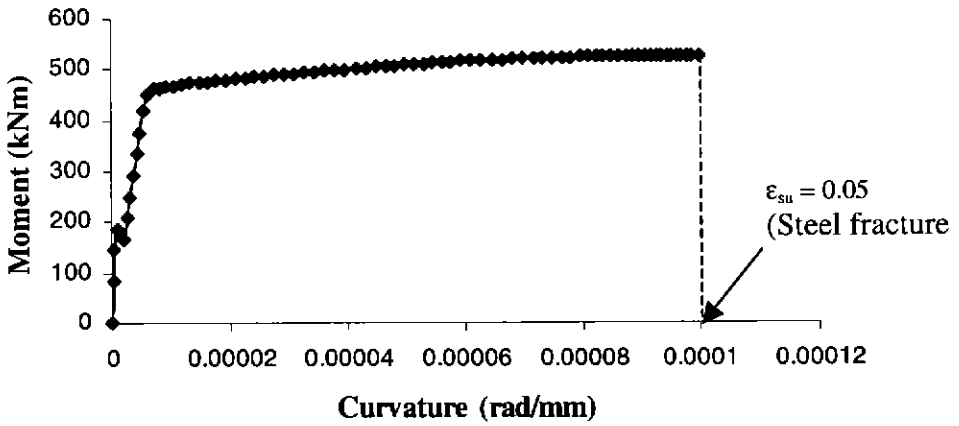

Fig. 3.6 Moment-Curvature Relationship for Maximum Positive Moment Section

Development of a moment-curvature relationship for maximum negative moment section

Figure 3.7 shows the details of the cross-section of the beam at the maximum negative moment section. The material properties are as follows:

Material properties

Compressive strength of concrete cylinder, f'_c = 40 MPa

Yield strength of steel, f_y = 500 MPa

Ultimate tensile strength of steel, f_t = 540 MPa

Modulus of elasticity of steel, E_s = 200,000 MPa

Ultimate strain of steel, ε_{su} = 0.05

Table 3.1 Moment-Curvature Relationships

Concrete Strain ε_c	Neutral Axis Depth d_n (mm)	Curvature κ (rad/mm)	Moment M_i (kNm)	Steel Strain ε_s	Concrete Strain ε_c	Neutral Axis Depth d_n (mm)	Curvature κ (rad/mm)	Moment M_i (kNm)	Steel Strain ε_s
0.00005	235.51	2.12E-07	84.09	-0.0001	0.0016	42.2	3.79E-05	497.77	-0.0189
0.0001	210.2	4.76E-07	147.02	-0.0002	0.00165	41.6	3.97E-05	499.33	-0.0198
0.00015	175	8.57E-07	183.73	-0.0003	0.0017	41	4.15E-05	500.9	-0.0207
0.0002	93	2.15E-06	166.99	-0.001	0.00175	40.5	4.32E-05	502.42	-0.0216
0.00025	93	2.69E-06	208.74	-0.0012	0.0018	40.1	4.49E-05	503.89	-0.0224
0.0003	93	3.23E-06	250.48	-0.0014	0.00185	39.7	4.66E-05	505.35	-0.0233
0.00035	93	3.76E-06	292.22	-0.0017	0.0019	39.4	4.82E-05	506.74	-0.0241
0.0004	93.1	4.30E-06	333.58	-0.0019	0.00195	39.1	4.99E-05	508.12	-0.025
0.00045	93.1	4.83E-06	375.26	-0.0022	0.002	38.8	5.15E-05	509.49	-0.0258
0.0005	93.1	5.37E-06	416.92	-0.0024	0.00205	38.6	5.31E-05	510.78	-0.0266
0.00055	91.8	5.99E-06	451.49	-0.0027	0.0021	38.4	5.47E-05	512.06	-0.0274
0.0006	85.8	6.99E-06	460.4	-0.0032	0.00215	38.2	5.63E-05	513.32	-0.0282
0.00065	79.8	8.15E-06	462.99	-0.0037	0.0022	38.1	5.77E-05	514.49	-0.029
0.0007	74.8	9.36E-06	465.4	-0.0044	0.00225	37.9	5.94E-05	515.72	-0.0298
0.00075	70.4	1.07E-05	467.61	-0.005	0.0023	37.7	6.10E-05	516.57	-0.0306
0.0008	66.7	1.20E-05	469.72	-0.0057	0.00235	37.4	6.28E-05	517.32	-0.0316
0.00085	63.5	1.34E-05	471.75	-0.0064	0.0024	37.1	6.47E-05	518.06	-0.0325
0.0009	60.6	1.49E-05	473.69	-0.0071	0.00245	36.8	6.66E-05	518.78	-0.0335
0.00095	58.2	1.63E-05	475.6	-0.0079	0.0025	36.6	6.83E-05	519.44	-0.0344
0.001	56	1.79E-05	477.46	-0.0086	0.00255	36.4	7.01E-05	520.1	-0.0353
0.00105	54	1.94E-05	479.27	-0.0095	0.0026	36.2	7.18E-05	520.73	-0.0362
0.0011	52.3	2.10E-05	481.07	-0.0103	0.00265	36.1	7.34E-05	521.31	-0.037
0.00115	50.7	2.27E-05	482.83	-0.0111	0.0027	36	7.50E-05	521.83	-0.0378
0.0012	49.3	2.43E-05	484.58	-0.0119	0.00275	35.9	7.66E-05	522.33	-0.0386
0.00125	48.1	2.60E-05	486.3	-0.0128	0.0028	35.9	7.80E-05	522.76	-0.0393
0.0013	47	2.77E-05	488	-0.0136	0.00285	35.8	7.96E-05	523.23	-0.0401
0.00135	45.9	2.94E-05	489.69	-0.0145	0.0029	35.8	8.10E-05	523.63	-0.0408
0.0014	45	3.11E-05	491.35	-0.0154	0.00295	35.8	8.24E-05	524.01	-0.0415
0.00145	44.2	3.28E-05	492.99	-0.0012	0.003	35.9	8.36E-05	524.31	-0.0421
0.0015	43.4	3.46E-05	494.62	-0.0172	0.00305	35.9	8.50E-05	524.67	-0.0428
0.00155	42.8	3.62E-05	496.2	-0.018	0.0031	36	8.61E-05	524.94	-0.0434

Concrete Strain ε_c	Neutral Axis Depth d_n (mm)	Curvature κ (rad/mm)	Moment M_i (kNm)	Steel Strain ε_s	Concrete Strain ε_c	Neutral Axis Depth d_n (mm)	Curvature κ (rad/mm)	Moment M_i (kNm)	Steel Strain ε_s
0.00315	36	8.75E-05	525.28	-0.0441	0.0035	37.1	9.43E-05	526.23	-0.0474
0.0032	36.1	8.86E-05	525.53	-0.0447	0.00355	37.3	9 52E-05	526.27	-0.0478
0.00325	36.2	8.98E-05	525.74	-0.0452	0.0036	37.5	9.60E-05	526.31	-0.0482
0.0033	36.4	9.07E-05	525.84	-0.0457	0.00365	37.7	9.68E-05	526.33	-0.0486
0.00335	36.5	9.18E-05	526.02	-0.0462	0.0037	37.8	9.79E-05	526.44	-0.0492
0.0034	36.7	9.26E-05	526.1	-0.0466	0.00375	38	9.87E-05	526.45	-0.0495
0.00345	36.9	9.35E-05	526.17	-0.047	0.0038	38.1	9.97E-05	526.54	-0.0501

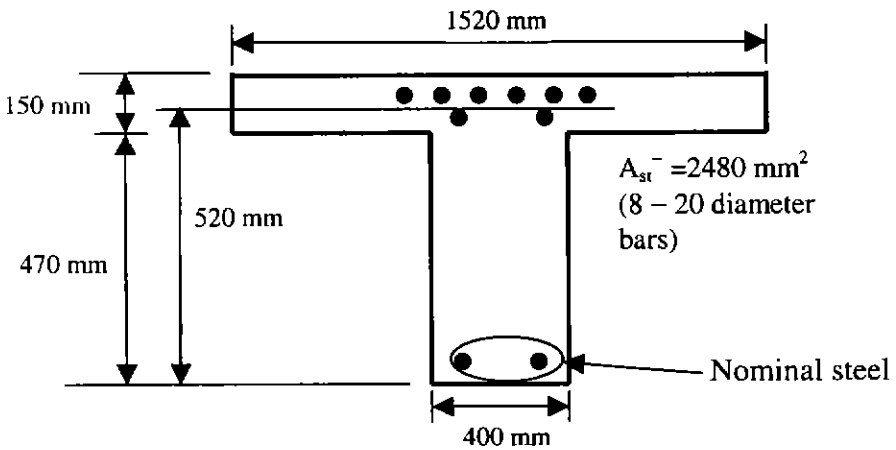

Fig. 3.7 Beam Cross-Section at Maximum Negative Moment Region

The results of the calculations are shown in Figure 3.8.

In this case, at ε_c = 0.0065, the moment-curvature curve unloads. The strain in the tensile steel ε_s at this stage is equal to 0.017, which is obviously less than the ultimate strain ε_{su}.

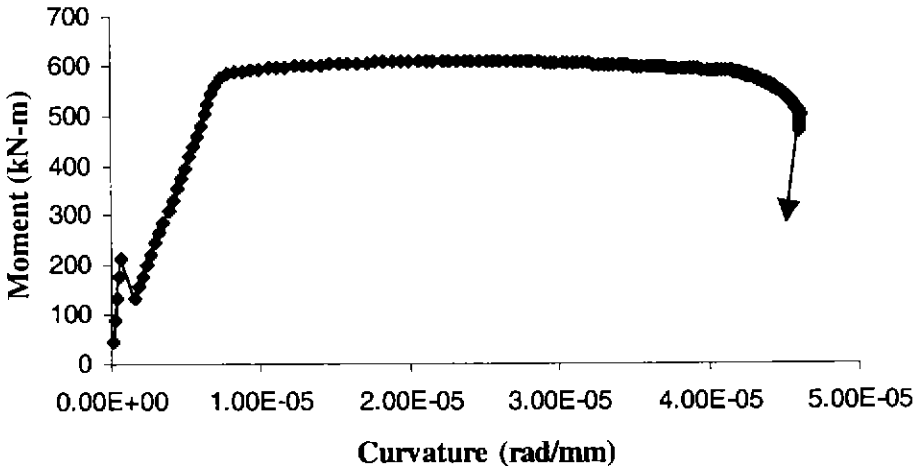

Fig. 3.8 Moment-Curvature Relationship for Maximum Negative Moment Section

3.3 Non-Linear analysis

The rotation and deflection of a beam are calculated by integrating the curvatures along the span lengths. For this purpose, the span is discretised into a number of rigid segments of finite length (Figure 3.9).

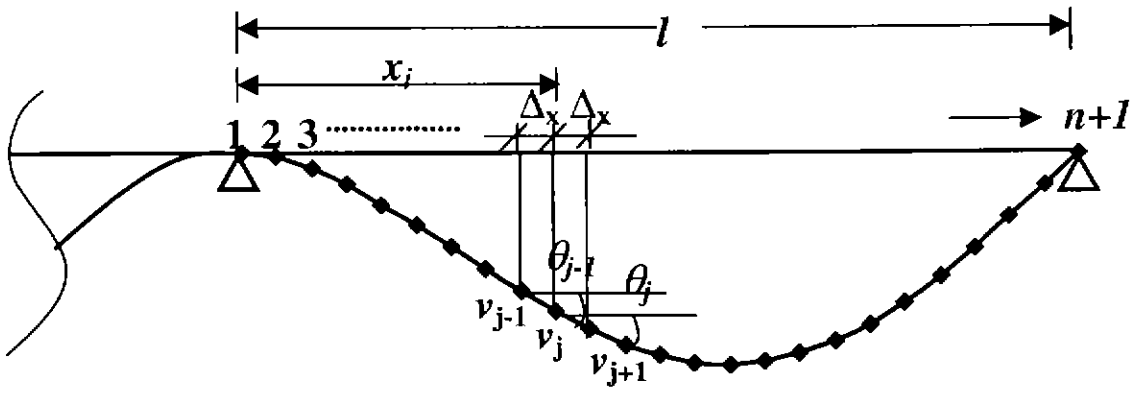

Fig. 3.9 Deflected Shape of a Continuous Beam

The curvature of the deflected shape at any point is the rate of change of the slope θ at that point. If the segments length is sufficiently small, the following expressions are valid (Figure 3.9).

$$\Delta\theta_j = \theta_j - \theta_{j-1} \tag{3.15}$$

and

$$\kappa_j \approx \frac{\Delta\theta_j}{\Delta x} \tag{3.16}$$

where,

$$\theta_j \approx \frac{v_{j+1} - v_j}{\Delta x} \tag{3.17}$$

$$\theta_{j-1} \approx \frac{v_j - v_{j-1}}{\Delta x} \tag{3.18}$$

From the Equation 3.16 we get

$$\kappa_j \approx \left(\frac{v_{j+1} - v_j}{\Delta x} - \frac{v_j - v_{j-1}}{\Delta x}\right).\frac{1}{\Delta x} \approx \frac{v_{j+1} - 2v_j + v_{j-1}}{(\Delta x)^2}$$

$$\text{or} \quad v_{j+1} = \kappa_j(\Delta x)^2 + 2v_j - v_{j-1} \tag{3.19}$$

Equation 3.19 can be rewritten in a generalised form as,

$$v_j = \kappa_{j-1}(\Delta x)^2 + 2v_{j-1} - v_{j-2} \tag{3.20}$$

In order to illustrate the analysis, we consider a propped cantilever beam, which approximately simulates the end span of a continuous beam. The numerical calculation starts from node 1 at the fixed support (Figure 3.10) for a given curvature κ_1. The corresponding bending moment $(M_{sup})_1$ at this node is obtained from the moment-curvature relationship of the section determined in accordance with the procedure described in Section 3.2.

Assume a trial value for the uniformly distributed load w_1 For this load w_1, the bending moment values at other nodes are now determined from the statics. The curvatures at various nodes are also calculated from the moment-curvature relationships of the corresponding sections.

The deflection at node 1 is zero, and Equation 3.20 calculates the deflections at all subsequent nodes. At node 2, the deflection is therefore given by

$$v_2 = \kappa_1(\Delta x)^2 + 2v_1 - v_0 \tag{3.21}$$

where, $v_1 = 0$

If we take the deflection curve to symmetrical about node 1, we can write, $v_0 = v_2$ and Equation 3.21 now becomes

$$v_2 = \frac{\kappa_1(\Delta x)^2}{2} \tag{3.22}$$

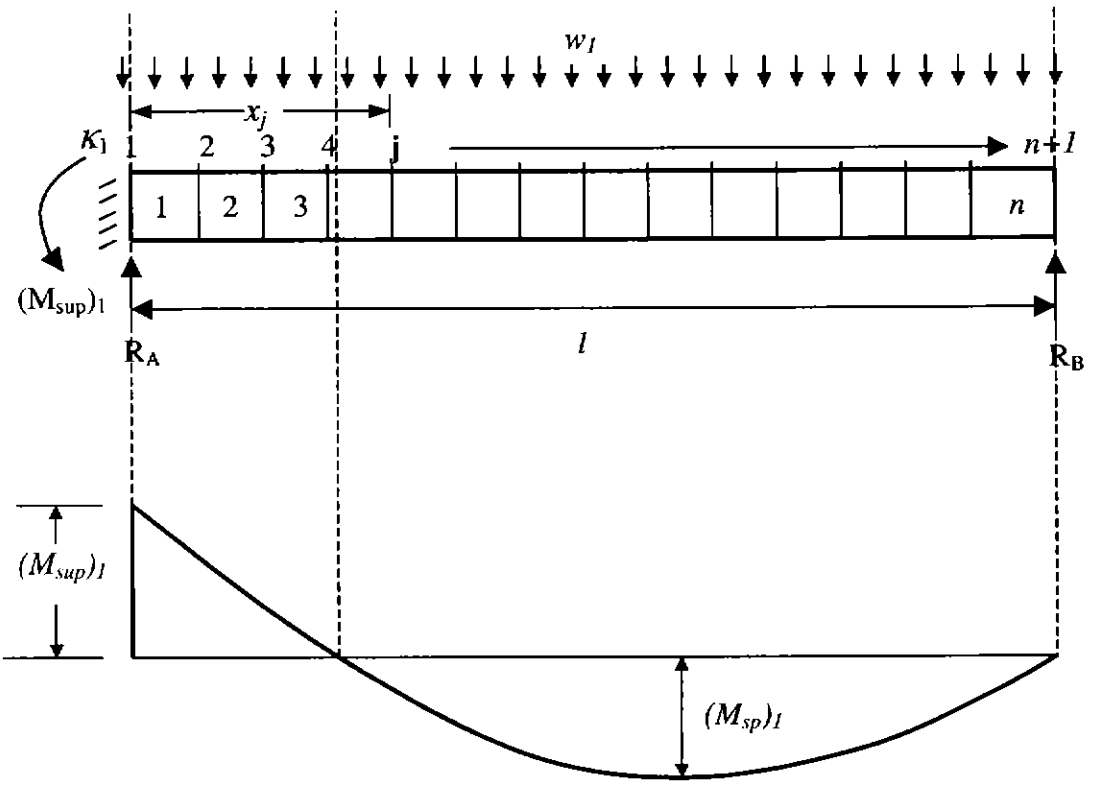

Fig. 3.10 Analysis of a Propped Cantilever Beam

The other boundary condition is that the deflection v_{n+1} at the simply supported end (i.e. node $n+1$) is also zero. We iterate the value of load w_1 until v_{n+1} becomes zero.

The above process is repeated for the new values of the curvature κ_1 at node 1 until the beam reaches the failure load. Failure of the propped cantilever occurs when the strain in the tensile steel reaches the failure strain either at the fixed support section or at the maximum positive moment section near the mid-span. Alternatively, failure may also occur due to crushing of the concrete compression zone at either of these regions. In this analysis, as mentioned earlier in Section 3.2.1, concrete crushing is assumed to occur when the moment-curvature curve at the appropriate section unloads and the failure load drops.

3.4 Discretisation

In this study, discretisation of the span length into a number of rigid segments of finite length is considered depending on the equivalent plastic hinge length. Various empirical equations have been proposed by investigators for the equivalent plastic hinge length, l_p based on beam tests. These expressions are based on experimental results, with very little rational explanations. Some of the available expressions are presented below:

- I.C.E Committee (1962)

$$l_p = k_1 k_2 k_3 (\frac{Z}{d}) d$$

- Baker and Amarakone (1964)

$$l_p = 0.8 k_1 k_3 (\frac{Z}{d}) k_u$$

- Corley (1966)

$$l_p = 0.5d + 0.2\sqrt{d}(\frac{Z}{d})$$

- Mattock (1967)

$$l_p = 0.5d + 0.05Z$$

- ACI-ASCE Committee 428 on Limit Design (1968)

Upper limit of l_p: the lesser of $R_e(\frac{d}{4} + 0.03Z^* R_m)$ and $R_e d$

Lower Limit of l_p: $R_e(\frac{d}{2} + 0.10Z^* R_m)$

- Tse and Darvall (1987)

$$\frac{l_p}{d} = 3.5\left(\frac{Z}{d}\right)^{0.49} \rho^{0.57}\left(1-\frac{p-p'}{p_b}\right)^{0.25}$$

where,

$k_1 = 0.7$ for mild steel or 0.9 for cold-worked steel

$k_2 = 1 + 0.5P_u/P_o$, where, P_u = axial compressive force in member and P_o = axial compressive strength of member without bending moment

$k_3 = 0.9\text{-}0.0128(f_c - 11.7)$ where f_c = concrete compressive strength in MPa

Z = distance of critical section to the point of point of contraflexure

d = effective depth of member

$R_e = \dfrac{0.004 - \varepsilon_{cue}}{\varepsilon_{cuo} - \varepsilon_{cue}}$ where, ε_{cue} = elastic component of maximum compression strain in concrete and εcue = basic maximum compressive strain in concrete

$R_m = \dfrac{M_m - M_e}{M_u - M_e}$ where, M_m = maximum moment in a length of member, M_e = elastic-limit moment, and M_u = ultimate moment

$Z^* = \dfrac{M_m \times 10^{-3}}{V_Z + 0.744\sqrt{w M_m R_m}}$ where, V_Z = the shear adjacent to a concentrated load or reaction at a section of maximum moment (in kN), w = the uniformly distributed load at section of maximum (in kN m) and M_m = the maximum moment (in kN m)

ρ = ratio of volume of stirrups to volume of concrete core measured to outside

$p = A_{st}/bd$ where A_{st} = area of reinforcement in a tensile zone of flexural member

$p' = A_{sc}/bd$ where A_{sc} = area of reinforcement in a compression zone of flexural member

It is to be noted that l_p refers to the length of plastic hinge on either side of a critical section.

Baker (1964) indicated that for the range of span/d and Z/d ratios normally found in practice, l_p lies between 0.4d and 2.4d. Tse and Darvall 1988; Foo and Darvall 1988

noted that a reasonable value for l_p is approximately equal to $D/2$. This value is used in the present study.

3.5 Calculation Procedure

The non-linear analysis described in the previous section may be carried out using the following steps:

Step 1: Input test beam data, viz dimensions of the beam section, span length of the beam, reinforcement details, material properties and loading conditions.

Step 2: Establish the moment-curvature relationships of the various sections (see Section 3.2).

Step 3: Discretise the beam into n rigid segments of length Δx with $n+1$ nodes. In this study the segment length is taken $D/2$ where D is the overall depth of the beam.

Step 4 Select a value for the curvature κ_1 at the node 1. Calculate the moment $(M_{sup})_1$ at the node 1 from the moment-curvature relationship

Step 5: Assume a trial value of load w_1. The first trial value taken as 0.05 times of plastic failure load and the increment of the load thereafter is 0.05% of plastic failure load.

Step 6: Calculate the moment at every node and the corresponding curvatures at every node from the moment-curvature relationships.

Step 7: Calculate the deflection at every node. The deflection at node 1 is zero. Equation 3.21 calculates the deflection at node 2 and Equation 3.20 is used for deflections at other nodes.

Step 8: Check the boundary condition at end node. If the magnitude of the load w_I is the correct value then deflection v_{n+1} will be zero subjected to a tolerance. In this study this tolerance is taken as ±1.0% of the maximum deflection of the beam.

If v_{n+1} is not within the prescribed tolerance limit, a new value of w_I must be selected and the process returns to Step-5.

Usually a positive value of the deflection v_{n+1} indicates that the current value of w_I is lower than the correct value and a negative deflection indicates a higher value of w_I. The value of w_I can be corrected by interpolation between the values of w_I for positive and negative deflection at the end node as shown in Figure 3.11. The method of false position (Regula Falsi) is used in this analysis to estimate the correct value of w_I. When the deflection at end node is within the prescribed tolerance, a convergence for the selected value of κ_I is obtained and the corresponding load, deflection and internal moment at every node are calculated.

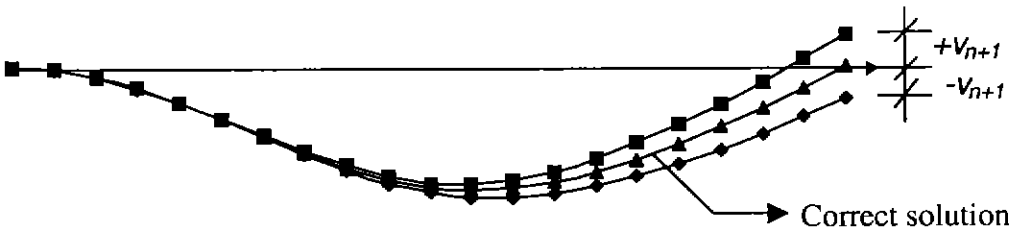

Fig. 3.11 Convergence of Solution

Step 9: Increase the value of curvature κ_I and repeat Steps 4 to 9 until the failure load is reached. Calculate the percentage of moment redistribution β at support as

$$\beta = (1 - \frac{M_{u-}}{M_{EL}})100\,(\%) \qquad (3.23)$$

where

M_{u-} = ultimate support moment at failure

M_{EL} = support moment calculated by elastic analysis for the failure load

The analysis procedure is explained by the flow chart shown in Figure 3.12.

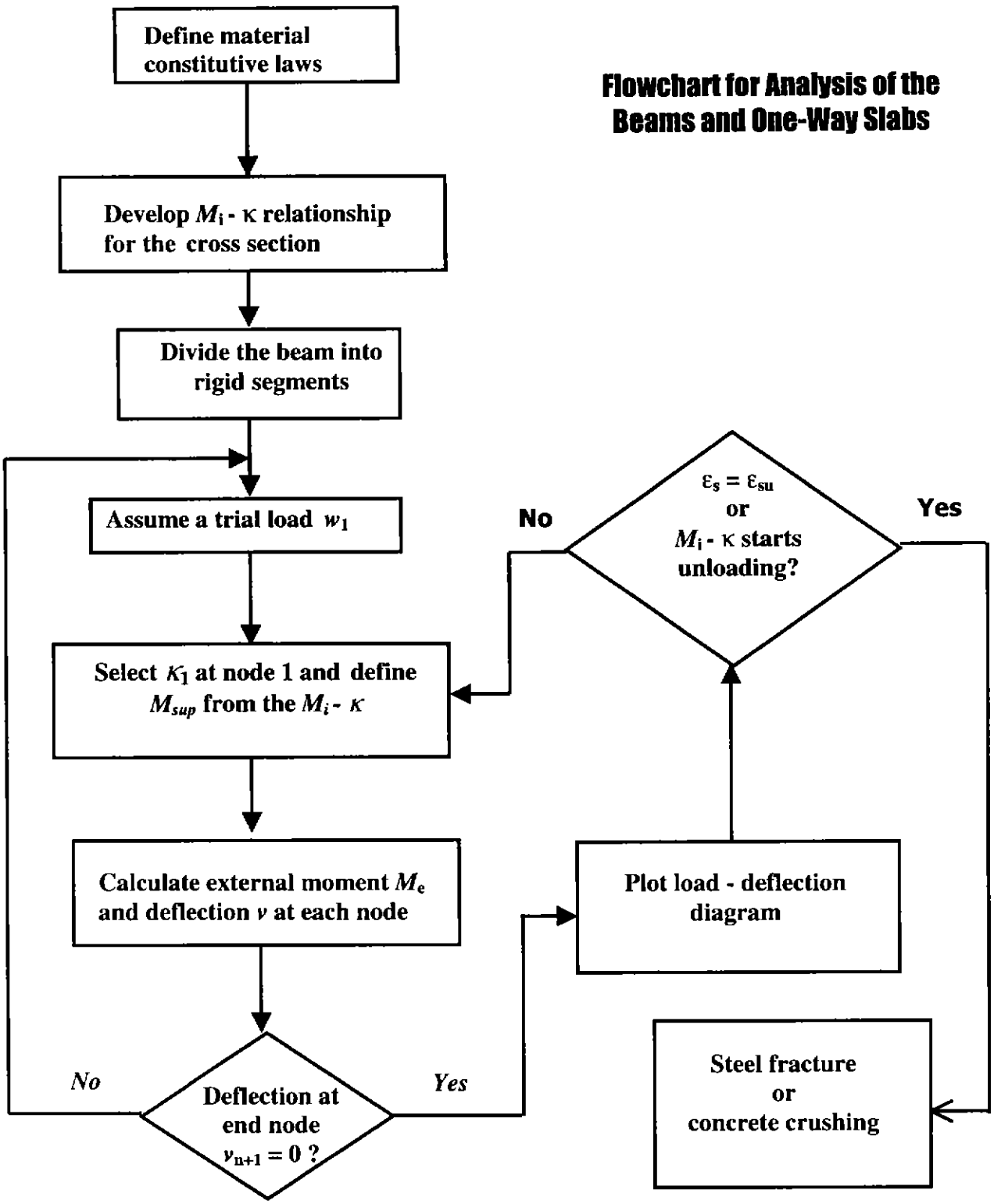

Fig. 3.12 Flow Chart of the Analytical Procedure

3.6 Example

The procedure of non-linear analysis described in the previous section is illustrated by the following example.

Steps 1 & 2: Data

The cross-section details and material properties of a propped cantilever beam are the same as those given in Section 3.2.5. The moment-curvature relationships are also given in Section 3.2.5. The span length is 8 m and the beam carries an uniformly distributed load.

Step 3: Discretisation

The beam length is divided into 25 rigid segments of length $\Delta x = 320$ mm which is equal to about half of the overall depth of the beam.

Step 4: Take $\kappa = 7.41 \times 10{-}6$ rad/mm. The corresponding moment is obtained from moment-curvature relationship as $(M_{sup})_1 = 574.23$ kNm.

Step 5: Let the trial value of load $w_1 = 70.4$ kN/m.

Step 6: From statics, the moment at every node is shown in Figure 3.12.Curvature at every node is given by the moment-curvature relationships.

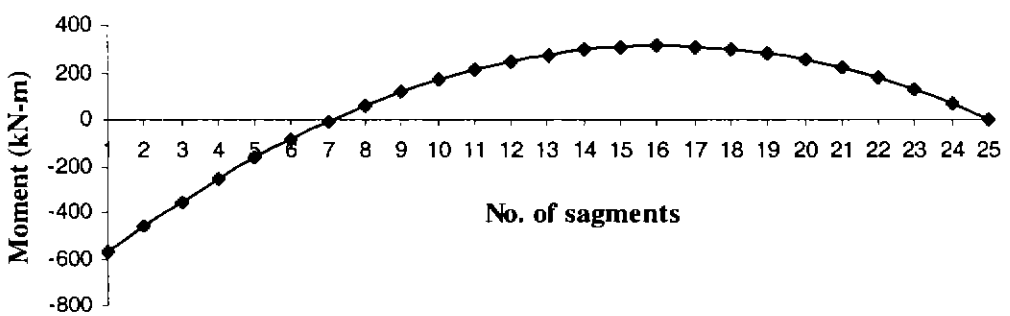

Fig. 3.13 Bending Moment Diagram ($w_1 = 70.4$ kN/m)

Step 7: The deflection at node 1 is zero Deflection at node 2 is calculated by Equation 3.22 and Equation 3.20 calculates the deflection of the subsequent nodes. Deflection at every node is shown in Figure 3.13.

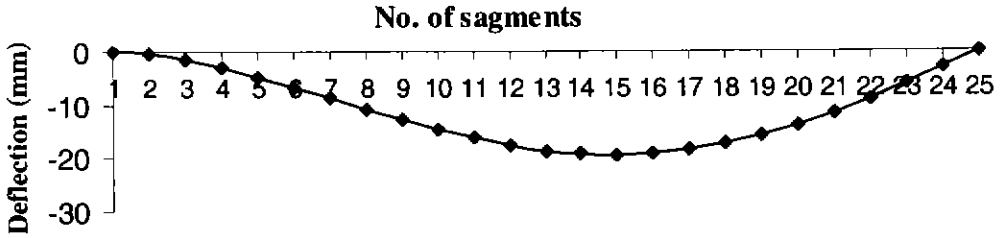

Fig. 3.14 Deflected Shape of Beam (w_1 = 70.4 kN/m)

Step 8: The deflection at the end node, v_{25} = 0.17 mm and the maximum deflection at node 15, v_{max} = 19.46 mm.

Now $\frac{v_{25}}{v_{\max}} \times 100\% = 0.87\%$ which is less than the tolerance limit. Therefore, the assumed load is accepted.

Step 9: The failure load is 90.47 kN/m which occurs due to concrete crushing at the fixed end when ε_c = 0.0065 and the corresponding steel strain, ε_s = 0.017 which is less than ε_{su} = 0.05. At that time the maximum positive moment is 458.55 kN-m which is less than the ultimate positive moment, M_{u+} = 523.37 kN-m. Therefore the failure is due to concrete crushing at fixed end.

At failure, the fixed end moment, M_{u-} = 586.36 kNm. The moment at the fixed end by usual elastic analysis, M_{EL} = 723.76 kNm. Therefore, the moment redistribution at fixed end, $\beta = \frac{723.76 - 586.36}{723.76} \times 100 = 18.98\,\%$.

The load-deflection diagram is shown in Figure 3.15 and the results of the example are given in Table 3.2.

Table 3.2 Summery of Calculations: Example

Curvature at fixed end, κ_f (rad/mm)	Maximum deflection v_{max} (mm)	Mid-span deflection (mm)	Load/span (kN)	
7.41E-07	1.72	1.65	225.40	
1.48E-06	2.29	2.16	234.41	
2.22E-06	2.87	2.68	241.96	
2.96E-06	3.44	3.20	249 09	
3.70E-06	6.92	6.41	294 54	
4.44E-06	9.43	8.80	339 30	
5.18E-06	12.87	12.22	403.65	
5.92E-06	14.65	13.95	453.20	
6.66E-06	17.71	16.94	520.35	
7.41E-06	19.46	18.65	563.11	
9.28E-06	20.76	19.95	588.29	
1.12E-05	21.74	20.95	602.28	
1.30E-05	22.67	21.90	615.06	
1.49E-05	23.56	22.82	627.45	
1.68E-05	24.46	23.75	638.64	
1.87E-05	25.37	24.67	651.03	
2.06E-05	26.19	25.50	661.82	
2.24E-05	26.88	26.21	670.22	
2.43E-05	27.49	26.85	677.41	
2.62E-05	28.10	27.48	683.01	
2.81E-05	28.64	28.06	688.20	
3.00E-05	29.20	28.63	692.60	
3.18E-05	29.75	29.19	696.19	
3.37E-05	30.49	29.93	702.19	
3.56E-05	31.29	30.73	708.18	
3.75E-05	32.09	31.54	714.58	
3.94E-05	33.01	32.44	720.57	
4.12E-05	34.06	33.45	723.77	← Failure
4.31E-05	34.79	34.16	719.77	
4.50E-05	34.86	34.28	705.79	

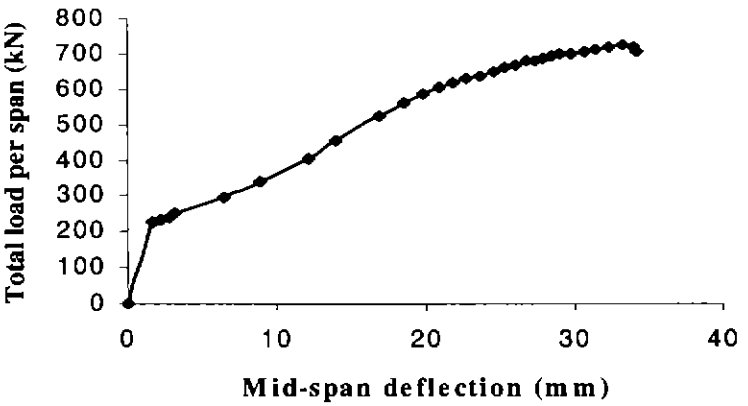

Fig. 3.15 Load-Deflection Diagram

CHAPTER 4

CORRELATION BETWEEN ANALYTICAL AND TEST RESULTS

4.1 Introduction

This chapter describes the ability of the non-linear analysis presented in Chapter 3 to predict the strength, failure modes and deformations and rotation capacity of continuous reinforced concrete beams and slabs. The following Sections present correlation of analytical results with test results reported in the literature.

4.2 Influence of Discritisation

In order to determine the influence of the segment length (into which beam was discretised) upon the predicted behaviour of the beam or one-way slab, three beams and one-way slabs were analysed using various segment lengths. The largest segment length was set approximately equal to depth of the cross section. The lower limit of the segment length was chosen to be approximately one-quarter of the cross-section.

Analyses were carried out on test Beam group 4 (Pisanty and Regan 1993), Test 2.0 (Eligehausen and Fabritius 1993) and Test ADF.BO2 (Patrick, Akbarshahi and Warner 1997). The results of the analyses presented in Table 4.1 and in Figure 4.1, show that the segment length has an influence upon the predicted results. It is observed from Table 4.1 and Figure 4.1 that as a general, segment length of *D/2* shows good correlation with test results. As a result of this investigation, it was decided to consider segment length as one-half of the depth of the cross-section i.e. *D/2*.

Table 4.1 Influence of Segment Length upon Predicted Results

Specimen	Discretis-ation Δ_x	Predicted total load per span, kN	Predicted /Test	Predicted Mid-span deflection/Support rotation	Predicted /Test
Beam Group 4	$\Delta_x = D/4$	52.8	1.11	15.0 (mm)	1.23
	$\Delta_x = D/2$	54.8	1.07	19.96 (mm)	0.93
	$\Delta_x = D$	55.0	1.06	22.34 (mm)	0.83
Test 2.0	$\Delta_x = D/4$	60.15	1.0	0.031 (rad)	1.16
	$\Delta_x = D/2$	63.1	0.95	0.039 (rad)	0 92
	$\Delta_x = D$	66.9	0.9	0.062 (rad)	0 58
Test ADF.BO2	$\Delta_x = D/4$	222.4	1.02	18.7 (mm)	1.4
	$\Delta_x = D/2$	245.8	0.92	23.8 (mm)	1.09
	$\Delta_x = D$	273.2	0.83	30.7 (mm)	0.85

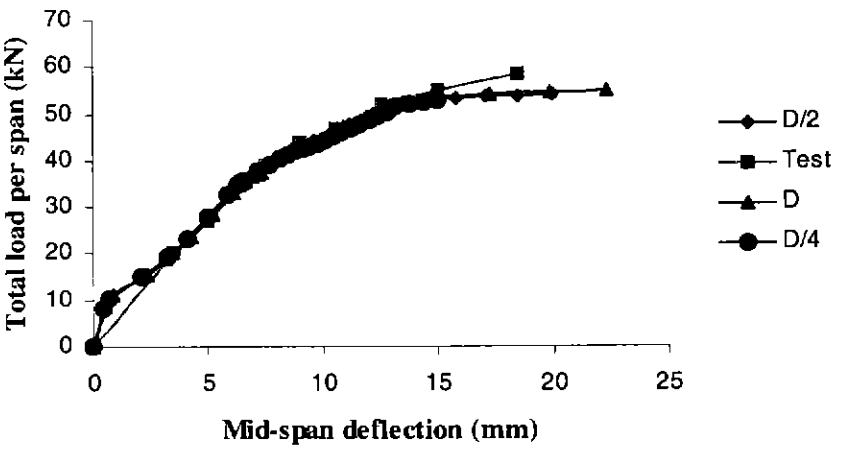

Beam Group 4 (Pisanty and Regan 1993)

Fig 4.1 Influence of Segment Length upon Predicted Results (Continued)

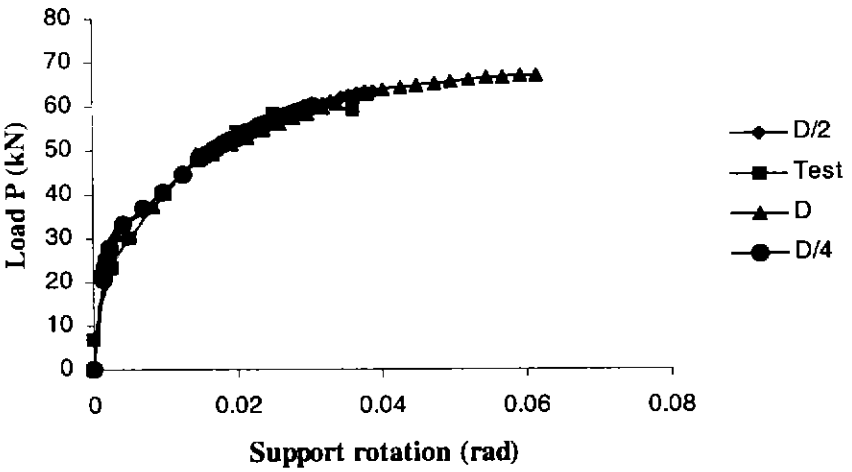

Test 2.0 (Eligehausen and Fabritius 1993)

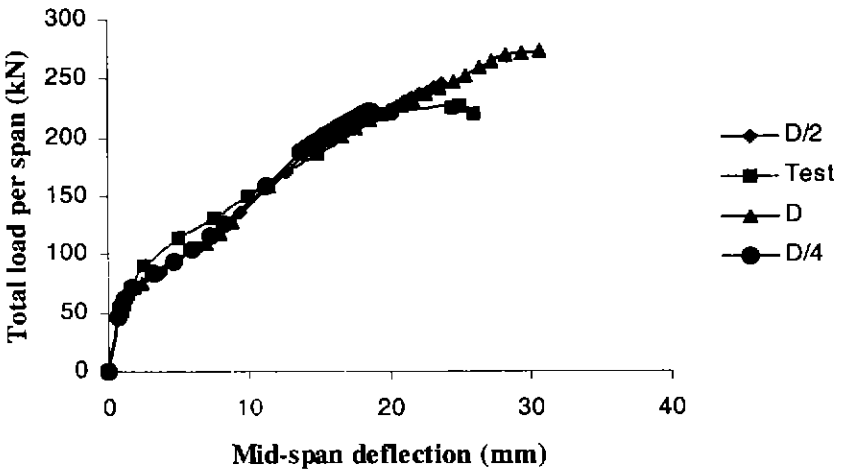

Beam ADF.BO2 (Patrick, Akbarshahi and Warner 1997)

Fig 4.1 Influence of Segment Length upon Predicted Results

4.3 Tests by Pisanty and Regan (1993)

4.3.1 Beam Details

An experimental study was under taken by Pisanty and Regan (1993) to investigate the behaviour of reinforced beams, designed for various redistribution of moments

conditions. Four beams were made as shown in Figure 4.1, all designed to carry four point loads of W = 20 kN The beams were initially designed for moment redistribution ratios of +15%, 0% -15%, -35% from the linear elastic moment at the interior support. However, in order to achieve the amount of the reinforcement shown in Figure 4.1, the redistribution ratios were modified to +15%, +5%, -10% and –35%, and the design loads for the four beams were modified to: 22.0, 22.5, 21.6, and 22.0 kN respectively.

The average concrete cube crushing strength was 40 MPa. By assuming the cylinder strength to be 85 % of cube strength, f'_c was taken as 34 MPa. From test observations, the average tensile properties for the steel were taken as follows: yield stress (0.2%) f_{sy} = 460 MPa, tensile strength f_t = 506 MPa and ultimate strain ε_{su} = 0.06.

4.3.2 Correlation of Results

Due to symmetry, each span was analysed as a propped cantilever. The beams were discretised into segments approximately equal to one-half of the overall beam depth. The analysis was carried out using the method described in Chapter 3. The results are presented in Table 4.1 and Figure 4.2.

Table 4.2 Correlation of Test and Calculated Results: Tests by Pisanty and Regan

Beam Group	Design Moment Redist-ribution	Failure Load, kN			Analysis Results					
		Test	Analysis	Test/ Analysis	Strain in Tensile Steel		Failure Location	Moments at Failure		Moment Redistribution
					support	span		support	span	
1	+15 %	31.0	28.1	1.10	0.017	0.048	span	29.3	14.8	+13.2 %
2	+5 %	30.0	28.3	1.06	0.031	0.044	span	24.2	15.7	+6.0 %
3	-10 %	30.0	27.25	1.10	0.038	0.017	support	19.4	16.9	-19.0 %
4	- 35 %	29.2	27.4	1.07	0.054	0.018	support	14.7	18.5	-39 %

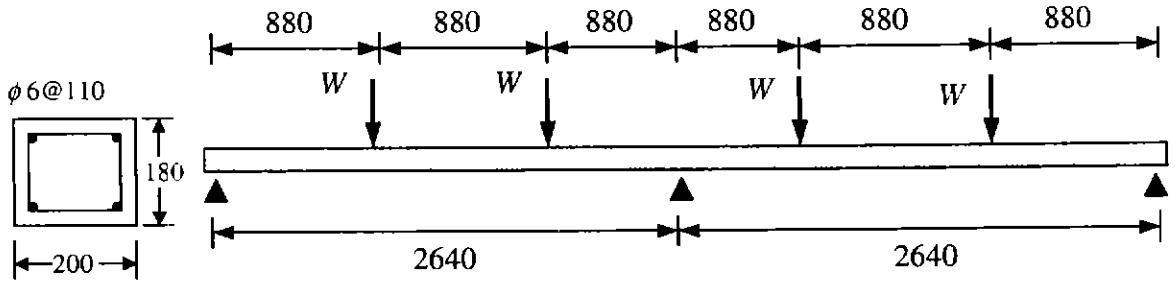

Dimensions are in mm

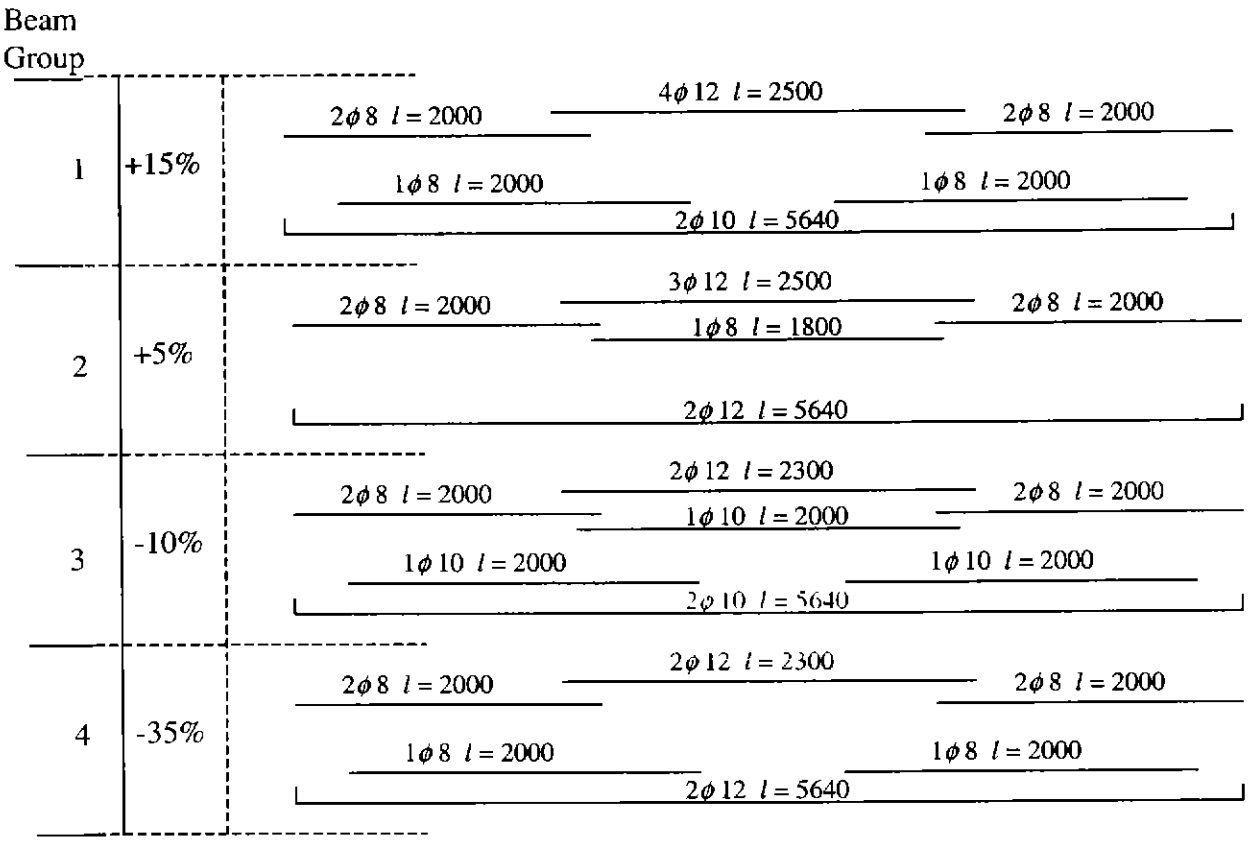

Fig. 4.2 Beams Tested by Pisanty and Regan (1993)

It can be seen from the Figure 4.2 that the correlation between the analytical and measured load-deflection curves of beams is very good. The predicted failure loads are conservative in every case.

The analysis showed that the Beam Group 1 (+15 %) and Beam Group 2 (+5 %) were failed by concrete crushing over the span whereas other two Beam Groups (-10 % and –35 %) failed by concrete crushing over the support. The predicted values of the maximum steel strains at failure sections ranged from 0.031 to 0.054. These values were still smaller than the ultimate value of 0.06 and therefore steel fracture did not occur in any of the beams.

The researchers did not report the observed moment redistribution. As steel was highly ductile, in every case the predicted moment redistribution generally reached the designed moment redistribution (Table 4.1).

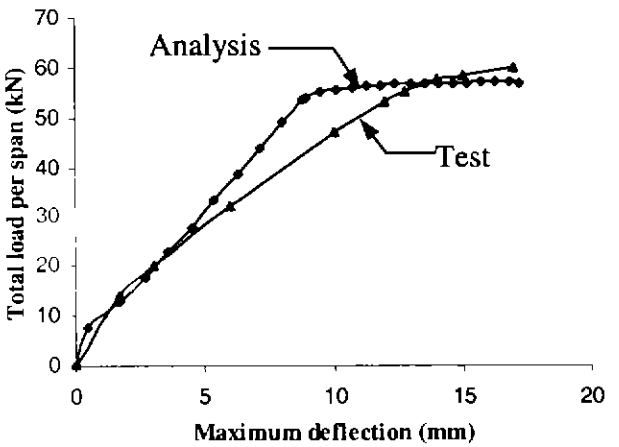

Beam Group 1 (+15 %)

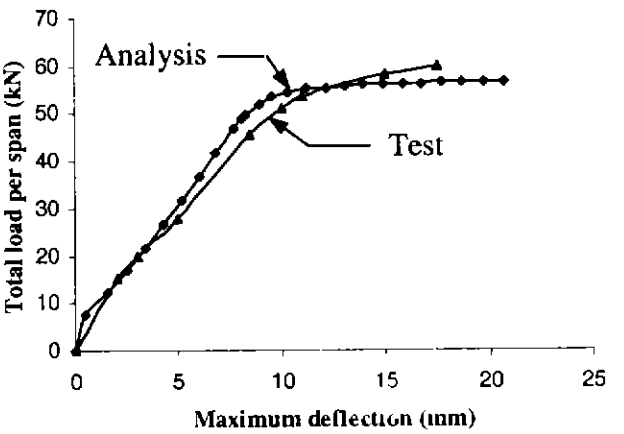

Beam Group 2 (+5 %)

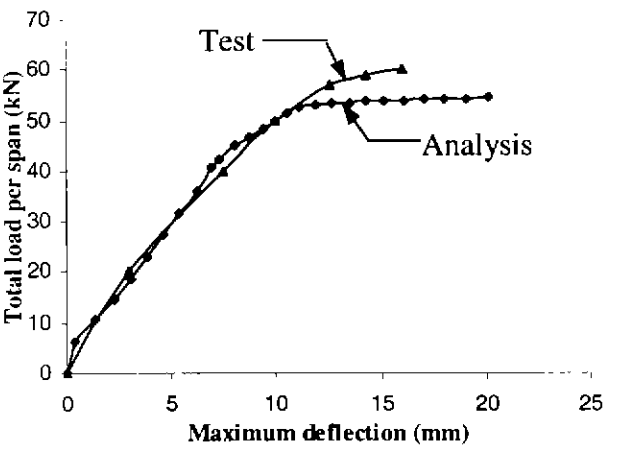

Beam Group 3 (– 10 %)

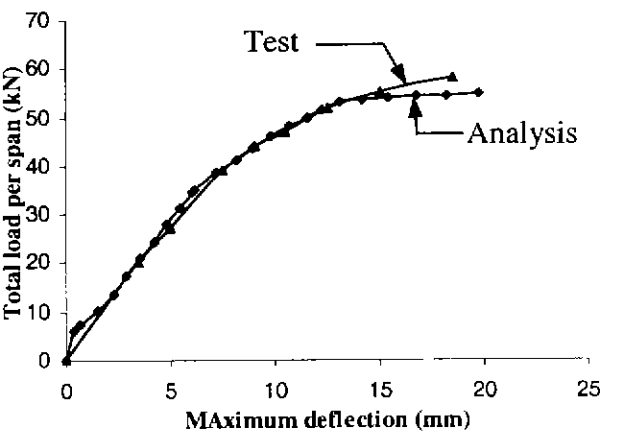

Beam Group 4 (– 35 %)

Fig. 4.3 Correlation of Test and Calculated Load-Deflection curves: Tests by Pisanty and Regan

4.4 Tests by Eligehausen and Fabritius (1993)

4.4.1 Specimen Details

Eligehausen and Fabritius (1993) tested seven continuous slabs reinforced with welded wire mesh. The details of test slabs are shown in Figure 4.3. In all slabs, the reinforcement percentage was 0.3 % in the span as well as over the support.

The average cube compressive strength of concrete was 61.5 MPa. Once again, the cylinder strength was taken as 85 % of the cube strength and $f'_c = 0.85 \times 61.5 = 52.3$ MPa. The properties of the steel reinforcement are given in Table 4.2.

Table 4.3 Properties of Reinforcing Steel

Steel parameters							
Specimen Number	Slab1.1	Slab 2.0	Slab 2.1	Slab 2.2	Slab 4.1	Slab 6.1	Slab 8.1
Reinforcement over support							
f_y (N/mm^2)	508	602	594	599	598	615	514
f_t (N/mm^2)	555	639	642	643	644	650	553
ε_{su} (%)	4.9	4.2	3.3	3.1	3.5	3.4	5.0
Reinforcement in the span							
f_y (N/mm2)	599	604	609	602	600	612	513
f_t (N/mm^2)	639	637	644	638	643	652	556
ε_{su} (%)	2.92	4.3	2.85	2.9	3.65	3.4	5.3

4.4.2 Correlation of Results

Once again, due to symmetry, each span was analysed as propped cantilever. Each span was discretised into segments approximately equal to one-half of the thickness of slab. The analysis was carried out using the method given in Chapter 3. The results are presented in Table 4.3 and Figure 4.4.

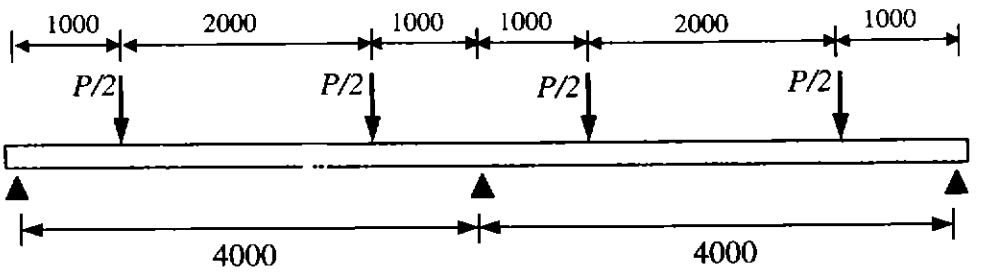

(a) Test set-up

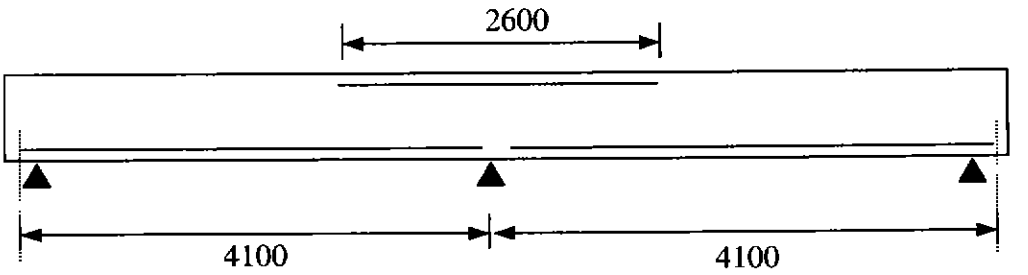

(b) Reinforcement details

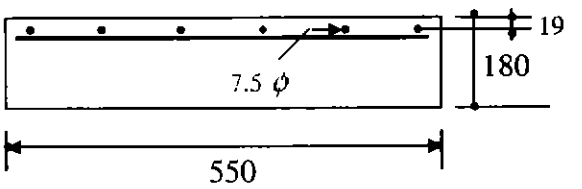

(c) Cross-section at interior support

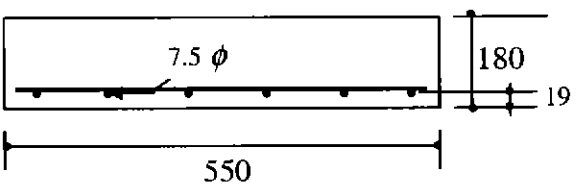

(d) Cross-section in span

Dimensions are in mm

Fig. 4.4 Slabs Tested by Eligehausen and Fabritius (1993)

Table 4.3 shows that test and analytical values of failure loads, moments at peak load, and moment redistribution percentage correlate well. The results of the analysis also indicated that failure occurred by steel fracture in all cases, which agreed with the test observations.

Figure 4.4 shows the correlation of test and predicted load versus support rotation curves. In the experimental work, the researchers calculated the support rotation using the measured deflections of test specimens at the support and points of inflexion. In the analysis, the support rotation was calculated by summing the curvatures between the support point and the inflexion points. It can be seen from the Figure 4.4 that the agreement between test and predicted curves is excellent in most cases. In Slab 2.1, the experimental curve is somewhat erratic for unknown reasons.

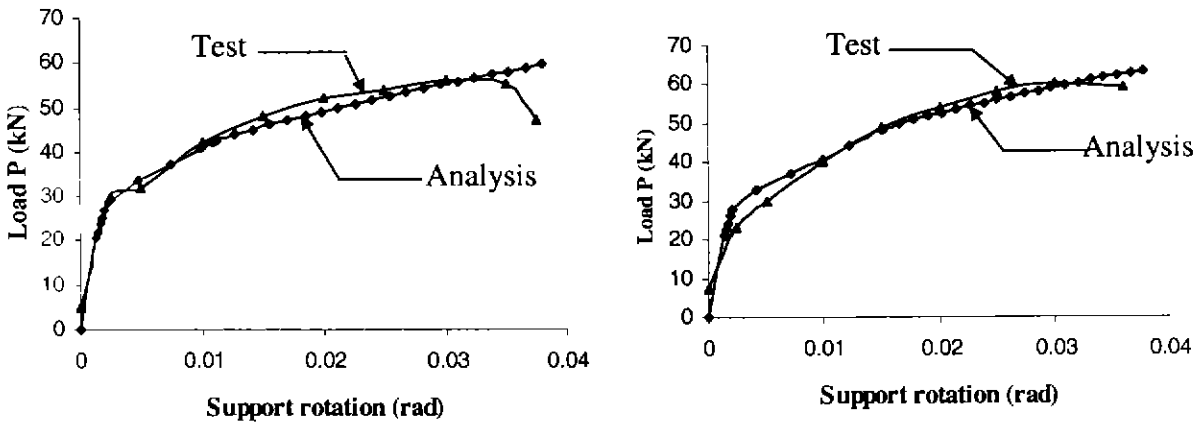

(a) Slab 1.1

(b) Slab 2.0

Fig. 4.5 Correlation of Test and Calculated Load-Support Rotation Curves: Tests by Eligehausen and Fabritius (Continued)

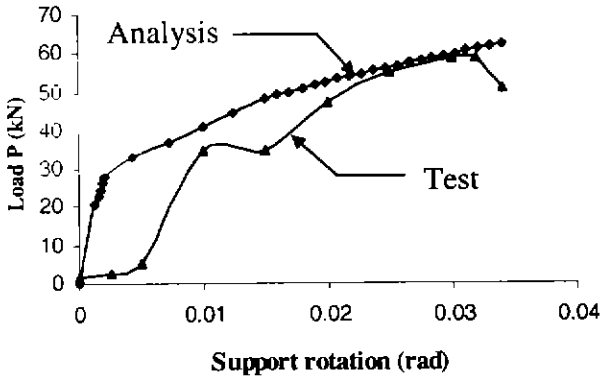

(c) Slab 2.1

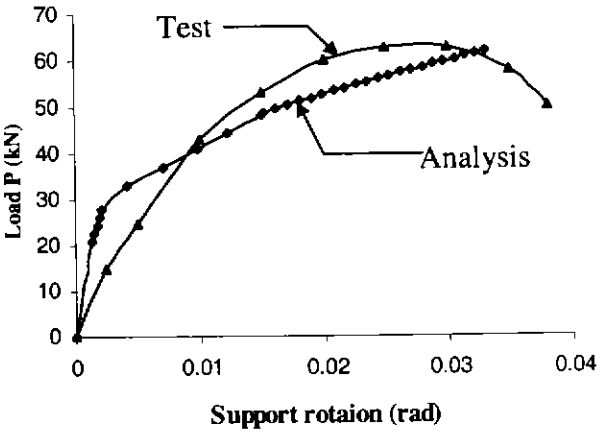

(d) Slab 2.2

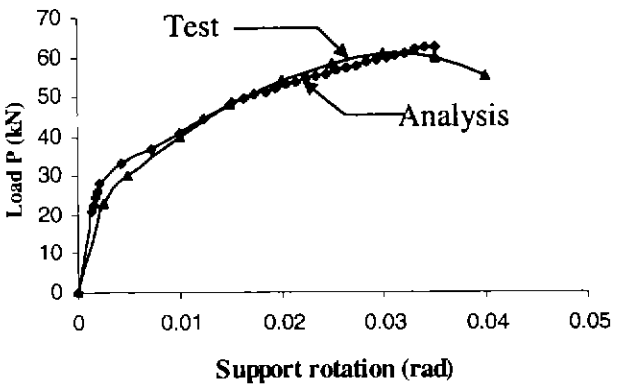

(e) Slab 4.1

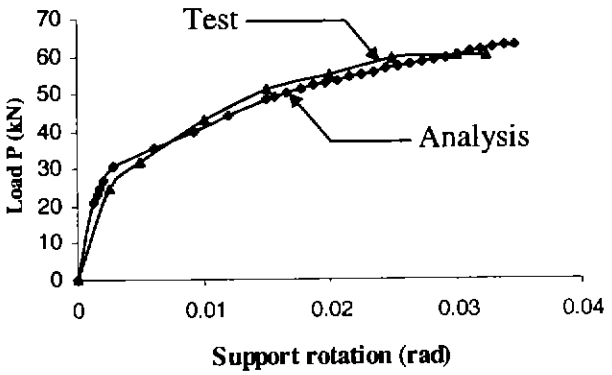

(f) Slab 6.1

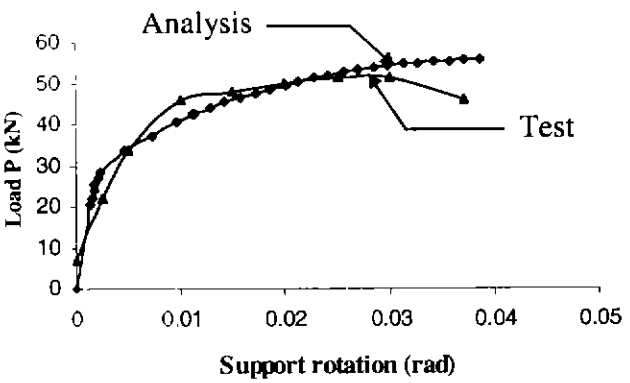

(g) Slab 8.1

Fig. 4.5 Correlation of Test and Calculated Load-Support Rotation Curves: Tests by Eligehausen and Fabritius

Table 4.4 Correlation of Test and Calculated Results: Tests by Eligehausen and Fabritius

Slab No.	1.1	2 0	2.1	2.2	4.1	6.1	8.1
Failure load, P_{max} (kN)							
Test	56.2	60.2	58.8	63.0	60.8	59.8	50.6
Analysis	59.5	63.1	62.2	61.82	62.2	62.71	55.7
Test/ Analysis	0.94	0.95	0.94	1.02	0.98	0.95	0.91
Interior Support moment at P_{max} (kN-m)							
Test	22.6	30.2	27.3	30.0	28.6	25.3	24.9
Analysis	23.27	26.7	27.1	27.1	27.1	27.26	23.1
Test/ Analysis	0.97	1.13	1.01	1.11	1.06	0.93	1.08
Span moments at P_{max} (kN-m)							
Test	26.0	26.4	26.1	28.1	27.3	27.3	22 7
Analysis	24.35	25.0	24.3	24.13	24.52	24.54	22 16
Test/ Analysis	1.07	1.06	1.07	1.16	1.11	1.11	1.02
Moment redistribution over the support at P_{max} (%)							
Test	37.0	22.5	23.5	24.0	27.9	34.1	28.0
Analysis	30.5	24.8	22.8	22.1	22.8	22.7	26.3
Test/ Analysis	1.21	0.91	1.03	1.09	1.22	1.5	1.08

4.5 Tests by Patrick, Akbarshahi and Warner (1997)

4.5.1 Beam Details

Three continuous reinforced concrete beams tests were reported by Patrick, Akbarshahi and Warner (1997) to determine the ductility limits for use in the design of continuous concrete structures containing high-strength, low elongation steel reinforcement. The beams varied in overall depth and in the amount of moment redistribution assumed in design.

The details of test specimens are shown in Figure 4.5. The longitudinal reinforcement continued uninterrupted along the full length of the members. Closely spaced Y12 stirrups were used to prevent shear failure. The reinforcement ratios in the top were for beams ADF.BO1, ASF.BO2 and ADF.BO3 were 0.73, 0.50 and 0.83 percent respectively. The beam ADF.BO3 was designed for no moment redistribution and the beam ADF.BO1 and ADF.BO2 were both designed for 30 percent moment redistribution from negative to positive moment regions.

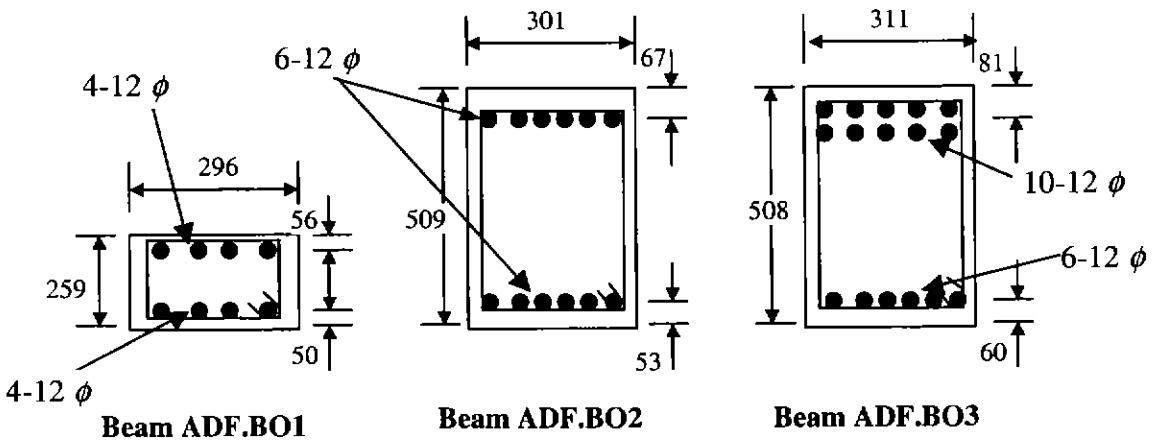

(a) Beam cross-sections

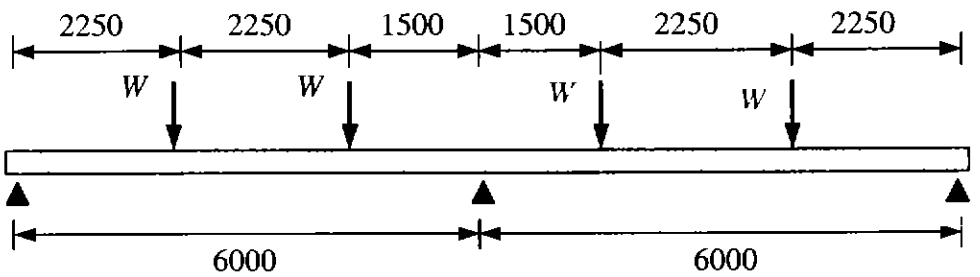

(b) Test set-up

Dimensions are in mm

Fig. 4.6 Beams Tested by Patrick, Akbarshahi and Warner (1997)

The beams were all cast from one batch of concrete, and tested at ages varying from 27 to 65 days, during which time the compressive strength varied from 40.0 to 46.0 MPa. The average of the compressive strengths was therefore taken as f'_c = 43.0 MPa. The average tensile properties for the steel were measured and reported as follows: yield stress (0.2%) f_{sy} = 648 MPa, tensile strength f_t = 685 MPa and ultimate strain ε_{su} = 0.016.

4.5.2 Correlation of Results

Once again, each span of the beam was analysed as a propped cantilever using the method of analysis given in Chapter 3. The span was discretised into segments approximately equal to one-half of the overall depth of beam. The results are presented in Table 4.4 and Figure 4.6.

In the tests, the specimens ADF.BO1 and ADF.BO2 failed by fracture of tensile steel over the interior support whereas the specimen ADF.BO3 failed by fracture of the tensile steel near the mid span of one of the spans. The analysis showed that all the three beams failed by fracture of the tensile steel at the interior support, although the beam ADF.BO3 was closed to forming a plastic mechanism with a ratio of failure load to plastic load equal to 0.97.

Figure 4.6 shows that test and calculated load-deflection curves agree well. Table 4.4 indicates the test failure loads are in reasonable agreement with calculated values. The specimens ADF.BO1 and ADF.BO2 did not reach the 30 percent moment redistribution they were designed for whereas the specimen ADF.BO3 achieved very little as was expected. The primary reason for the behaviour of specimens ADF.BO1 and ADF.BO2 is suspected to be the low ultimate strain of the steel bars, which fractured at failure of the specimens.

Table 4.5 Correlation of Test and Calculated Results: Tests by Patrick, Akbarshahi and Warner

Specimen Mark	Design Moment Redistribution (percent)	Calculated Moment Redistribution (percent)	Failure Load per Span (kN)		
			Test	Predicted	Test/ Predicted
ADF.BO1	30.0	9.0	68.0	64.1	1.06
ADF.BO2	30.0	20.0	227.0	245.8	0.92
ADF.BO3	0.0	3.0	303.0	311.7	0.97

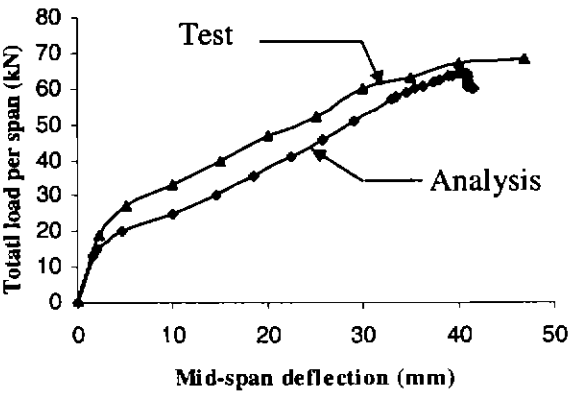

(a) Beam ADF.BO1

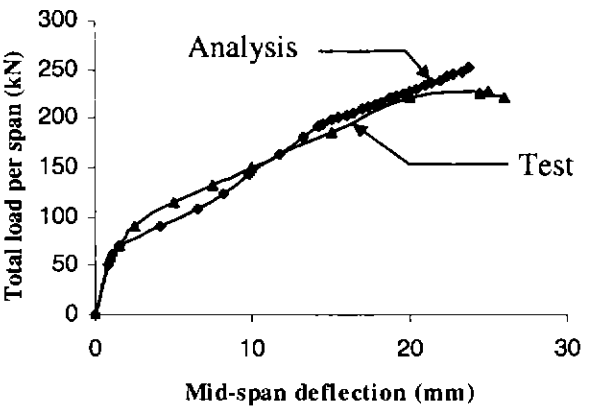

(b) Beam ADF.BO2

Fig. 4.7 Correlation of Test and Calculated Load-Deflection Curves: Tests by Patrick, Akbarshahi and Warner (Continued)

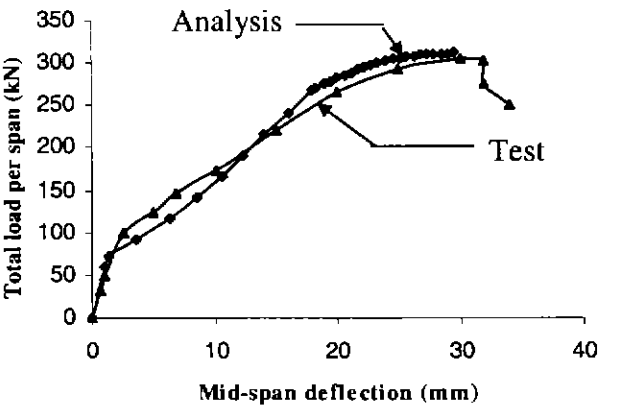

(c) Beam ADF.BO3

Fig. 4.7 Correlation of Test and Calculated Load-Deflection Curves: Tests by Patrick, Akbarshahi and Warner

4.6 Tests by Alvarez, Koppel and Marti (2000)

4.6.1 Specimen Details

To investigate the ductility of reinforcing steel on the behaviour of structural members, Alvarez, Koppel and Marti (2000) tested three continuous slab specimens. The details of the test specimens are given in Figure 4.7 and Table 4.5.

The average concrete compressive strength of specimens 1, 2, and 3 were respectively 49, 51, and 50 MPa. Cold-deformed, coiled reinforcing bars were used. Table 4.6 shows the results of the tension tests on samples with a free length of 1 m. For each diameter, six tests were performed (Figure 4.8). The strains were measured over the central 300 mm of the free length of the test samples. The values of the yield strength f_{sy} given in Table 4.6 correspond to a strain of 0.2%. It can be seen from the Figure 4.8 that the ultimate strain ε_{su} showed considerable scatter and the values given in Table 4.6 are mean values.

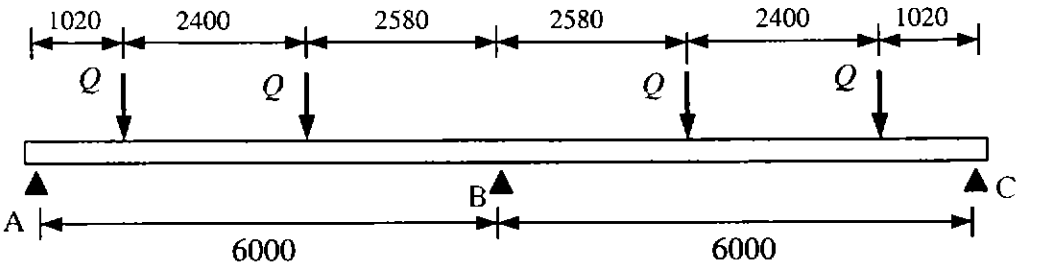

(a) Test set-up

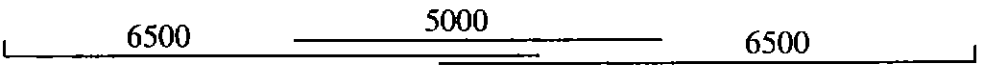

(b) Steel layout along the span

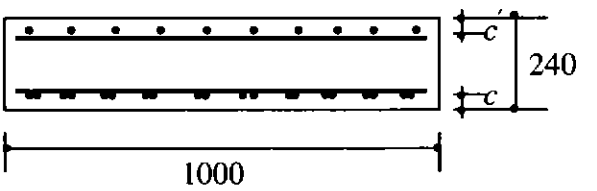

(c) Specimen cross-section at interior support B

Dimensions are in mm

Fig. 4.8 Specimens Tested by Alvarez, Koppel and Marti (2000)

Table 4.6 Bar Diameters, Covers to Bar Centres and Cross-Sectional Areas of Reinforcement of Specimens Tested by Alvarez, Koppel and Marti (2000)

Specimen	Bottom reinforcement			Top reinforcement		
	ϕ, mm	c, mm	A_s, mm^2	ϕ', mm	c', mm	A'_s, mm^2
1	10	30	785	12	33	1131
2	14	32	1539	12	29	1131
3	10	30	785	8	30	503

Note: ϕ = bar diameter, c = cover to bar centre, A_s = area of steel.

Table 4.7 Mean Values of Reinforcing Steel Properties

ϕ, mm	f_{sy}, MPa	f_{su}, MPa	f_{su}/f_{sy}	ε_{su}, %
8	630	663	1.05	1.9
10	632	674	1.07	2.2
12	623	679	1.09	2.8
14	593	631	1.06	2.7

4.6.2 Correlation of Results

Once again, each span of test specimens was analysed as a propped cantilever using the method of analysis of Chapter 3. The span was discretised into segments approximately equal to one-half of the depths of test specimens.

The correlation of test and analytical results is presented in Table 4.7 and Figure 4.9. In the tests, all specimens failed by fracture of the top reinforcement at the interior support B. The analysis also predicted the same mode of failure in all specimens.

The correlation of analytical and test results is in good agreement for Specimen 1 and 2. The researchers reported the behaviour of Specimen 3 was poor due to more pronounced scatter of the ultimate strain of steel ε_{su} (Figure 4.8). This is also reflected by the poor correlation of results in Table 4.7 and Figure 4.9 (c).

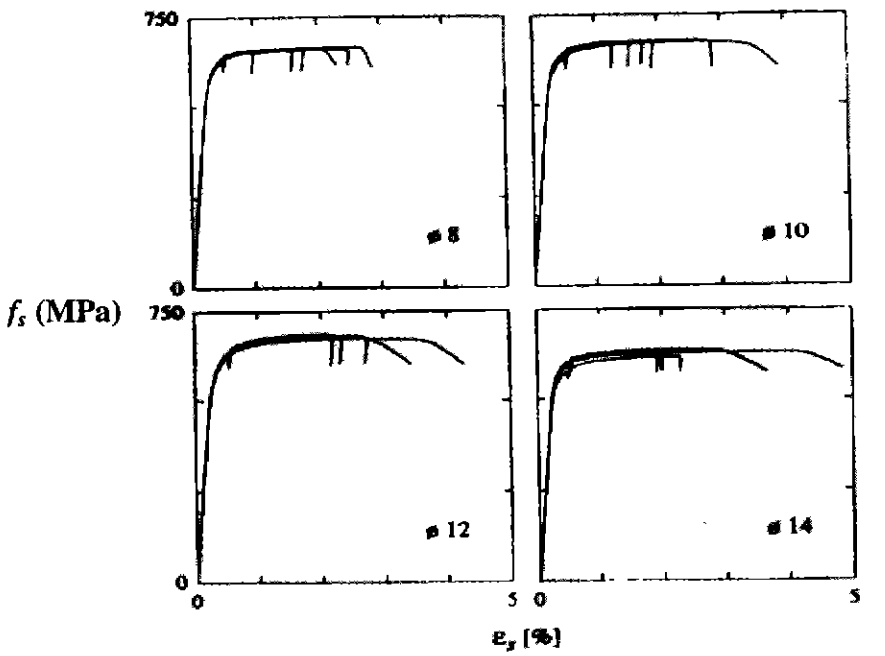

Fig. 4.9 Stress-strain Diagrams for Reinforcing Bars- Tests by Alvarez, Koppel and Marti (2000)

Table 4.8 Correlation of Test and Analytical Results: Tests by Alvarez, Koppel and Marti

Specimen Number	At Failure				
	Load, Q (kN)			Moment Redistribution (percent)	
	Test	Analysis	Test/Analysis	Test	Analysis
1	85	92.75	0.92	10.5	7.2
2	127	119.2	1.06	22.2	24.6
3	47	58 75	0.80	26.5	25.4

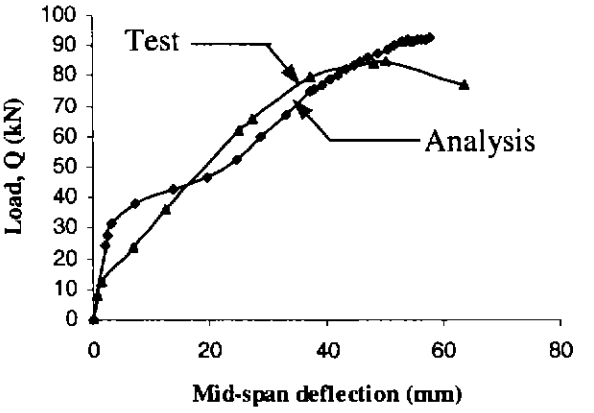

(a) Specimen 1

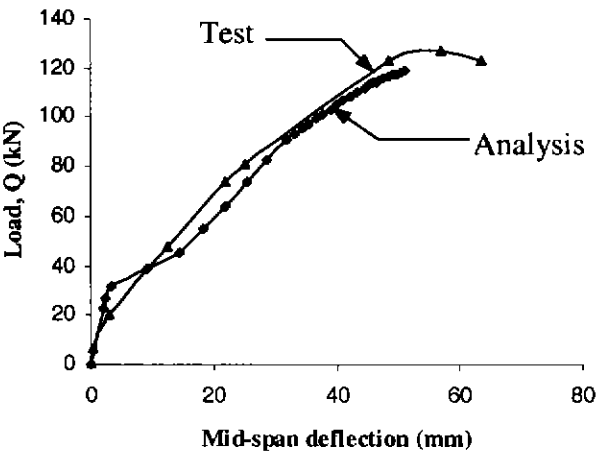

(b) Specimen 2

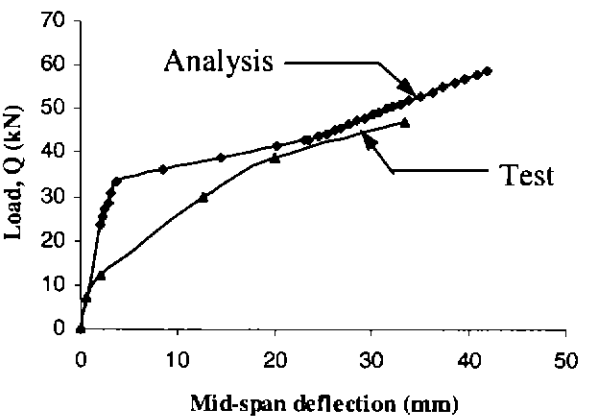

(c) Specimen 3

Fig. 4.10 Correlation of Test and Calculated Load-Deflection Curves: Tests by Alvarez, Koppel and Marti

CHAPTER 5

PARAMETRIC STUDY

5.1 Introduction

The moment redistribution allowed by AS 3600-2001 for statically indeterminate members depends on the neutral axis parameter, κ_u in the critical moment regions. According to the Standard, all the main reinforcement in a member are Class N steel and where κ_u is less or equal to 0.2 in all peak moment regions, the redistribution is not greater than 30 %. Where κ_u exceeds 0.2 in one or more peak moment regions, but does not exceed 0.4, the redistribution does not exceed $75(0.4 - \kappa_u)\%$ and where κ_u exceeds 0.4 in any peak moment region, no redistribution is allowed. Where ductility Class L reinforcement is used, moment redistribution is not permitted unless a rigorous analysis, as specified in Clause 7.6.8.1, is undertaken.

The results of the analytical study presented in Chapters 3 and 4 indicate that moment redistribution depends on many factors and not just on κ_u only.

This chapter describes a study carried out to establish the effects of various parameters on the extent of moment redistribution of reinforced concrete beams and one-way slabs. The non-linear analysis described in Chapter 3, which has shown good correlation with experimental data reported in the literature, was used for this purpose.

5.2 Parameters Selected for the Study

The parametric study was conducted for two-span continuous members subjected to uniformly distributed load with the cross-sections shown in Figures 5.1 and 5.2.

The details of Class N and Class L 500 MPa steel used in the study are as follows:

- Class N Steel 'normal ductility'

  $f_t/f_y = 1.08$ and $\varepsilon_{su} = 0.050$

- Class L Steel 'low ductility'

  $f_t/f_y = 1.03$ and $\varepsilon_{su} = 0.015$

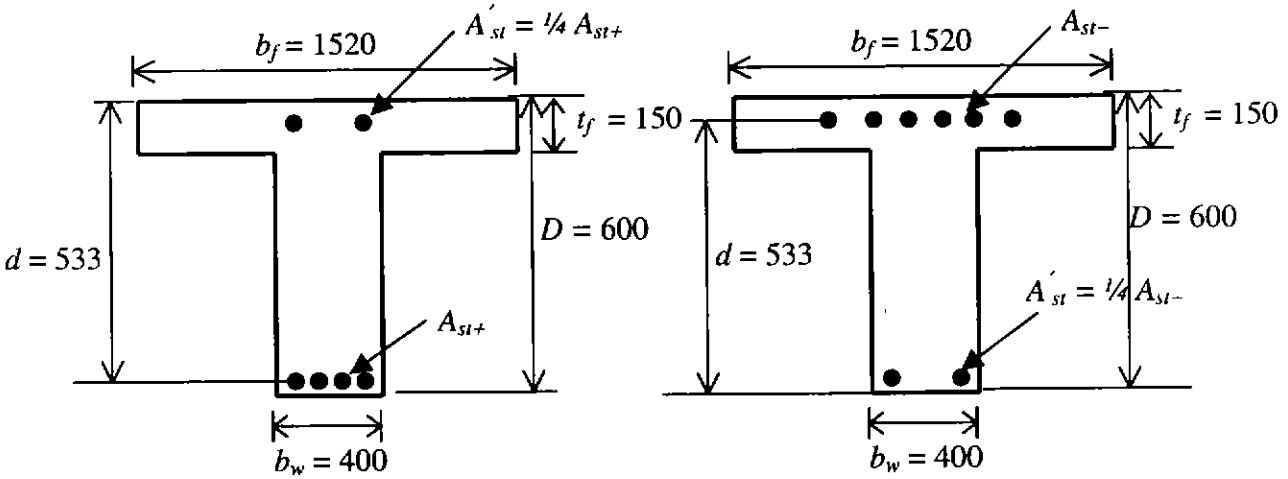

(a) Cross-section at mid-span

(b) Cross-section at support

Fig. 5.1 Cross-Sections of T-Beam (Dimensions are in mm)

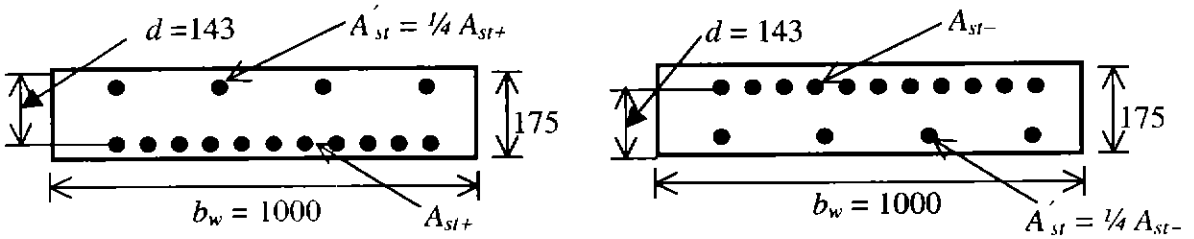

(a) Cross-section at mid-span

(b) Cross-section at support

Fig. 5.2 Cross-Sections of One-Way Slab (Dimensions are in mm)

The variables selected for the study were the ratio of neutral axis parameter at support to that value at mid-span, ultimate steel strain, and concrete compressive strength. The parameters were varied in the range they usually occur in practical beams and one-way slabs. In all cases, the compression reinforcement was taken one-quarter of the tension reinforcement. The values of the parameters used in this study are as follows:

For one-way slab:

A_{st-}/A_{st+} = 0.75, 1.0, 1.33, 1.5, 2.0

κ_{u-} = 0.1, 0.15, 0.2, 0.25, 0.3 and 0.4 (for 25 MPa concrete compressive strength)

κ_{u-} = 0.084, 0.11, 0.168, 0.2, 0.3 and 0.4 (for 30 MPa concrete compressive strength)

ε_{su} = 0.015 and 0.05

f_c' = 25, 30 MPa

l/d = 35

The minimum $\kappa_{u\pm}$ is 0.1 and 0.084 for concrete compressive strength of 25 and 30 MPa respectively (see Section 5.3)

For T-beam:

A_{st-}/A_{st+} = 0.75, 1.0, 1.33, 1.6

κ_{u-} = 0.244, 0.3, 0.35 and 0.4 (for 25 MPa concrete compressive strength)

κ_{u-} = 0.168, 0.2, 0.3 and 0.4 (for 40 MPa concrete compressive strength)

κ_{u-} = 0.136, 0.2, 0.3 and 0.4 (for 60 MPa concrete compressive strength)

ε_{su} = 0.015 and 0.05

f_c' = 25, 40 and 60 MPa

l/d = 15

The minimum values of κ_{u-} and κ_{u+} are 0.244 and 0.04 when f_c' = 25 MPa, 0.168 and 0.028 when f_c' = 40 MPa, and 0.136 and 0.0223 when f_c' = 60 MPa respectively (see Section 5.3).

Note that A_{st-}/A_{st+} = ratio of the area of tensile reinforcement over support to that at mid-span

A_{st-} = area of reinforcement in a tensile zone over support

A_{st+} = area of reinforcement in a tensile zone at mid-span

κ_{u-} = neutral axis parameter at support

κ_{u+} = neutral axis parameter at mid-span region

ε_{su} = ultimate steel strain

f'_c = concrete compressive strength

l/d = ratio of effective span length to effective depth of the cross-section

The neutral axis parameter, κ_u is the ratio of depth of neutral axis (measured from the compression zone) to effective depth.

5.3 Minimum Value of Neutral Axis Parameter

For crack control purposes, the Australian Standard AS 3600–2001 recommends that the minimum area of reinforcement in a tensile zone of a flexural member should be–

$$A_{st.min.} = 3\, k_s A_{ct}/f_s \qquad (5.1)$$

where

k_s = a coefficient that takes into account the shape of the stress distribution within the section immediately prior to cracking, as well as the effect of non-uniform self-equilibrating stresses, and is taken as 0.6

A_{ct} = the area of concrete in the tensile zone, being that part of the section in tension assuming the section is uncracked

f_s = the maximum tensile stress permitted in the reinforcement

immediately after formation of a crack, which shall be the lesser of the yield strength of the reinforcement (f_y) and the maximum steel stress given in Table 5.1 or Table 5.2 for the largest nominal diameter (d_b) of the bars in the section.

The minimum area of reinforcement in a tensile zone over support, $(A_{st.min})_-$ and that value at mid-span, $(A_{st.min})_+$ were calculated using Equation 5.1.The largest nominal diameter of the bars for the beam was taken as 20 mm and that for one-way slab was12 mm.

Table 5.1 Maximum Steel Stress for Flexure in Beams (AS 3600-2001)

Nominal bar diameter (d_b) mm	**Maximum steel stress MPa**
10	360
12	330
16	280
20	240
24	210
28	185
32	160
36	140
40	120

The neutral axis parameters corresponding to the minimum area of tensile steel are-

T-Beam:

$$(\kappa_{u-})_{\min} = \frac{(A_{st\ \min})_- \times f_y}{\alpha \times \gamma \times f_c' \times b_w \times d} \qquad (5.2)$$

and $$(\kappa_{u+})_{\min} = \frac{(A_{st\ \min})_+ \times f_y}{\alpha \times \gamma \times f_c' \times b_{ef} \times d} \qquad (5.3)$$

where α and γ are rectangular stress block parameters given by

$$\alpha = 0.85 - 0.004(f_c' - 55)$$
$$= 0.75 \le \alpha \le 0.85$$
$$\gamma = 0.85 - 0.008(f_c' - 30)$$
$$= 0.65 \le \gamma \le 0.85$$

One-way Slab:

$$(\kappa_{u\pm})_{\min} = \frac{A_{st.\min} \times f_y}{\alpha \times \gamma \times f_c' \times b \times d} \qquad (5.4)$$

The values of κ_u selected in the parametric study were not less than the minimum values given by Equations 5.2, 5.3, or 5.4, as appropriate.

Table 5.2 Maximum Steel Stress for Flexure in Slabs (AS 3600-2001)

Nominal bar diameter (d_b) mm	**Maximum steel stress (MPa) for overall depth, D_s, (mm) of:**	
	≤ 300	**≥ 300**
6	375	450
8	345	400
10	320	360
12	300	330
16	265	280
20	240	
24	210	

5.4 Moment Redistribution

The percentage of moment redistribution β was calculated as follows:

$$\beta = (1 - \frac{M_{(u.fail)^-}}{M_{EL}})100(\%) \qquad (5.5)$$

where

$M_{(u.fail)}^-$ = ultimate support moment at failure

M_{EL} = support moment calculated by elastic analysis for the failure load

5.5 Presentation and Discussion of Results

Calculations were performed using the method of analysis presented in Chapter 3. Some typical results are shown in Figures 5.3 to 5.11. Comprehensive data obtained from parametric study are given in Appendix A to C.

5.5.1 Effect of A_{st-}/A_{st+}

The effect of A_{st-}/A_{st+} on moment redistribution is shown in Figures 5.3 and 5.4 for T-beams and in Figures 5.5 and 5.6 for one-way slabs when $f_c' = 25$ MPa for N and L type steel. Other similar results are given in Appendix C. These results show that the moment redistribution increases when A_{st-}/A_{st+} decreases. Smaller value of A_{st-}/A_{st+} means that the moment capacity of the support section M_{u-} is smaller than that of the mid-span section. The first hinge develops at the support section and large failure load needed to reach the moment capacity of the mid-span section. For such a large failure load, the elastic analysis will yield a large value of M_{EL} at the support. A combination of relatively small value of M_{u-} and large value of M_{EL} means, accordingly to Equation 5.5, a large value of percentage of moment redistribution β.

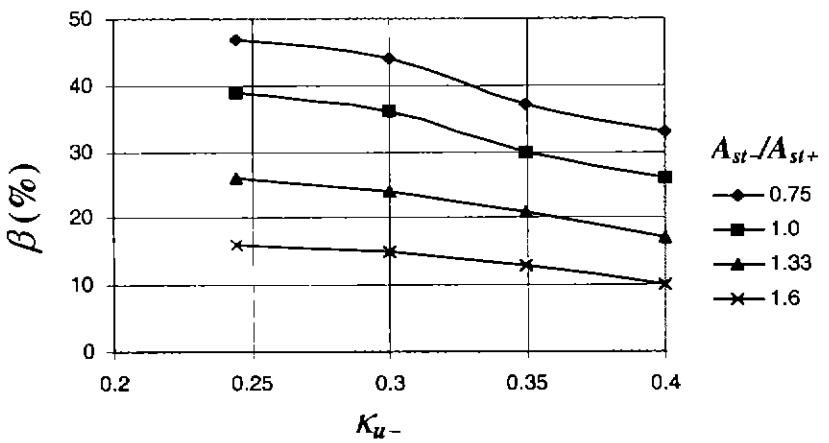

Fig. 5.3 T-beam: Effect of A_{st-}/A_{st+} on Degree of Moment Redistribution for Steel N ($l/d = 15, f_c' = 25$ MPa)

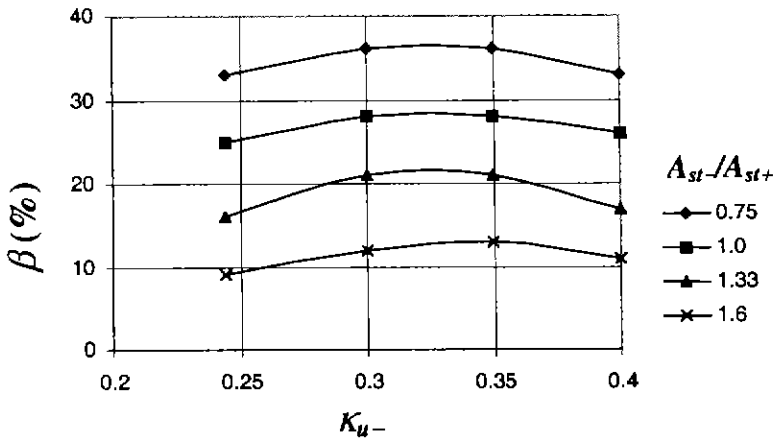

Fig. 5.4 T-beam: Effect of A_{st-}/A_{st+} on Degree of Moment Redistribution for Steel L (l/d = 15, f_c' = 25 MPa)

On the other hand, when A_{st-} is greater than the A_{st+}, moment capacity of the positive critical section is less than that of the support section. In this case, after the formation of first hinge at the support, the load increases only marginally to reach the moment capacity at mid-span. The failure load, therefore, may not be much larger than the load at which the first hinge developed. The net effect is that M_u/M_{EL} is large and hence the effect of moment redistribution β is small (Equation 5.5).

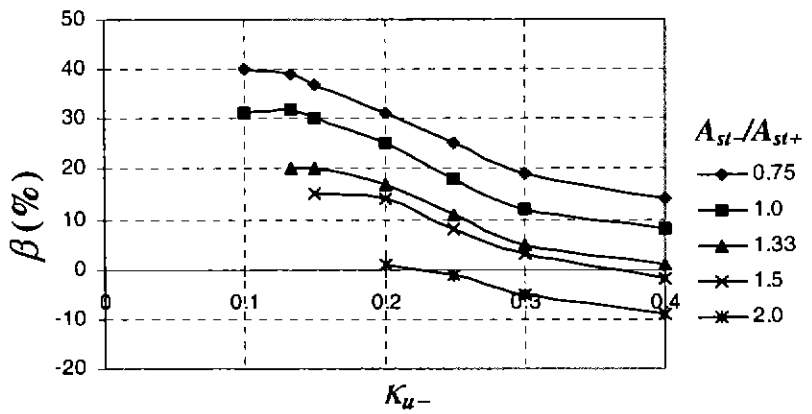

Fig. 5.5 One-way slab: Effect of A_{st-}/A_{st+} on Degree of Moment Redistribution for Steel N (l/d = 35, f_c' = 25 MPa)

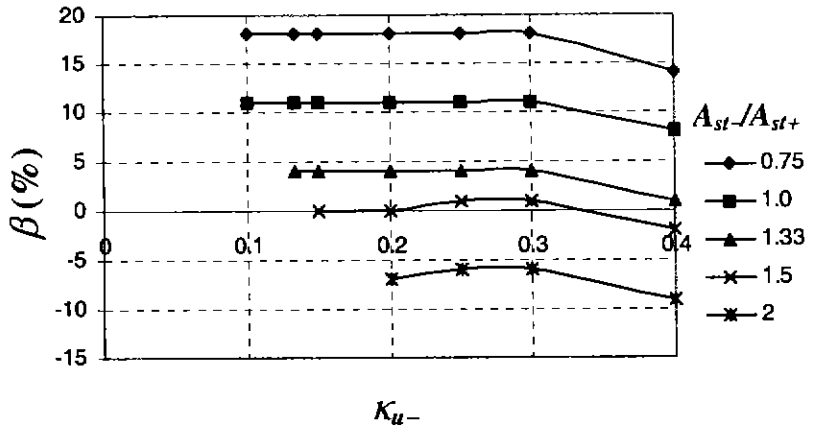

Fig. 5.6 One-way slab: Effect of A_{st-}/A_{st+} on Degree of Moment Redistribution for Steel L ($l/d = 35, f'_c = 25$ MPa)

5.5.2 Effect of Ultimate Steel Strain (ε_{su})

Figures 5.7 and 5.8 show the effect of ultimate steel strain on moment redistribution. Similar results for one-way slabs and T-beams with the other values of A_{st-}/A_{st+} are given in Figures C10 to C29 in Appendix C. When failure is due to concrete crushing there is no effect of ultimate steel strain on moment redistribution. Obviously, the moment redistribution for Class L steel is much smaller than that for Class N steel.

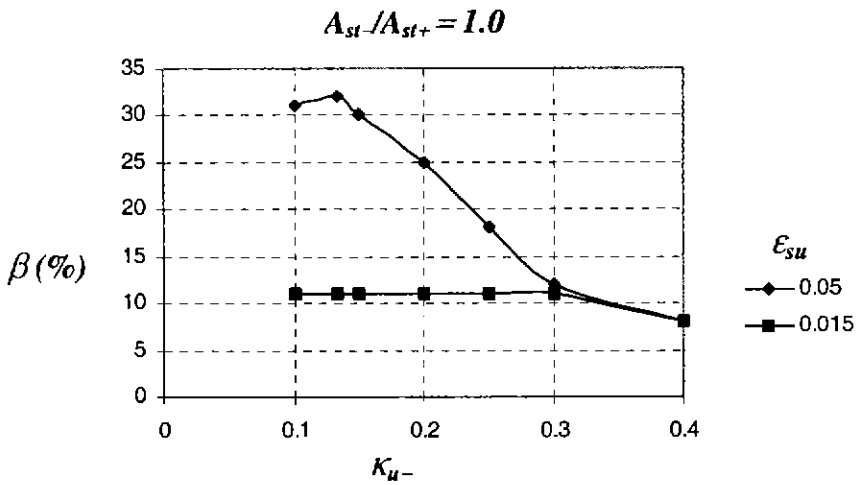

Fig. 5.7 One-way slab: Variation of Moment Redistribution with Ultimate Steel Strain (l/d = 35 and f'_c = 25 MPa)

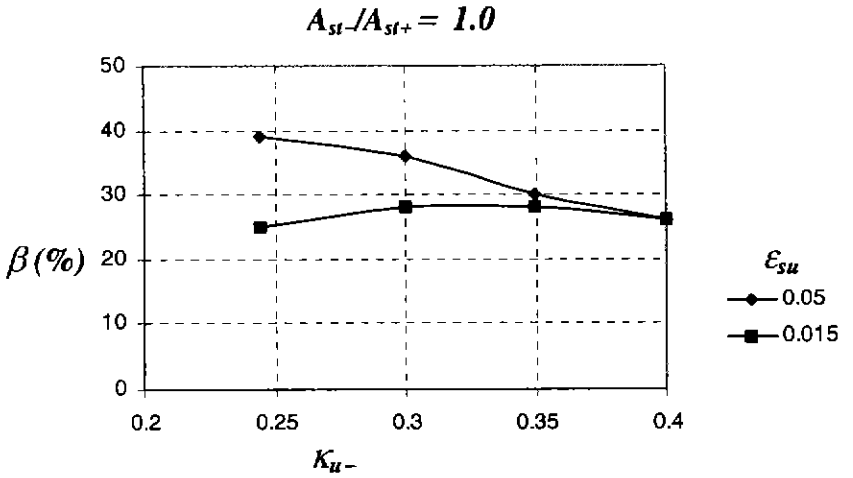

Fig. 5.8 T-beam: Variation of Moment Redistribution with Ultimate Steel Strain (l/d = 15 and f_c' = 25 MPa)

Figures 5.9 shows that for Class N steel, premature failure by steel fracture occurs when K_{u-} = 0.133 and for Class L steel, steel fractures when K_{u-} = 0.3 when f_c' = 25 MPa. Similar results given in Figures C7 to C9 in Appendix C, show that steel fracture occurs for Class N steel when K_{u-} is 0.1, 0.075 and 0.05 and for Class L steel, when K_{u-} is 0.27, 0.24 and 0.2, respectively, for f_c' = 30 MPa, 40 MPa, or 60 MPa.

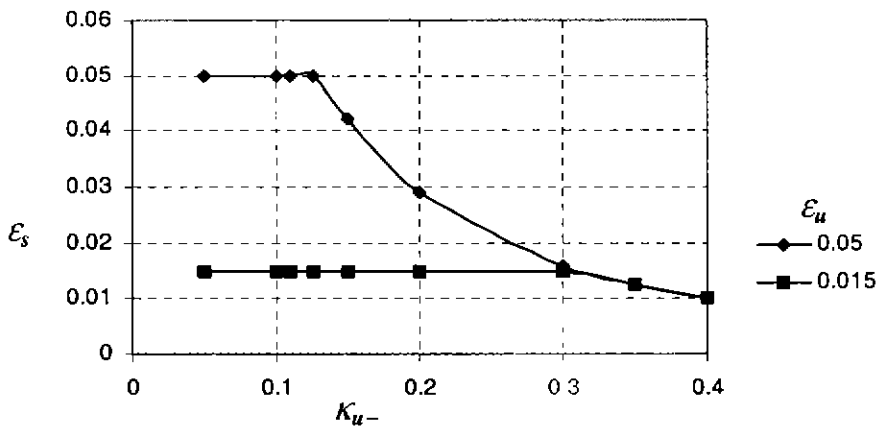

Fig. 5.9 Variation of Steel Strain at Failure with Neutral Axis Parameter at Support Section (f_c' = 25 MPa)

The results of parametric study therefore show that the ultimate steel strain should be more than 0.05 to produce failure by concrete crushing rather than steel fracture when f_c' is low and the member is lightly reinforced.

5.5.3 Effect of Concrete Strength (f_c')

Figures 5.10 and 5.11 illustrate that the effect of concrete strength on moment redistribution for one-way slabs and T-beams. Similar results are shown in Figures C30 to C36 in Appendix C. It can be seen from the Figures that the moment redistribution decreases with the increase of concrete strength.

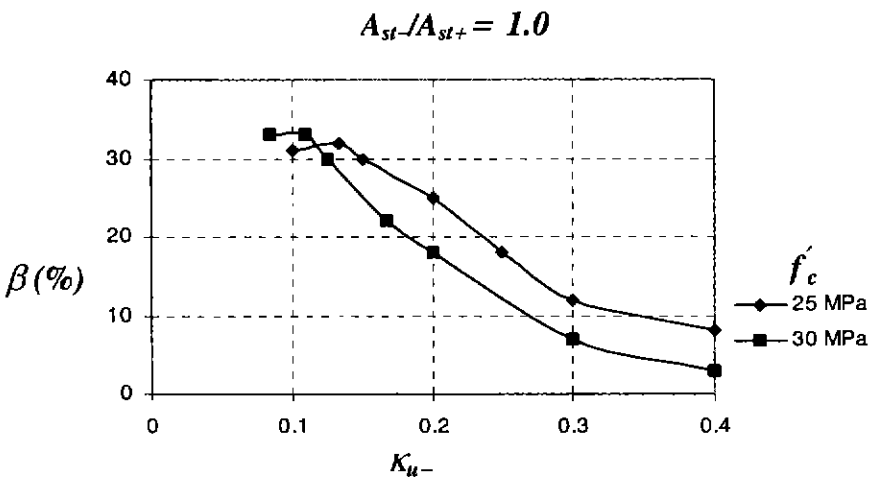

Fig. 5.10 One-way slab: Variation of Moment Redistribution with Concrete Compressive Strength (l/d = 35 and ε_{su} = 0.05)

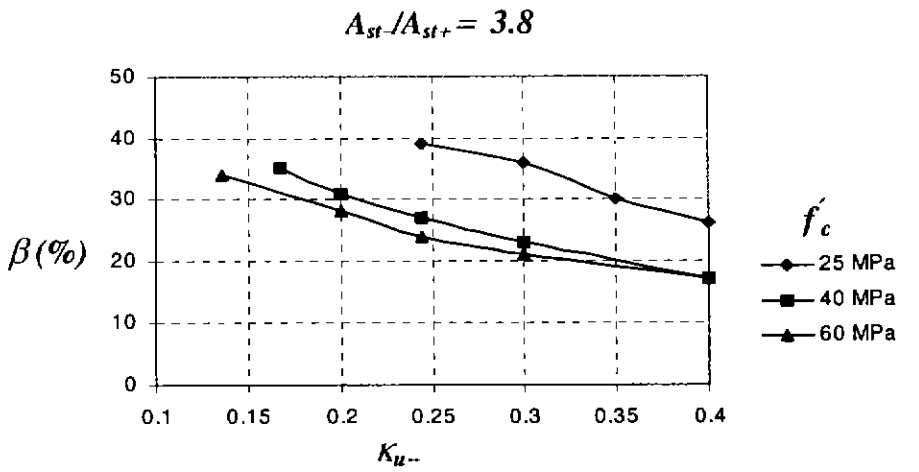

Fig. 5.11 T-beam: Variation of Moment Redistribution with Concrete Compressive Strength (l/d = 15 and ε_{su} = 0.05)

5.6 Summary

In summery, the extent of moment redistribution in T-beams and one-way slabs significantly varies with A_{st-}/A_{st+}, κ_{u-}, f'_c and ε_{su}. The results of the parametric study presented in Figures in this Chapter and Appendix C may be used to develop design proposals. The outcomes of parametric study are as follows:

i) Moment redistribution increases with decrease of A_{st-}/A_{st+}, although the strength of beam or slab increases significantly with increase of A_{st-}/A_{st+}

ii) Moment redistribution increases with increase of in steel ductility. When steel fracture is dominant rather than concrete crushing, with the increase in steel ductility, the moment redistribution increases significantly.

iii) In case of lightly reinforced flexural members, ultimate steel strain (ε_{su}) should be more than 0.05 to produce failure by concrete crushing rather than steel fracture. This is especially true when concrete compressive strength is low.

iv) Premature failure occurs by the fracture of the reinforcing steel in lightly reinforced regions, particularly when Class L reinforcement is used.

v) Increase in concrete compressive strength decreases the degree of moment redistribution. With increase of concrete compressive strength, strength of beams and slabs increases significantly but moment redistribution decreases significantly due to premature failure by concrete crushing rather than steel fracture.

CHAPTER 6

SUMMARY, CONCLUSIONS AND RECOMMENDATIONS

6.1 Summary

Steel reinforcement characterising yield stress of 500 MPa has been adopted as a standard for the production of Australian reinforcing steels. Two main ductility classifications (Classes L and N for Low and Normal ductility, respectively) define minimum acceptable values for the uniform elongation (strain at peak stress) and tensile-to-yield stress ratio of the reinforcement. Although 500 MPa steel possess higher strength than 400 MPa hot-rolled reinforcement traditionally used in reinforced concrete structures, it is less ductile.

In developing new design provisions for the use of 500 MPa steel reinforcement, Australian Standard AS 3600 restricted the use of Class L steel in flexural members in situations where significant amounts of moment redistribution can occur. In the present Australian concrete design standard, AS 3600-2001, the neutral axis parameter κ_u is used as a convenient, but approximate, measure of available ductility in high moment region of a flexural member.

A detailed literature survey showed that there is limited information available regarding the design provisions for the moment redistribution. This research work was, therefore, conducted to establish the moment redistribution that occurs in T-beams and one-way slabs using 500 MPa steel reinforcement.

An iterative numerical procedure was developed to analyse reinforced two span continuous concrete T-beams and one-way slabs taking the material and geometrical non-linearities into account. The deflected shape of the beam and one-way slab was calculated by dividing the span length into a number of rigid segments. The entire

numerical method was implemented in a computer program written in FORTRAN language so that any change for a specific purpose could be made. The program calculates the failure load and deflection with the geometrical and material properties of beam and one-way slab as input data. The analytical method was compared with the test results reported in the literature. The results for load-deflection graphs and moment redistribution showed a good agreement between analytical and test results.

In order to understand the effect of different parameters on moment redistribution of T-beams and one-way slabs, a parametric study was conducted using the proposed analytical method. The ratio of the area of support to span tensile reinforcement (A_{st-}/A_{st+}), ultimate steel strain (ε_{su}), and concrete compressive strength (f'_c) were included in this study as variables. The results are presented in numerous graphs

6.2 Conclusions

Based on the research reported in the thesis, the following conclusions are drawn:

1. The effect of the ratio tensile reinforcements (A_{st-}/A_{st+}) on the moment redistribution is significant; moment redistribution increases with the decrease of A_{st-}/A_{st+}

2. Increase in concrete compressive strength decreases the degree of moment redistribution.

3. As expected, the ductility of a peak moment region of a beam or one-way slab depends on the quantity, properties and arrangement of the reinforcing steel as well as concrete compressive strength. Highly reinforced regions failed by premature crushing of the concrete in the compression zone.

4. Premature failure occurs by the fracture of the reinforcing steel in lightly reinforced regions, particularly when Class L reinforcement is used.

5. In case of lightly reinforced flexural members, ultimate steel strain (ε_{su}) should be more than 0.05 to produce failure by concrete crushing rather than steel failure. This is especially true when concrete compressive strength is low.

6. Only the neutral axis parameter (κ_u) as a measure of extent of moment redistribution as recommended by AS 3600 is inadequate. Data presented in Figures 5.3 to 5.11 and Figures C1 to C36 in Appendix C is useful to estimate the degree of moment redistribution in reinforced concrete beams and one-way slabs.

6.3 Recommendations for Further Work

Although this research work provided some important information regarding the strength and ductility of reinforced concrete beams and one-way slabs using 500 MPa steel, questions regarding some other issues are yet to be answered. Therefore, the following further works are recommended:

1. Comprehensive experimental work is needed to study the effect of the ratio of tensile reinforcements (A_{st-}/A_{st+}), steel ultimate strain (ε_{su}), and concrete compressive strength (f_c') on moment redistribution.

2. More analytical work should be carried out on other forms of statically indeterminate structures such as frames and two-way slabs to evaluate the effect of the ratio of tensile reinforcements (A_{st-}/A_{st+}), steel ultimate strain (ε_{su}) and concrete compressive strength (f_c') on moment redistribution.

3. Based on the extensive analytical data, simple design rules should be developed.

REFERENCES

ACI-ASCE Committee 428, "Progress Report on Code Clauses for Limit Design", ACI Journal of the American Concrete Institute, Vol. 65, No. 9, September 1968, pp. 713-715.

ACI Committee 439, "Uses and Limitations of High Strength Steel Reinforcement", Journal of the American Concrete Institute, ACI Proceedings, Vol. 70, No. 2, February 1973, pp.77-104.

Alvarez, M., Köppel, S. and Marti, P., "Rotation Capacity of Reinforced Concrete Slabs" ACI Structural Journal, March-April 2000, pp.235-242.

Baker, A.L.L. and Amarakone, A.M.N., "Inelastic Hyperstatic Frame Analysis", Proceedings International Symposium on the Flexural Mechanics of Reinforced Concrete, Miami, ACI SP-12, 1964, pp. 85-142.

Beeby, A.W., "Ductility in Reinforced Concrete: Why is it Needed and How is it Achieved?" The Structural Engineer, 75 (18), September 1997, pp.311-318.

Chick, C., Patrick, M. and Wong, K., "Ductility of Reinforced-Concrete Beams and Slabs, and AS 3600 Design Requirements", Concrete 99, Concrete Institute of Australia, May 1999, pp.570-578.

Calvi, G.M., Cantù, E., Macchi, G. and Magenese, G., "Rotation Capacity of RC Slabs as a Function of Steel Properties", CEB Bulletin d'Information No.218, August 1993, pp.45-63.

Collins, M.P., Mitchell, D. and Macgregor, J.G., "Structural Design Considerations for High-Strength Concrete", ACI Concrete International, May 1993, pp.27-34.

Corley, W.G., "Rotational Capacity of Reinforced Concrete Beams", Journal of the Structural Division, ASCE, Vol. 92, No. ST5, October 1966, pp. 121-126.

Cosenza, E., Greco, C. and Pecca, M, "Nonlinear Design of Reinforced Concrete Continuous Beam", Structural Engineering International, No.1/91, 1991, pp.19-27.

Eligehausen, R. and Fabritius, E., "Tests on Continuous Slabs Reinforced with Welded Wire Mesh", CEB Bulletin d'Information No.218, August 1993, pp.133-148.

Gilbert, R.I., "The Impact of 500 MPa Reinforcement on the Ductility of Concrete Structures-Revision of AS 3600", Proceedings of the 20th Biennial Conference of the Concrete Institute of Australia, Perth, 11 – 14 September 2001, pp.597-6561.

Gravina, R.J. and Warner, R.F., "Moment Re-distribution in Indeterminate RC Beams and Slabs Constructed with 500 MPa Grade, Class L and Class N Reinforcing Steel", Proceedings of the 20th Biennial Conference of the Concrete Institute of Australia, Perth, 11 – 14 September 2001, pp.613-618.

I.C.E. Research Committee, "Ultimate Load Design of Concrete Structures", Proceedings I.C.E. (London), Vol. 21, February 1962, pp. 399-442.

Mattock, A.H., "Rotational Capacity of Hinging Regions in Reinforced Concrete Beams." Proceedings International Symposium on the Flexural Mechanics of Reinforced Concrete, Miami, ACI SP-12, 1964, pp. 143-181.

Patrick, M., Akbarshahi, E. and Warner, R.F, "Ductility Limits for the Design of Concrete Structures Containing High-Strength, Low-Elongation Steel Reinforcement", Concrete 97, Concrete Institute of Australia, May 1997,pp.65-71.

Patrick, M., Turner, M. and Warner, R., "Utilisation of Ductility of 500 MPa Steel Reinforcement in Reinforced-Concrete Structures Designed to AS 3600-2001", Concrete Institute of Australia, Perth, Conference Proceedings, Perth, 11 – 14 September 2001, pp.613-618.

Pisanty, A. and Regan, P.E., "Redistribution of Moments and the Possible Demand for Ductility", CEB Bulletin d'Information No.218, August 1993, pp.149-162.

Popovics, S., "A Numerical Approach to the Complete Stress-Strain Curves of Concrete", Cement and Concrete Research, Vol. 3, No. 5, September 1973, pp.583-599.

Pulmano, V.A. and Shin, Y.S., "Simplified Finite-Element Analysis of Deflections of Reinforced Concrete Beams", ACI Structural Journal, July-Augaust 1987, pp.342-348.

Russwurm, D., "Steel Properties and Plastic Behaviour of Reinforced Concrete Constructions", CEB Bulletin d'Information No.218, August 1993, pp.199-221.

Standards Australia, "Amendment No.1 to AS3600-1994", AS3600/Amdt/1996-08-05, August 1996.

Standards Australia, (Committee BD/2), " Progress Report, Working Group 1 – Ductility", BD/2/98-5. February 1998

Standards Australia, "Concrete Structures", Australian Standard AS 3600-2001, Sydney, 2001, pp.176.

Stolze, R, Bühler, A and Eibl. J., "Rotational Behaviour of reinforced Concrete Slabs", CEB Bulletin d'Information No.218, August 1993, pp.65-118.

Tse, D. and Darvall, P.LeP., "Softening Hinges in Reinforced Concrete Beams", Proceedings First National Structural Engineering Conference, The Institute of Engineers, Melbourne, Australia, August, pp. 483-488

Appendix A

Results of Parametric Study – One-Way Slabs

Table SA1 $f'c$ **= 25 MPa,** l/d **= 35,** ε_{su} **= 0.05**

K_{u-}	A_{st-}	A_{st+}	Q_{PL} (kN)	Q_{FL} (kN)	Q_{FL}/Q_{PL}	$M_{(u,fail)}^{-}$ (kNm)	$M_{(u,fail)}^{+}$ (kNm)	Failure Region (C/S)	β (%)
0.1	516.6	516.6	87.1	80.8	0.93	34.6	34.7	Support (S)	31
0.1	516.6	678.1	104.9	91.7	0.87	34.6	41.25	Support (S)	40
0.133	678.1	516.6	93.9	88	0.94	44	35.2	Support (S)	20
0.133	678.1	678.1	111.7	103.1	0.92	44	44.3	Support (S)	32
0.133	678.1	929.9	136	115.6	0.85	44	51.9	Support (S)	39
0.15	774.9	516.6	97.5	91.5	0.94	48.8	35.3	Support (C)	15
0.15	774.9	578.6	103.9	97.5	0.94	48.8	38.9	Support (C)	20
0.15	774.9	774.9	123.9	111.7	0.90	48.8	47.5	Support (C)	30
0.15	774.9	1033.2	149.6	124.1	0.83	48.8	55	Support (C)	37
0.2	1033.2	516.6	107.5	100.2	0.93	62.3	35	Support (C)	1
0.2	1033.2	678.1	125.2	113.6	0.91	61.2	43.65	Support (C)	14
0.2	1033 2	774.9	133.9	118	0.88	61.2	46.3	Support (C)	17
0.2	1033 2	1033.2	159.6	129.7	0.81	61.2	53.3	Support (C)	25
0.2	1033 2	1379.3	192.6	141.7	0.74	61.2	60 6	Support (C)	31
0.25	1219.5	645.7	130.5	122.2	0.94	77.1	42 6	Support (C)	-1
0.25	1219.5	862.7	152.4	131.9	0.87	75.6	49	Support (C)	8
0.25	1219.5	971.2	163.2	136.5	0.84	75.6	51.8	Support (C)	11
0.25	1219.5	1219.5	194.1	148	0.76	75.6	58.6	Support (C)	18
0.25	1219.5	1704.7	233.5	161.6	0.69	75.6	66.7	Support (C)	25
0.3	1549.8	774.9	153	140.9	0.92	92.9	47.9	Support (C)	-5
0.3	1549.8	1033.2	178.6	152.1	0.85	92.5	54.4	Support (C)	3
0.3	1549.8	1162.3	191.1	156.5	0.82	92.5	57	Support (C)	5
0.3	1549.8	1549.8	227.4	169	0.74	92.5	64.5	Support (C)	12
0.3	1549.8	2066.4	272.8	182.7	0.67	92.5	72.6	Support (C)	19
0.4	2066.4	1033.2	196.3	176.1	0.90	120.3	58.5	Support (C)	- 9
0.4	2066.4	1379.3	229.4	188.3	0.82	119.5	65.6	Support (C)	- 2
0.4	2066.4	1549.8	245.1	193.9	0.79	119.5	68.8	Support (C)	1
0.4	2066.4	2066.4	290.6	207.6	0.71	119.5	77	Support (C)	8
0.4	2066.4	2753.4	346.2	223	0.64	119.5	86	Support (C)	14

Note:
Support (S) – Support failure by steel fracture.
Support (C) – Support failure by concrete crushing.

Table SA2 $f'c = 25$ MPa, $l/d = 35$, $\varepsilon_{su} = 0.015$

K_{u-}	A_{st-}	A_{st+}	Q_{PL} (kN)	Q_{FL} (kN)	Q_{FL}/Q_{PL}	$M_{(u,fail)}^{-}$ (kNm)	$M_{(u\,fail)}^{+}$ (kNm)	Failure Region (C/S)	β (%)
0.1	516.6	516.6	88.4	66.8	0.76	37.2	25.2	Support (S)	11
0.1	516.6	678.1	106	72.6	0.68	37.2	28.7	Support (S)	18
0.133	678.1	516.6	95.3	80.3	0.84	48.2	29	Support (S)	4
0.133	678.1	678.1	112.9	87.1	0.77	48.2	33	Support (S)	11
0.133	678.1	929.9	137.3	93.9	0.68	48.2	37	Support (S)	18
0.15	774.9	516.6	98.8	86.1	0.87	53.6	30.36	Support (S)	0
0.15	774.9	578.6	105.2	88.9	0.85	53.6	31.96	Support (S)	4
0.15	774.9	774.9	125.3	95.9	0.76	53.6	35.9	Support (S)	11
0.15	774.9	1033.2	150.9	103.6	0.69	53.6	40.7	Support (S)	17
0.2	1033.2	516.6	108.7	101.7	0.94	68.3	33.9	Support (S)	- 7
0.2	1033.2	678.1	126.3	109.8	0.87	68.3	38.7	Support (S)	0
0.2	1033.2	774.9	135.2	112.8	0.83	68.3	40.4	Support (S)	3
0.2	1033.2	1033.2	160.8	122.2	0.76	68.3	45.9	Support (S)	11
0.2	1033.2	1379.3	193.9	131.7	0.68	68.2	51.7	Support (S)	17
0.25	1219.5	645.7	131.8	122.9	0.93	81.6	41.5	Support (S)	- 7
0.25	1219.5	862.7	153.7	131.9	0.86	81.6	46.8	Support (S)	1
0.25	1219.5	971.2	164.4	136.3	0.83	81.6	49.4	Support (S)	4
0.25	1219.5	1219.5	195.3	146.5	0.75	81.6	55.4	Support (S)	11
0.25	1219.5	1704.7	234.5	158.7	0.68	81.6	62.6	Support (S)	18
0.3	1549.8	774.9	154.2	142.1	0.92	94.2	47.95	Support (S)	- 6
0.3	1549.8	1033.2	179.8	153.0	0.85	94.2	54.5	Support (S)	1
0.3	1549.8	1162.3	192.3	157.5	0.82	94.2	56.97	Support (S)	4
0.3	1549.8	1549.8	228.5	170.1	0.74	94.2	64.4	Support (S)	11
0.3	1549.8	2066.4	273.9	183.5	0.67	94.2	72.4	Support (S)	18
0.4	2066.4	1033.2	197.6	177.8	0.90	121.2	58.8	Support (C)	- 9
0.4	2066.4	1379.3	230.5	189.2	0.82	120.3	65.9	Support (C)	- 2
0.4	2066.4	1549.8	246.2	194.8	0.79	120.3	69.1	Support (C)	1
0.4	2066.4	2066.4	291.6	208.5	0.72	120.3	77.2	Support (C)	8
0.4	2066.4	2753.4	347.2	223.8	0.64	120.3	86.3	Support (C)	14

Note:
Support (S) – Support failure by steel fracture.
Support (C) – Support failure by concrete crushing.

Table SB1 $f'c = 30$ MPa, $l/d = 35$, $\varepsilon_{su} = 0.05$

K_{u-}	A_{st-}	A_{st+}	Q_{PL} (kN)	Q_{FL} (kN)	Q_{FL}/Q_{PL}	$M_{(u.fail)}^{-}$ (kNm)	$M_{(u.fail)}^{+}$ (kNm)	Failure Region (C/S)	β (%)
0.084	520.7	520.7	89.3	81.1	0.91	34	35.1	Support (S)	33
0.084	520.7	694.3	107.5	91.7	0.85	34	41.6	Support (S)	41
0.11	681.9	520.7	95.9	87.8	0.92	42.8	35.6	Support (C)	22
0.11	681.9	681.9	112.8	101.8	0.90	42.8	44.1	Support (C)	33
0.11	681.9	929.9	138.3	113.84	0.82	42.8	51.3	Support (C)	40
0.126	781.1	520.7	99.9	90.7	0.91	47.7	35.5	Support (C)	16
0.126	781.1	588.9	107.1	97	0.91	47.7	39.3	Support (C)	21
0.126	781.1	781.1	127.1	108.4	0.85	47.7	46.2	Support (C)	30
0.126	781.1	1041.4	153.5	120.3	0.78	47.7	53.4	Support (C)	37
0.168	1041.4	520.7	110.2	100.8	0.91	62.7	35.6	Support (C)	0
0.168	1041.4	694.3	128.4	114.4	0.89	62.7	43.5	Support (C)	12
0.168	1041.4	781.1	137.4	117.9	0.86	62.7	45.7	Support (C)	15
0.168	1041.4	1041.4	163.8	129.2	0.79	62.7	52.4	Support (C)	22
0.168	1041.4	1388.6	197.8	141.3	0.71	62.7	59.7	Support (C)	29
0.2	1239.8	619.9	128.3	117.8	0.92	74.5	66.7	Support (C)	- 1
0.2	1239.8	824.5	149.5	128.5	0.86	74	47.6	Support (C)	8
0.2	1239.8	929.9	160.2	133.5	0.83	74	50.5	Support (C)	11
0.2	1239.8	1239.8	191	144.6	0.76	74	57.15	Support (C)	18
0.2	1239.8	1655.1	230.6	158.1	0.69	74	65.3	Support (C)	25
0.3	1859.7	929.9	183	164	0.90	112.5	54.1	Support (C)	- 10
0.3	1859.7	1239.8	213.8	175.5	0.82	112.5	60.8	Support (C)	- 3
0.3	1859.7	1394.8	228.8	180.9	0.79	112.5	63.95	Support (C)	0
0.3	1859.7	1859.7	272.2	194.3	0.71	112.5	71.9	Support (C)	7
0.3	1859.7	2479.6	326.5	208.6	0.64	112.5	80.4	Support (C)	14
0.4	2479.6	1239.8	235	208.8	0.89	147.6	67.12	Support (C)	- 13
0.4	2479.6	1655.1	274.6	223.1	0.81	147.6	75.4	Support (C)	- 6
0.4	2479.6	1859.7	293.4	228.8	0.78	147.6	78.7	Support (C)	- 3
0.4	2479.6	2479.6	347.6	244.2	0.70	147.6	87.8	Support (C)	3
0.4	2479.6	3304.1	413.8	260.9	0.63	147.6	97.6	Support (C)	9

Note:
Support (S) – Support failure by steel fracture.
Support (C) – Support failure by concrete crushing.

Table SB2 $f'c$ = 30 MPa, l/d = 35, ε_{su} = 0.015

K_{u-}	A_{st-}	A_{st+}	Q_{PL} (kN)	Q_{FL} (kN)	Q_{FL}/Q_{PL}	$M_{(u.fail)}^{-}$ (kNm)	$M_{(u.fail)}^{+}$ (kNm)	Failure Region (C/S)	β (%)
0.084	520.7	520.7	90.5	68.5	0.76	37.9	26.1	Support (S)	11
0.084	520.7	694.3	108.96	73.4	0.67	37.9	28.7	Support (S)	17
0.11	681.9	520.7	97.3	81.4	0.84	48.6	29.6	Support (S)	4
0.11	681.9	681.9	114.3	87.2	0.76	48.6	32.6	Support (S)	11
0.11	681.9	929.9	139.7	93.9	0.67	48.6	36.9	Support (S)	17
0.126	781.1	520.7	101.3	88.4	0.88	55	31.5	Support (S)	0
0.126	781.1	588.9	108.5	91.2	0.84	55	32.7	Support (S)	4
0.126	781.1	781.1	128.5	97.8	0.76	55	36.5	Support (S)	10
0.126	781.1	1041.4	154.9	105.7	0.68	55	41.4	Support (S)	17
0.168	1041.4	520.7	111.6	104.4	0.94	70.2	34.9	Support (S)	- 8
0.168	1041.4	694.3	129.9	112.5	0.87	70.2	39.6	Support (S)	0
0.168	1041.4	781.1	138.8	115.5	0.83	70.2	41.3	Support (S)	3
0.168	1041.4	1041.4	165.2	124.9	0.76	70.2	46.9	Support (S)	10
0.168	1041.4	1388.6	199.1	134.8	0.68	70.2	72.85	Support (S)	17
0.2	1239.8	619.9	129.7	119.5	0.92	80.4	40.2	Support (S)	- 8
0.2	1239.8	824.5	150.9	128.9	0.85	80.4	45.4	Support (S)	0
0.2	1239.8	929.9	161.6	133.3	0.82	80.4	48	Support (S)	3
0.2	1239.8	1239.8	192.4	143.3	0.74	80.4	53.9	Support (S)	10
0.2	1239.8	1655.1	231.9	155.4	0.67	80.4	61.13	Support (S)	17
0.3	1859.7	929.9	184.4	165.1	0.90	113.4	54.3	Support (C)	- 10
0.3	1859.7	1239.8	215.2	176.7	0.82	113.4	61.1	Support (C)	- 3
0.3	1859.7	1394.8	230.1	182	0.79	113.4	64.15	Support (C)	0
0.3	1859.7	1859.7	273.5	195.5	0.71	113.4	72.1	Support (C)	7
0.3	1859.7	2479.6	327.7	209.9	0.64	113.4	80.6	Support (C)	14
0.4	2479.6	1239.8	236.3	209.6	0.89	148.3	67.4	Support (C)	- 13
0.4	2479.6	1655.1	275.9	224	0.81	148.3	75.7	Support (C)	- 6
0.4	2479.6	1859.7	294.7	229.8	0.78	148.3	79 1	Support (C)	- 3
0.4	2479.6	2479.6	348.9	245.1	0.70	148.3	88	Support (C)	3
0.4	2479.6	3304.1	415	261.9	0.63	148.3	97 9	Support (C)	9

Note:
Support (S) – Support failure by steel fracture.
Support (C) – Support failure by concrete crushing.

Appendix B

Results of Parametric Study – T–Beams

Table TA1 $f'c$ = 25 MPa, l/d = 15, ε_{su} = 0.05

K_{u-}	A_{st-}	A_{st+}	Q_{PL} (kN)	Q_{FL} (kN)	Q_{FL}/Q_{PL}	$M_{(u,fail)}^{-}$ (kNm)	$M_{(u,fail)}^{+}$ (kNm)	Failure Region (C/S)	β (%)
0.244	1879.3	1170.7	556.9	494	0.89	416.8	308.6	Support (C)	16
0.244	1879.3	1404.8	617.3	552.8	0.90	410.1	366.6	Support (C)	26
0.244	1879.3	1873.1	737.9	665.7	0.90	405.2	478.5	Support (C)	39
0.244	1879.3	2487.7	894.6	781	0.87	416.8	587.4	Support (C)	47
0.3	2310.6	1434.1	662.8	600.8	0.91	513 6	371.9	Support (C)	15
0.3	2310.6	1726.8	737.8	668.1	0.91	508 9	436.8	Support (C)	24
0.3	2310.6	2326.7	891.8	769.2	0.86	494 9	547	Support (C)	36
0.3	2310.6	3073	1079	867.2	0.80	485.4	627.5	Support (C)	44
0.35	2695.7	1685.8	760.5	693.6	0.91	601	425.5	Support (C)	13
0.35	2695.7	2019.4	846.4	750.8	0.89	590.6	485.4	Support (C)	21
0.35	2695.7	2692.6	1017	829.4	0.82	583.3	562.7	Support (C)	30
0.35	2695.7	3570.6	1235.6	918.6	0.74	583.3	659.7	Support (C)	37
0.4	3080.7	1931.6	855.8	761.6	0.89	683.5	459.9	Support (C)	10
0.4	3080.7	2312.1	952.9	808.5	0.85	673.3	506.5	Support (C)	17
0.4	3080.7	3073	1144	893.6	0.78	663.4	591.8	Support (C)	26
0.4	3080.7	4097.4	1396	99.3	0.71	663.4	681.2	Support (C)	33

Note:
Support (S) – Support failure by steel fracture.
Support (C) – Support failure by concrete crushing.

Table TA2 $f'c = 25$ MPa, $l/d = 15$, $\varepsilon_{su} = 0.015$

K_{u-}	A_{st-}	A_{st+}	Q_{PL} (kN)	Q_{FL} (kN)	Q_{FL}/Q_{PL}	$M_{(u.fail)}^{-}$ (kNm)	$M_{(u.fail)}^{+}$ (kNm)	Failure Region (C/S)	β (%)
0.244	1879.3	1170.7	575.8	508.2	0.88	460.7	303.9	Support (S)	9
0.244	1879.3	1404.8	638.3	551.2	0.86	460.7	344.6	Support (S)	16
0.244	1879.3	1873.1	761.7	613.6	0.81	460.7	404.1	Support (S)	25
0.244	1879.3	2487.7	921.4	685.5	0.74	460.7	474.4	Support (S)	33
0.3	2310 6	1434.1	685	612	0.89	537.5	373.6	Support (S)	12
0.3	2310 6	1726.8	761.6	680.8	0.89	537.5	438.7	Support (S)	21
0.3	2310 6	2326.7	915.9	750.6	0.82	537.5	506.3	Support (S)	28
0.3	2310.6	3073	1102.7	838.6	0.76	537.5	592.2	Support (S)	36
0.35	2695.7	1685.8	780.2	696	0.89	607	426.8	Support (C)	13
0.35	2695.7	2019.4	866.7	736	0.85	585.1	473.1	Support (C)	21
0.35	2695.7	2692.6	1035.8	814.6	0.79	585.1	549.9	Support (C)	28
0.35	2695.7	3570.6	1254.7	916	0.73	588.5	647.4	Support (C)	36
0.4	3080.7	1931.6	875.8	763.7	0.87	679.6	461.6	Support (C)	11
0.4	3080.7	2312.1	973	810	0.83	672.4	508.4	Support (C)	17
0.4	3080.7	3073	1163.8	892.6	0.77	656.4	598.5	Support (C)	26
0.4	3080.7	4097.4	1415.5	974.6	0.69	656.4	682.7	Support (C)	33

Note:
Support (S) – Support failure by steel fracture.
Support (C) – Support failure by concrete crushing.

Table TB1 $f'c$ **= 40 MPa,** l/d **= 15,** ε_{su} **= 0.05**

K_{u-}	A_{st-}	A_{st+}	Q_{PL} (kN)	Q_{FL} (kN)	Q_{FL}/Q_{PL}	$M_{(u,fail)}^{-}$ (kNm)	$M_{(u,fail)}^{+}$ (kNm)	Failure Region (C/S)	β (%)
0.168	1875.4	1187.8	577.3	516.7	0.90	450.2	316	Support (C)	13
0.168	1875.4	1399.9	635.1	572.8	0.90	449.2	366	Support (C)	22
0.168	1875.4	1866.5	760.8	679.2	0.89	444.5	469.3	Support (C)	35
0.168	1875.4	2502.8	929.2	770.3	0.83	425.1	572.2	Support (C)	45
0.2	2232.6	1399.9	668.6	606.7	0.91	435.7	368.4	Support (C)	12
0.2	2232.6	1675.6	743	666.1	0.90	524.5	429	Support (C)	21
0.2	2232.6	2248.3	895.8	767	0.86	525 4	531.1	Support (C)	31
0.2	2232.6	2969.4	1048	868.4	0.83	519 8	628	Support (C)	40
0.244	2723.8	1696.8	793.7	721.5	0.91	642 7	429.6	Support (C)	11
0.244	2723.8	2036.2	884 5	783.2	0.89	631.5	502.4	Support (C)	19
0.244	2723.8	2714.9	1063	867.9	0.82	636.5	575.9	Support (C)	27
0.244	2723.8	3605.7	1293	960.85	0.74	620.9	670.7	Support (C)	35
0.3	3348 9	2078 6	951	850.9	0.89	774.2	507.8	Support (C)	9
0.3	3348 9	2502 8	1063	897.3	0.84	754.7	559.3	Support (C)	16
0.3	3348 9	3372 4	1288	1011	0.78	780.7	657 5	Support (C)	23
0.3	3348.9	4454.1	1563.9	1104	0.71	780.7	745	Support (C)	29
0.4	4465.3	2799.7	1235	1070.9	0.87	1001.8	628 6	Support (C)	6
0.4	4465.3	3351.2	1377.8	1135	0.82	1015.6	685.4	Support (C)	11
0.4	4465.3	4454.1	1658	1222	0.74	1012.7	767.7	Support (C)	17
0.4	4465.3	5938.8	2029	1342	0.66	1002	885.2	Support (C)	25

Note:
Support (S) – Support failure by steel fracture.
Support (C) – Support failure by concrete crushing.

Table TB2 $f'c$ **= 40 MPa,** l/d **= 15,** ε_{su} **= 0.015**

K_{u-}	A_{st-}	A_{st+}	Q_{PL} (kN)	Q_{FL} (kN)	Q_{FL}/Q_{PL}	$M_{(u,fail)}^{-}$ (kNm)	$M_{(u,fail)}^{+}$ (kNm)	Failure Region (C/S)	β (%)
0.168	1875.4	1187.8	597	518.8	0.87	479.2	306.9	Support (S)	8
0.168	1875.4	1399.9	655	558.1	0.85	479.2	344.1	Support (S)	14
0.168	1875.4	1866.5	780.6	617	0.79	479.2	399.9	Support (S)	22
0.168	1875.4	2502.8	949.5	694.5	0.73	479.2	475.4	Support (S)	31
0.2	2232.6	1399.9	688.5	610	0.89	555.3	364.2	Support (S)	9
0.2	2232.6	1675.6	763	660	0.87	555.3	411.6	Support (S)	16
0.2	2232.6	2248.3	915.4	735	0.80	555.3	483	Support (S)	24
0.2	2232.6	2969.4	1105	819.2	0.74	555.3	565	Support (S)	32
0.244	2723.8	1696.8	813.7	722.9	0.89	642.6	737.3	Support (C)	11
0.244	2723.8	2036.2	904	788.4	0.87	643.5	502	Support (C)	18
0.244	2723.8	2714.9	1083	874.2	0.81	649.8	578.6	Support (C)	26
0.244	2723.8	3605.7	1313.9	968.7	0.74	647.6	672.9	Support (C)	33
0.3	3348.9	2078.6	974.2	856.8	0.88	788.4	509.8	Support (C)	8
0.3	3348.9	2502.8	1083	909.3	0.84	779.8	560.9	Support (C)	14
0.3	3348.9	3372.4	1309	1014	0.77	788.4	660.2	Support (C)	22
0.3	3348.9	4454.1	1585	1108.7	0.70	788.4	751	Support (C)	29
0.4	4465.3	2799.7	1253	1078.3	0.86	1017	629.8	Support (C)	6
0.4	4465.3	3351.2	1398	1138.3	0.81	1017	686.6	Support (C)	11
0.4	4465.3	4454.1	1679.5	1226	0.73	1017	769.6	Support (C)	17
0.4	4465.3	5938.8	2050	1348	0.66	1017	885.6	Support (C)	25

Note:
Support (S) – Support failure by steel fracture.
Support (C) – Support failure by concrete crushing.

Table TC1 $f'c$ **= 60 MPa,** l/d **= 15,** ε_{su} **= 0.05**

K_{u-}	A_{st-}	A_{st+}	Q_{PL} (kN)	Q_{FL} (kN)	Q_{FL}/Q_{PL}	$M_{(u.fail)}^{-}$ (kNm)	$M_{(u.fail)}^{+}$ (kNm)	Failure Region (C/S)	β (%)
0.136	1877.2	1169.6	586.2	511.4	0.87	452.5	310.2	Support (C)	12
0.136	1877.2	1405.7	652	571.8	0.88	452.5	367.3	Support (C)	21
0.136	1877.2	1877.7	782.4	688.6	0.88	452.5	480.8	Support (C)	34
0.136	1877.2	2465.1	942.1	797	0.85	452.5	586.7	Support (C)	43
0.2	2760.5	1730.8	826.3	737	0.89	652.6	446.8	Support (C)	11
0.2	2760.5	2071.8	919.6	811.5	0.88	653.7	516.9	Support (C)	19
0.2	2760.5	2779.8	1110.7	905.2	0.81	653	605.9	Support (C)	28
0.2	2760.5	3671.5	1345.5	1017.9	0.76	653	717.5	Support (C)	36
0.244	3367.8	2098.0	983	883.2	0.90	792.5	531.4	Support (C)	10
0.244	3367.8	2517.6	1096.6	946.1	0.86	791.2	589.6	Support (C)	16
0.244	3367.8	3356.8	1319.2	1041.5	0.79	792.5	681.2	Support (C)	24
0.244	3367.8	4473.9	1609.7	1139.6	0.71	791	774.1	Support (C)	31
0.3	4140.8	2570.0	1180.3	1047	0.89	966.5	619.5	Support (C)	8
0.3	4140.8	3094.5	1319.7	1099	0.83	957.3	670.7	Support (C)	13
0.3	4140.8	4143.5	1595	1219	0.76	957.3	785.9	Support (C)	21
0.3	4140.8	5507.2	1943.5	1343	0.69	960.7	904.7	Support (C)	28
0.4	5521.0	3461.7	1535	1321	0.86	1250	770	Support (C)	5
0.4	5521.0	4143.5	1713	1393	0.81	1250.4	837.5	Support (C)	10
0.4	5521.0	5507.2	2062	1515	0.73	1260	955.5	Support (C)	17
0.4	5521.0	7343.0	2523	1643	0.65	1250.4	1074	Support (C)	24

Note:
Support (S) – Support failure by steel fracture.
Support (C) – Support failure by concrete crushing.

Table TC2 $f'c = 60$ MPa, $l/d = 15$, $\varepsilon_{su} = 0.015$

K_{u-}	A_{st-}	A_{st+}	Q_{PL} (kN)	Q_{FL} (kN)	Q_{FL}/Q_{PL}	$M_{(u.fail)}^{-}$ (kNm)	$M_{(u.fail)}^{+}$ (kNm)	Failure Region (C/S)	β (%)
0.136	1877.2	1169.6	608.5	523	0.86	491.4	306	Support (S)	6
0.136	1877.2	1405.7	675	569.7	0.84	491.4	350.2	Support (S)	14
0.136	1877.2	1877.7	805.8	620.9	0.77	491.4	398.7	Support (S)	21
0.136	1877.2	2465.1	965.3	665	0.69	491.4	441.3	Support (S)	26
0.2	2760.5	1730.8	849.5	747.2	0.88	679.4	448	Support (S)	9
0.2	2760.5	2071.8	943.1	812.5	0.86	679.4	507.9	Support (S)	16
0.2	2760.5	2779.8	1134.2	900	0.79	679.4	594	Support (S)	25
0.2	2760.5	3671.5	1370	1004.3	0.73	679.4	695.9	Support (S)	32
0.244	3367.8	2098.0	1006.4	883.6	0.88	791.8	533	Support (C)	10
0.244	3367.8	2517.6	1119.9	945.2	0.84	791.8	591.3	Support (C)	16
0.244	3367.8	3356.8	1343.5	1050	0.78	802.1	685	Support (C)	24
0.244	3367.8	4473.9	1635	1141.3	0.70	791.8	780.3	Support (C)	31
0.3	4140.8	2570.0	1203.6	1056.7	0.88	980.5	623.3	Support (C)	7
0.3	4140.8	3094.5	1343.7	1102.5	0.82	980.5	669.5	Support (C)	11
0.3	4140.8	4143.5	1625.8	1225	0.75	980.5	785.5	Support (C)	20
0.3	4140.8	5507.2	1969.5	1346.1	0.68	980.5	902.5	Support (C)	27
0.4	5521.0	3461.7	1559.6	1328.8	0.85	1267.3	772.2	Support (C)	5
0.4	5521.0	4143.5	1737.9	1400	0.81	1267.3	839.5	Support (C)	9
0.4	5521.0	5507.2	2088	1525.5	0.73	1267.3	959	Support (C)	17
0.4	5521.0	7343.0	2550	1649.8	0.65	1267.3	1076.4	Support (C)	23

Note:
Support (S) – Support failure by steel fracture.
Support (C) – Support failure by concrete crushing.

Appendix C

Results of Parametric Study

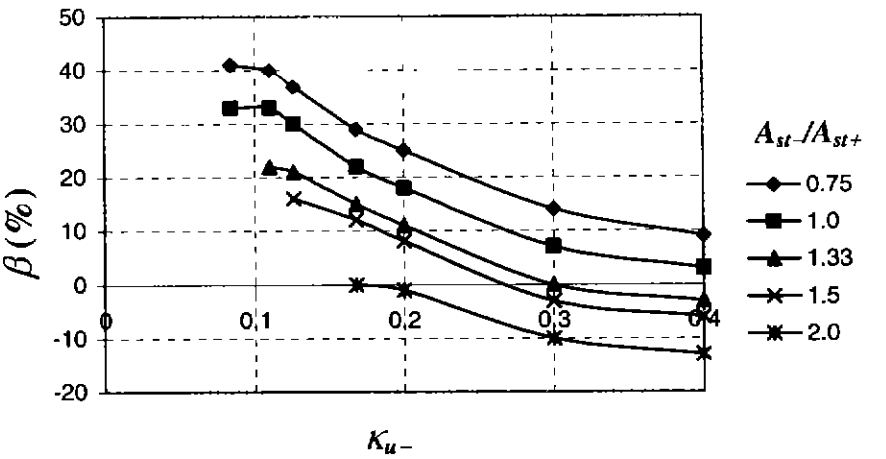

Fig. C1 One-Way Slab: Effect of A_{st-}/A_{st+} on Degree of Moment Redistribution for Steel *N* ($l/d = 35, f'_c = 30$ MPa)

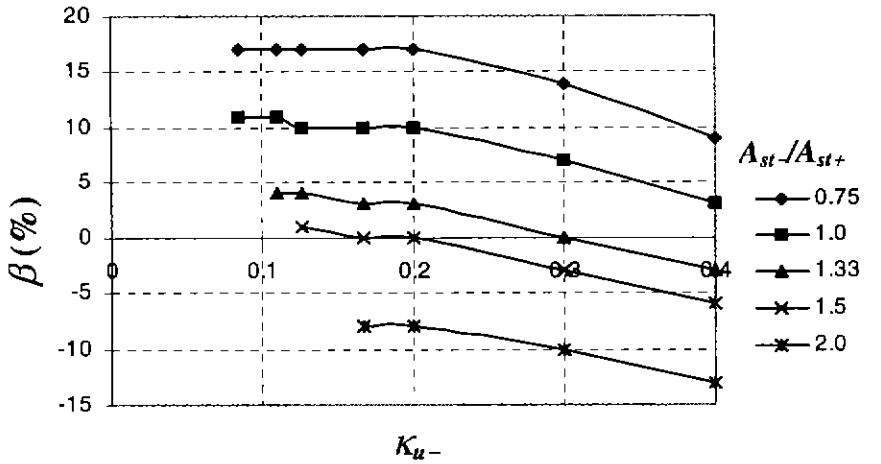

Fig. C2 One-Way Slab: Effect of A_{st-}/A_{st+} on Degree of Moment Redistribution for Steel *L* ($l/d = 35, f'_c = 30$ MPa)

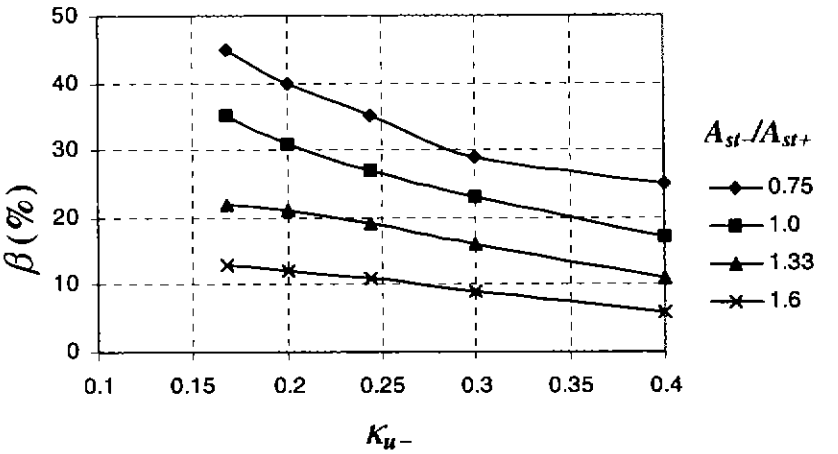

Fig. C3 T-BeamEffect of A_{st-}/A_{st+} on Degree of Moment Redistribution for Steel *N* ($l/d = 15, f'_c = 40\ MPa$)

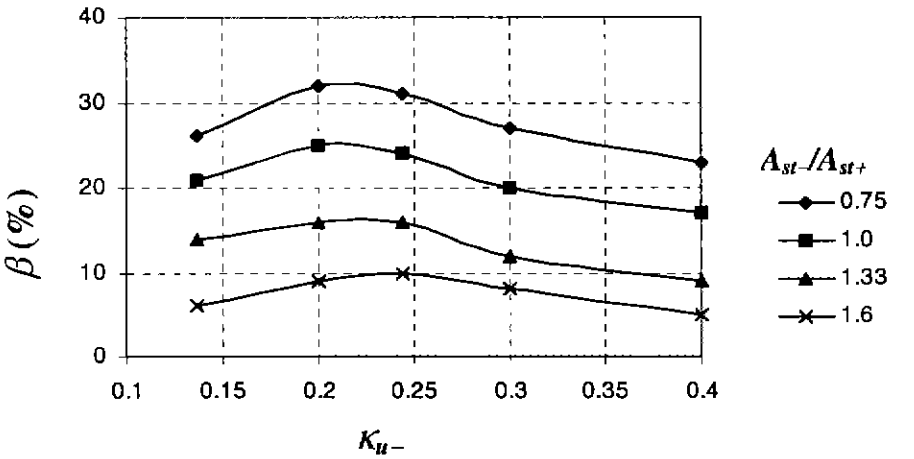

Fig. C4 T-Beam: Effect of A_{st-}/A_{st+} on Degree of Moment Redistribution for Steel *L* ($l/d = 15, f'_c = 40\ MPa$)

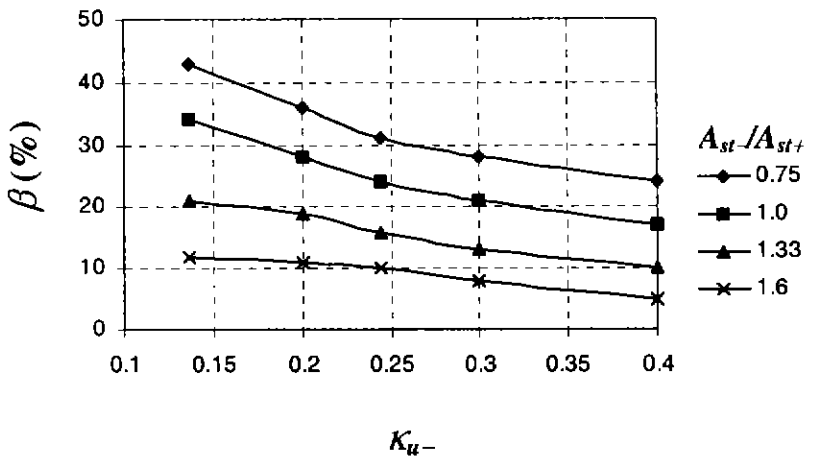

Fig. C5 T-Beam: Effect of A_{st-}/A_{st+} on Degree of Moment Redistribution for Steel *N* ($l/d = 15, f_c' = 60\ MPa$)

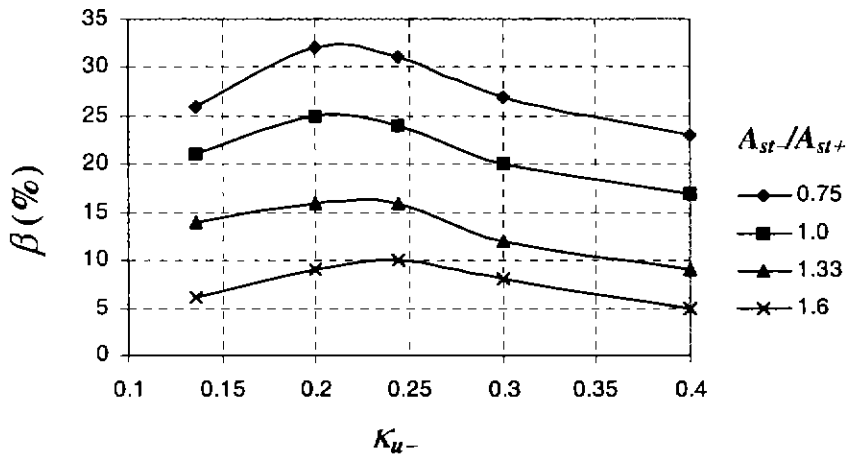

Fig. C6 T-Beam: Effect of A_{st-}/A_{st+} on Degree of Moment Redistribution for Steel *L* ($l/d = 35, f_c' = 60\ MPa$)

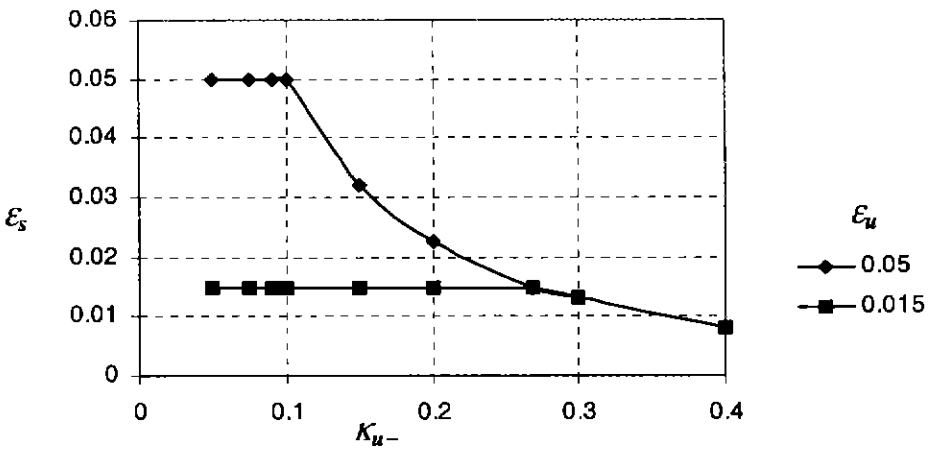

Fig. C7 Variation of Steel Strain at Failure with Neutral Axis Parameter at Support Section (f'_c = *30 MPa*)

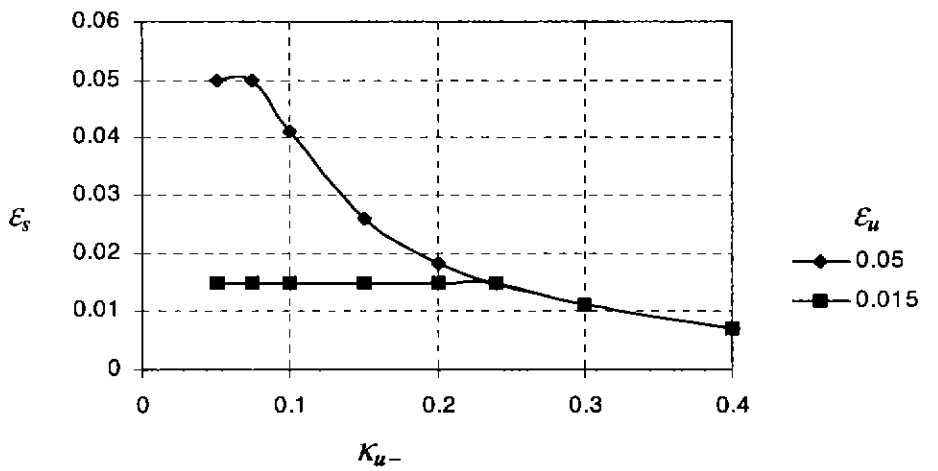

Fig. C8 Variation of Steel Strain at Failure with Neutral Axis Parameter at Support Section (f'_c = *40 MPa*)

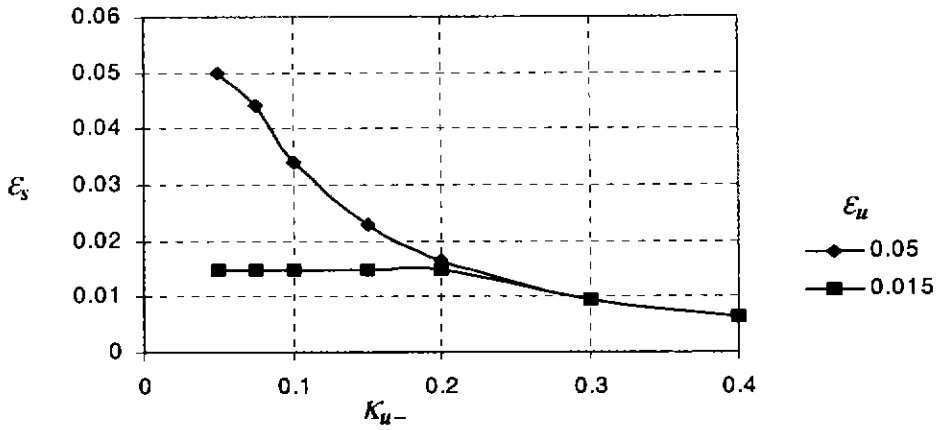

Fig. C9 Variation of Steel Strain at Failure with Neutral Axis Parameter at Support Section (f'_c = 60 MPa)

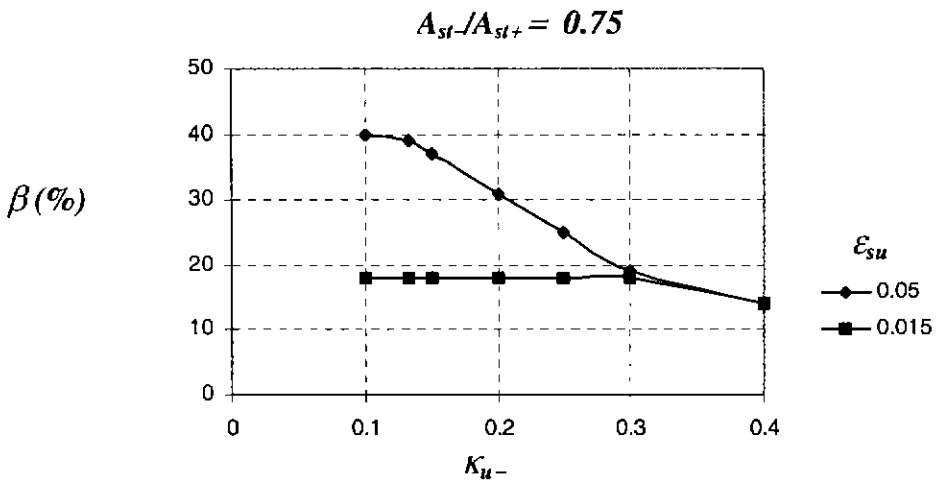

Fig. C10 One-way slab: Variation of Moment Redistribution with Ultimate Steel Strain (l/d = 35 and f'_c = 25 MPa)

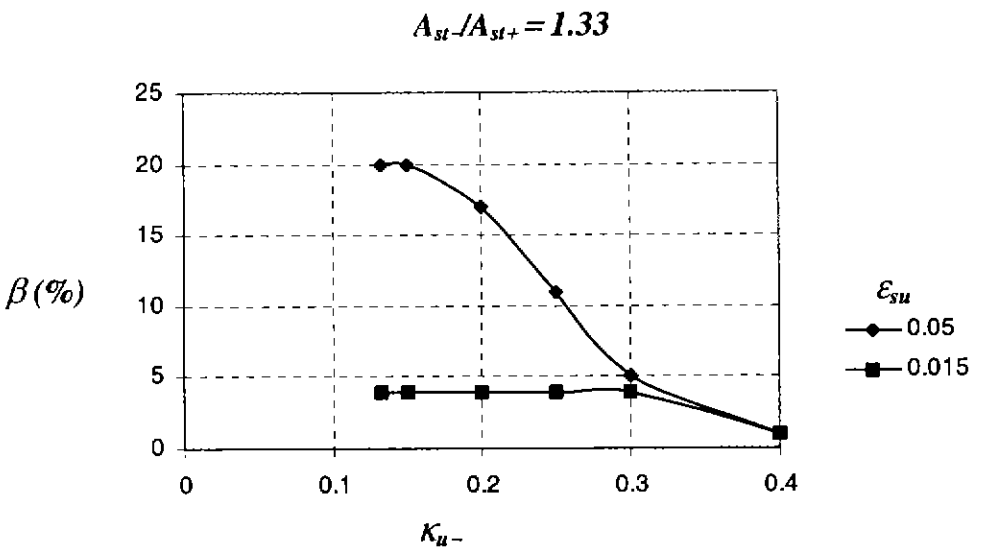

Fig. C11 One-way slab: Variation of Moment Redistribution with Ultimate Steel Strain (l/d = 35 and f_c' = 25 MPa)

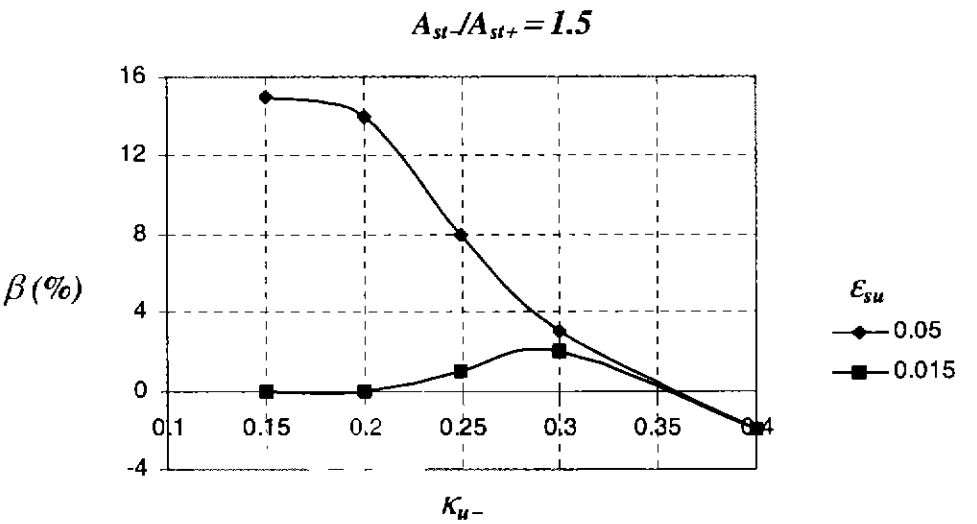

Fig. C12 One-way slab: Variation of Moment Redistribution with Ultimate Steel Strain (l/d = 35 and f_c' = 25 MPa)

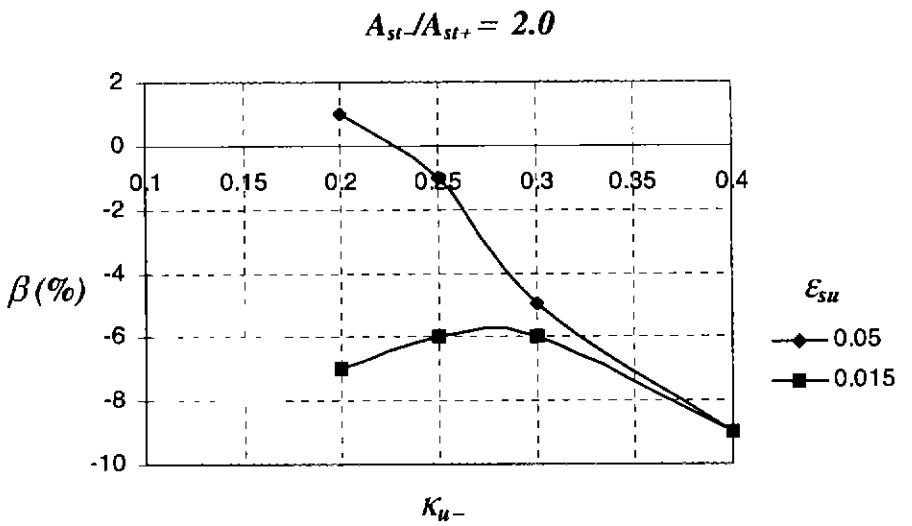

Fig. C13 One-way slab: Variation of Moment Redistribution with Ultimate Steel Strain (l/d = 35 and f_c' = 25 MPa)

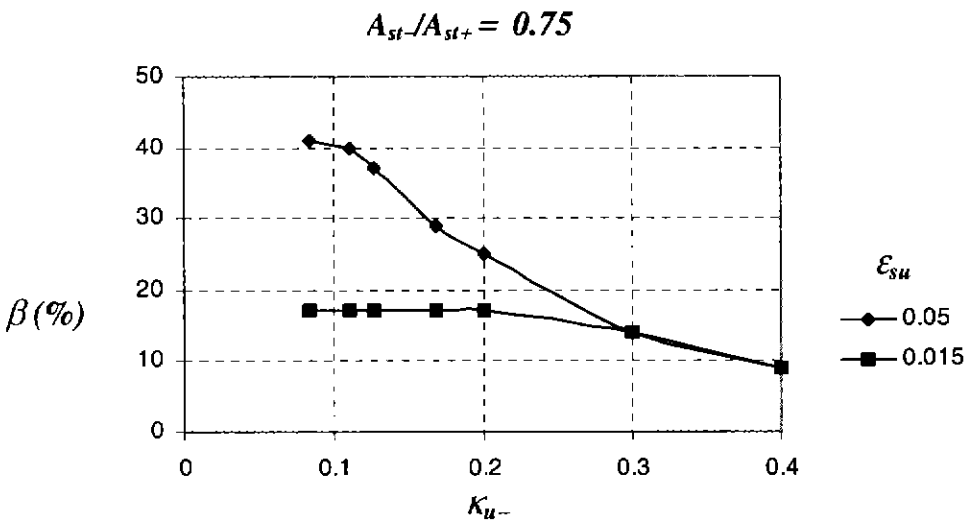

Fig. C14 One-way slab: Variation of Moment Redistribution with Ultimate Steel Strain (l/d = 35 and f_c' = 30 MPa)

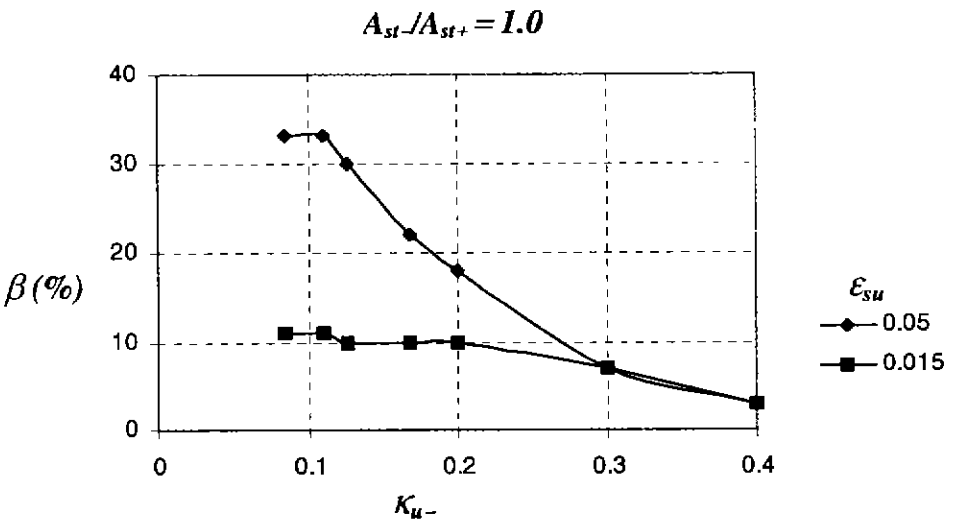

Fig. C15 One-way slab: Variation of Moment Redistribution with Ultimate Steel Strain (l/d = 35 and f_c' = 30 MPa)

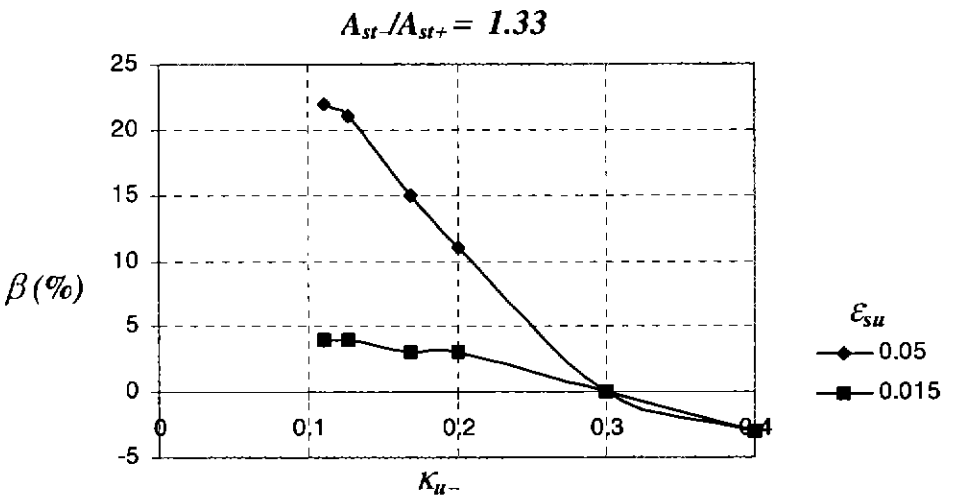

Fig. C16 One-way slab: Variation of Moment Redistribution with Ultimate Steel Strain (l/d = 35 and f_c' = 30 MPa)

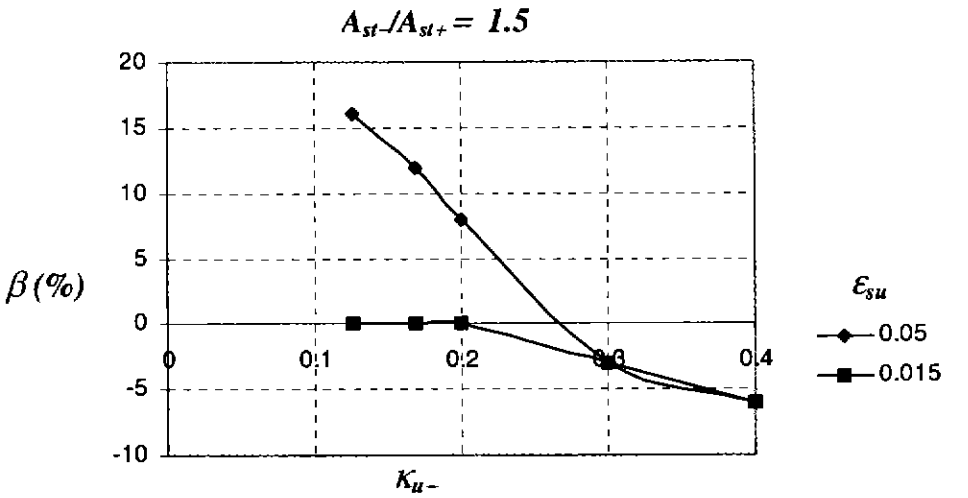

Fig. C17 One-way slab: Variation of Moment Redistribution with Ultimate Steel Strain (l/d = 35 and f_c' = 30 MPa)

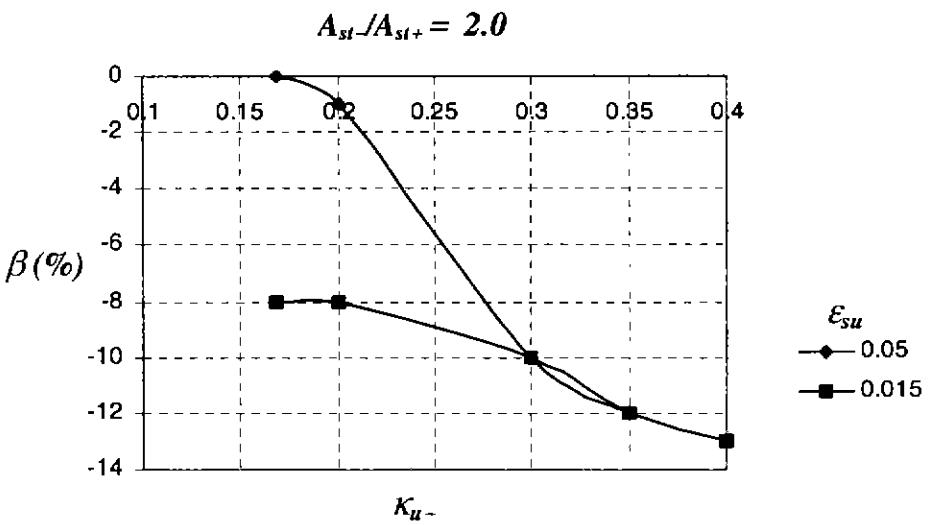

Fig. C18 One-way slab: Variation of Moment Redistribution with Ultimate Steel Strain (l/d = 35 and f_c' = 30 MPa)

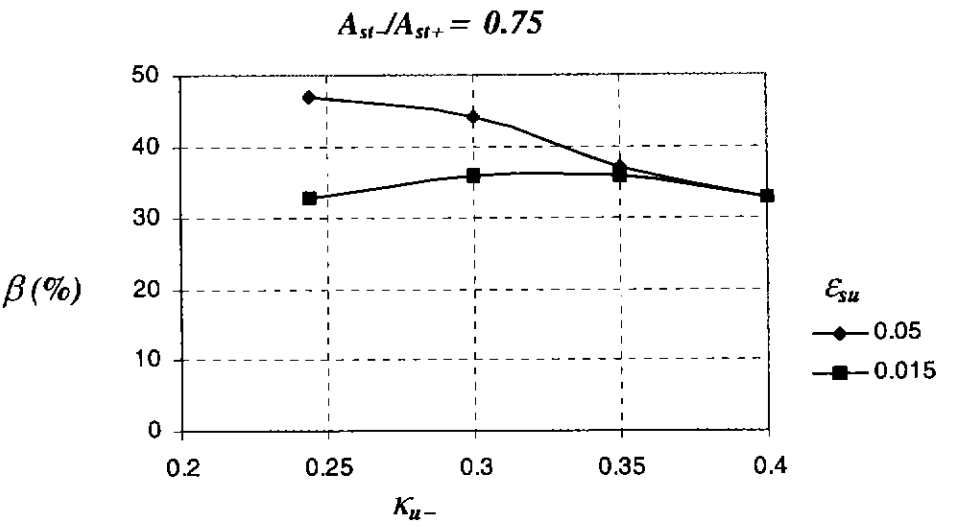

Fig. C19 T-beam: Variation of Moment Redistribution with Ultimate Steel Strain (l/d = 15 and f_c' = 25 MPa)

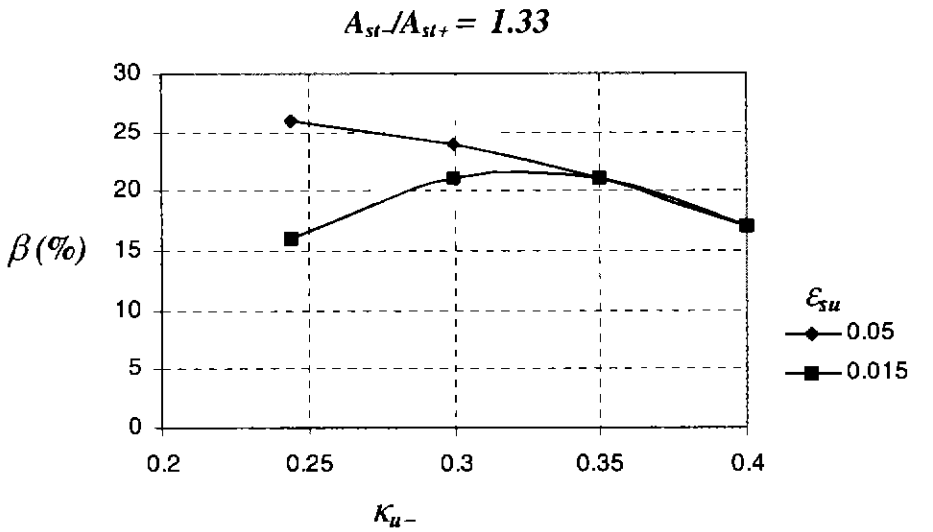

Fig. C20 T-beam: Variation of Moment Redistribution with Ultimate Steel Strain (l/d = 15 and f_c' = 25 MPa)

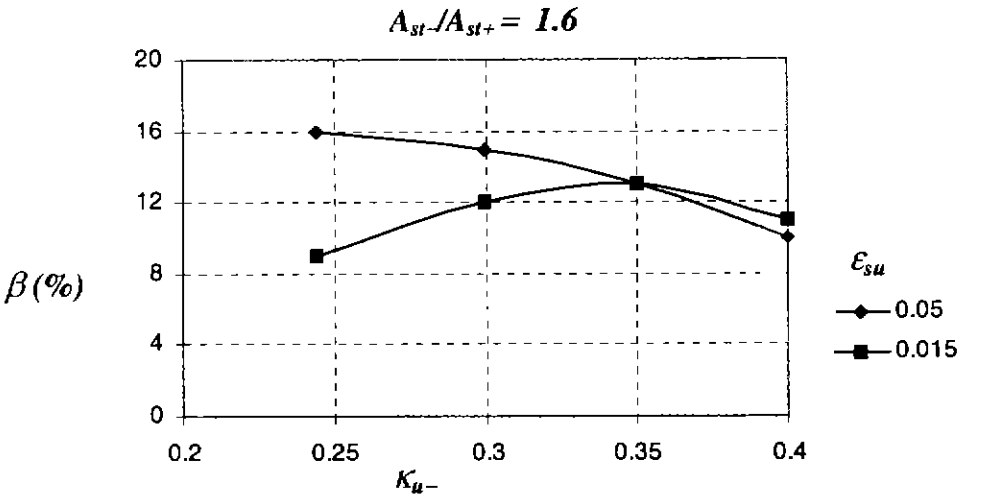

Fig. C21 T-beam: Variation of Moment Redistribution with Ultimate Steel Strain (l/d = 15 and f_c' = 25 MPa)

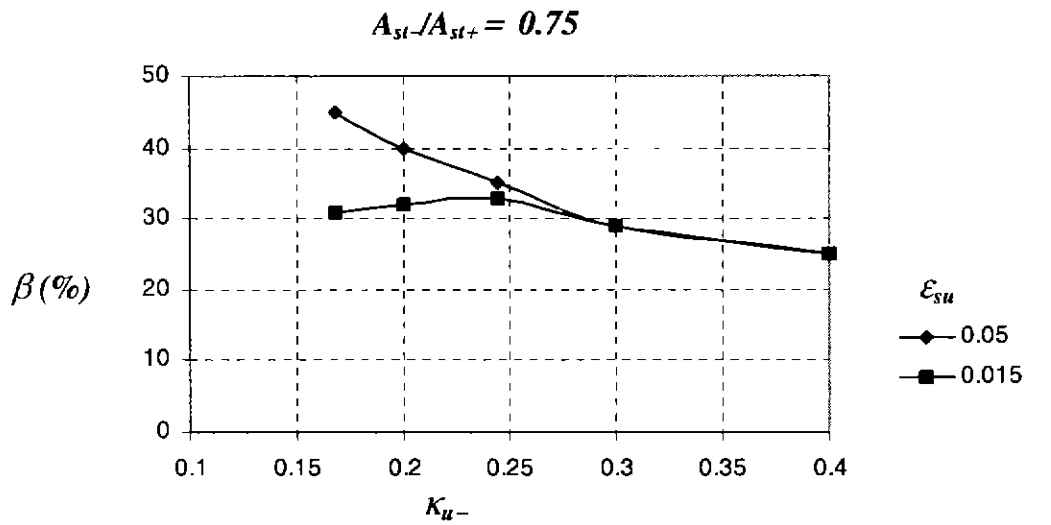

Fig. C22 T-beam: Variation of Moment Redistribution with Ultimate Steel Strain (l/d = 15 and f_c' = 40 MPa)

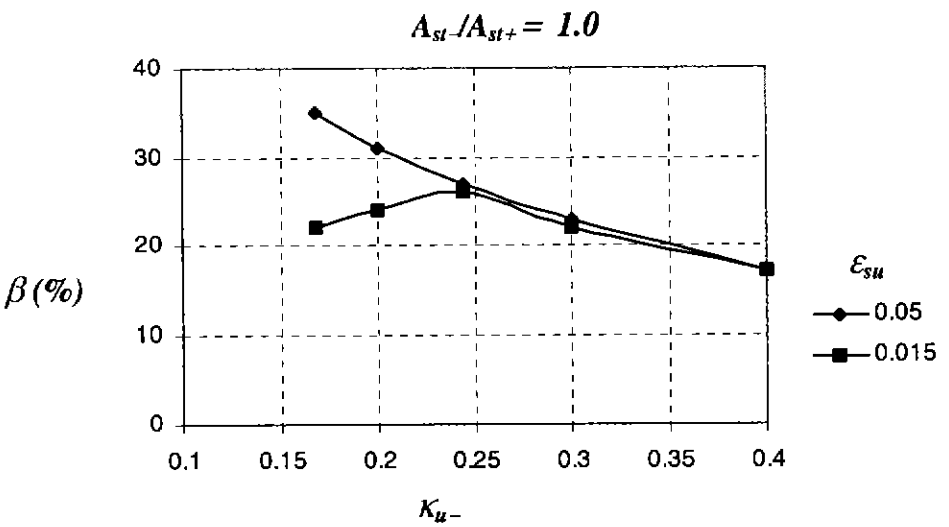

Fig. C23 T-beam: Variation of Moment Redistribution with Ultimate Steel Strain (l/d = 15 and f_c' = 40 MPa)

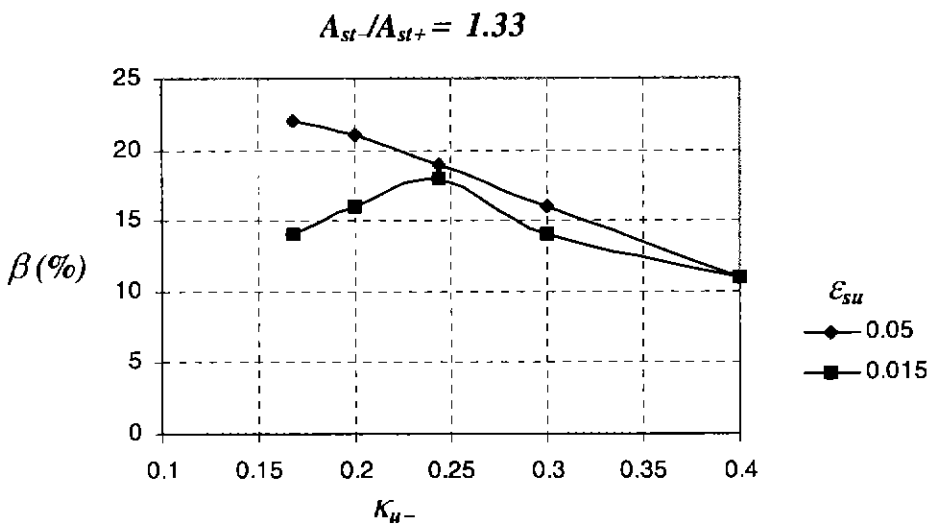

Fig. C24 T-beam: Variation of Moment Redistribution with Ultimate Steel Strain (l/d = 15 and f_c' = 40 MPa)

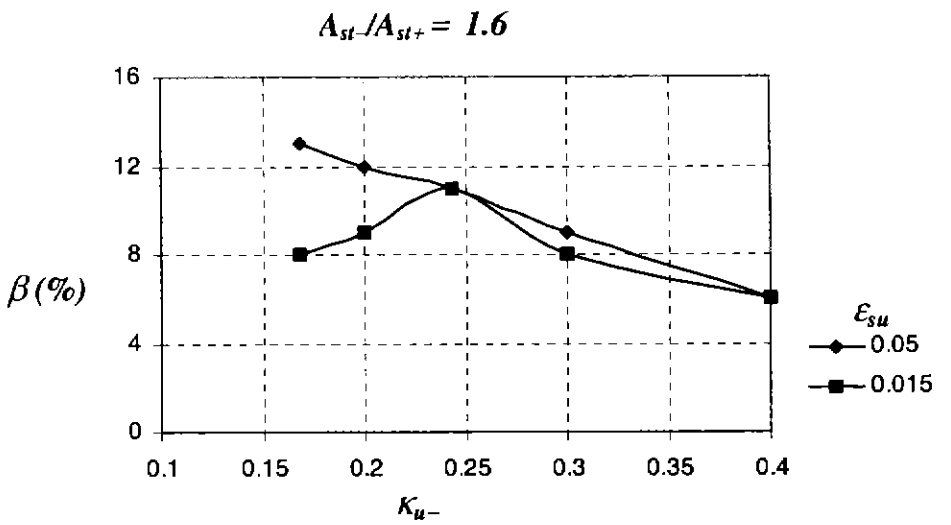

Fig. C25 T-beam: Variation of Moment Redistribution with Ultimate Steel Strain (l/d = 15 and f_c' = 40 MPa)

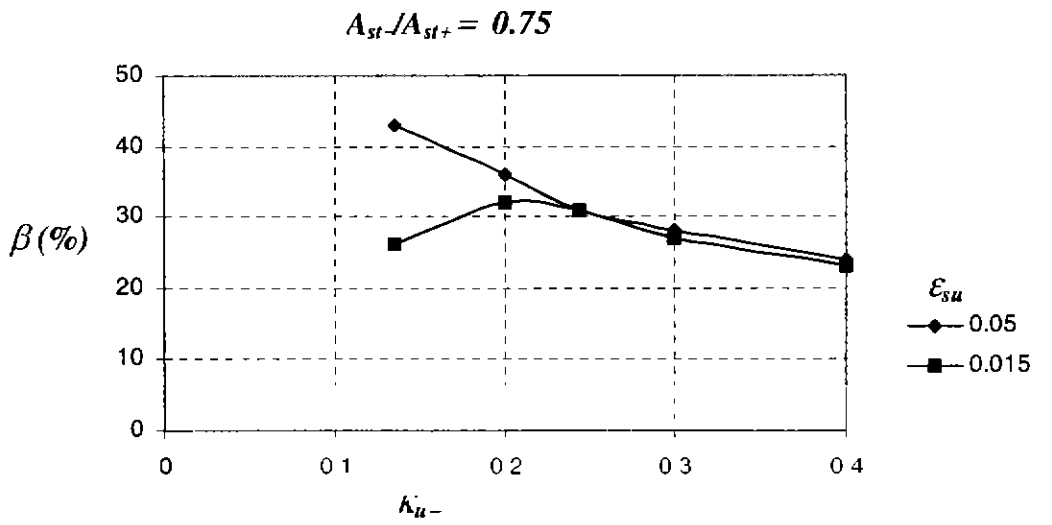

Fig. C26 T-beam: Variation of Moment Redistribution with Ultimate Steel Strain (l/d = 15 and f_c' = 60 MPa)

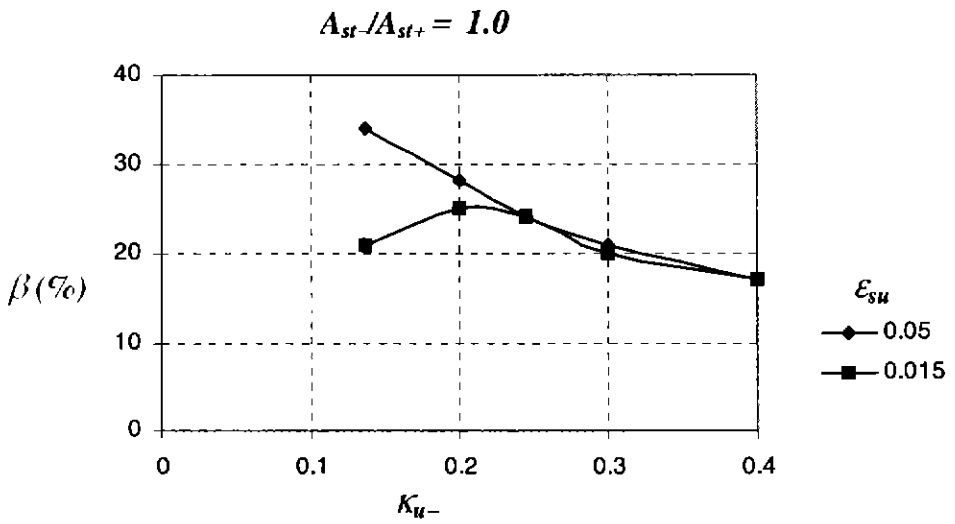

Fig. C27 T-beam: Variation of Moment Redistribution with Ultimate Steel Strain (l/d = 15 and f_c' = 60 MPa)

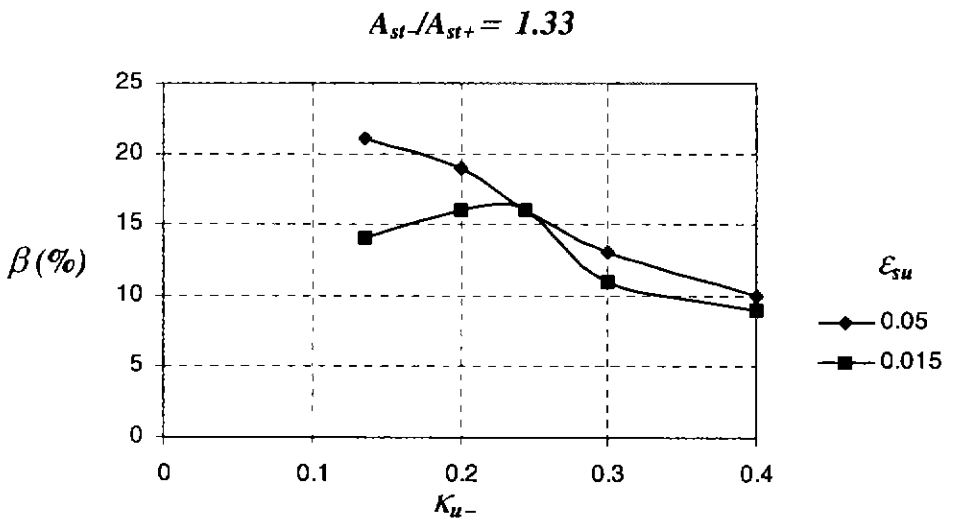

Fig. C28 T-beam: Variation of Moment Redistribution with Ultimate Steel Strain (l/d = 15 and f_c' = 60 MPa)

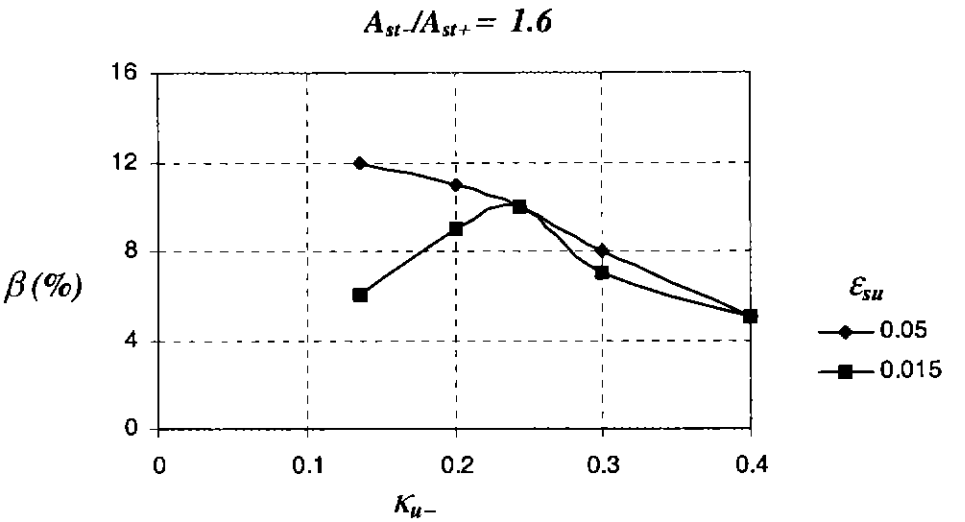

Fig. C29 T-beam: Variation of Moment Redistribution with Ultimate Steel Strain (l/d = 15 and f_c' = 60 MPa)

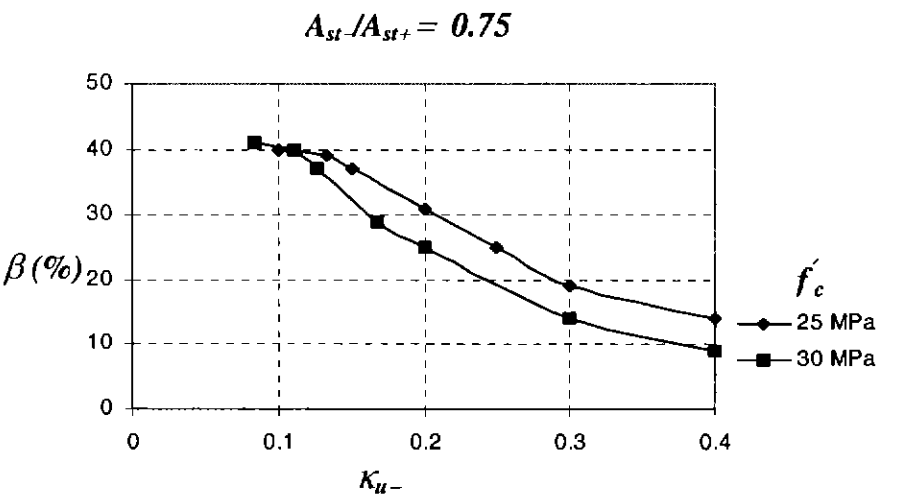

Fig. C30 One-way slab: Variation of Moment Redistribution with Concrete Compressive Strength (l/d = 35 and ε_{su} = 0.05)

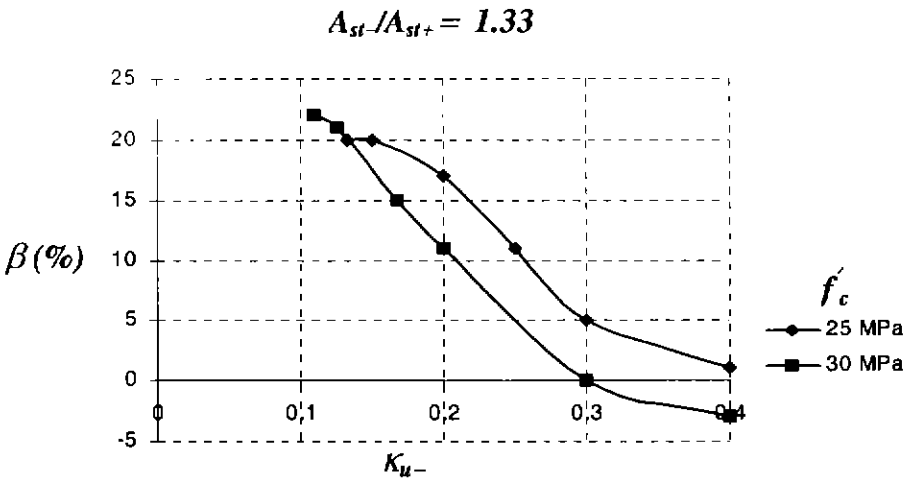

Fig. C31 One-way slab: Variation of Moment Redistribution with Concrete Compressive Strength (l/d = 35 and ε_{su} = 0.05)

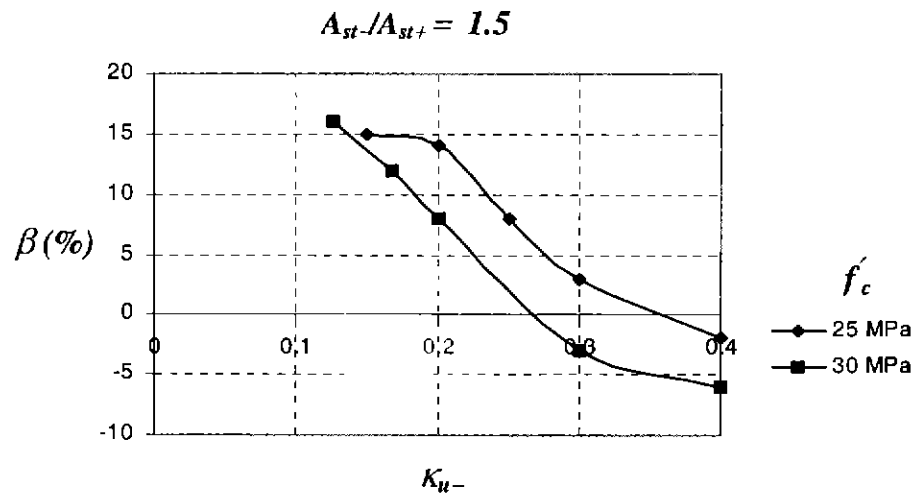

Fig. C32 One-way slab: Variation of Moment Redistribution with Concrete Compressive Strength (l/d = 35 and ε_{su} = 0.05)

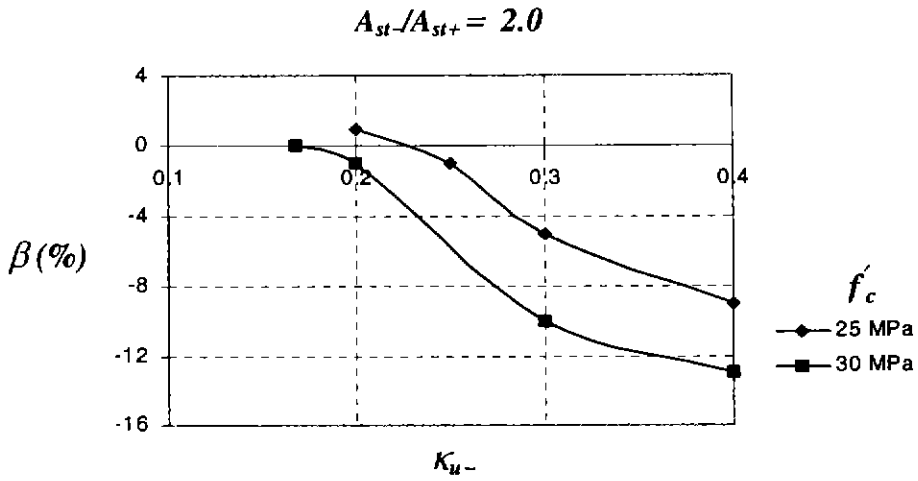

Fig. C33 One-way slab: Variation of Moment Redistribution with Concrete Compressive Strength (l/d = 35 and ε_{su} = 0.05)

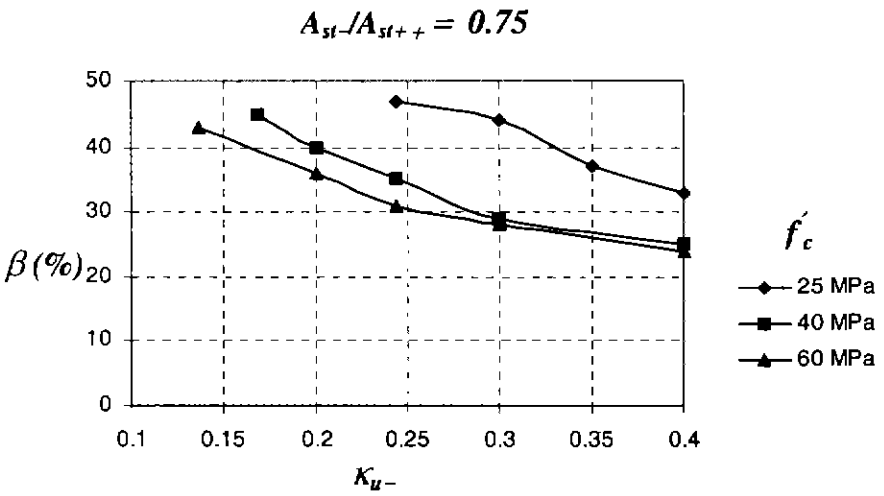

Fig. C34 T-beam: Variation of Moment Redistribution with Concrete Compressive Strength (l/d = 15 and ε_{su} = 0.05)

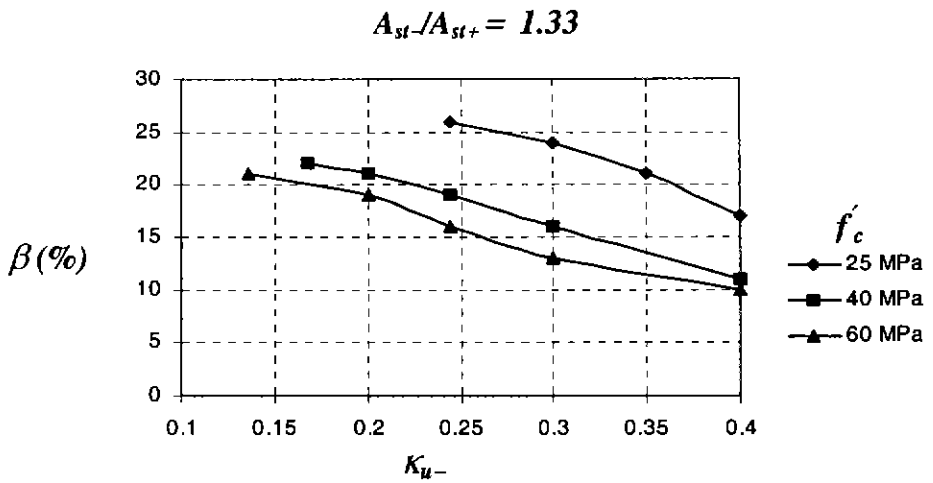

Fig. C35 T-beam: Variation of Moment Redistribution with Concrete Compressive Strength (l/d = 15 and ε_{su} = 0.05)

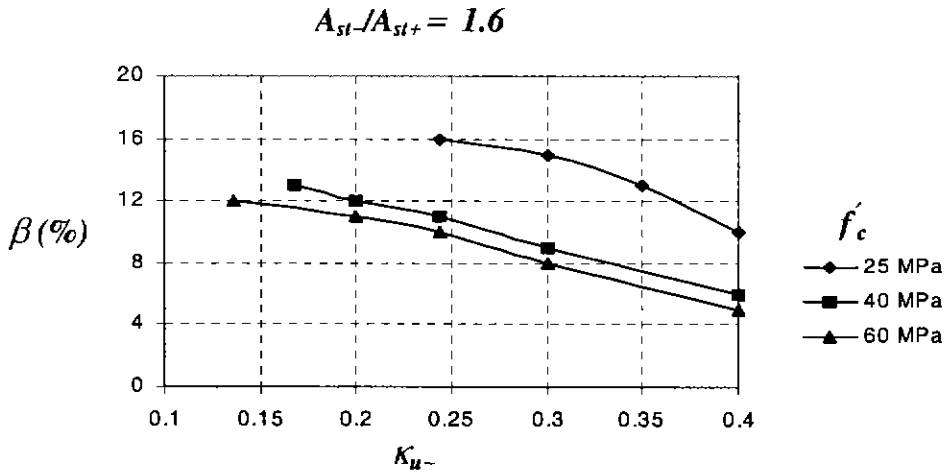

Fig. C36 T-beam: Variation of Moment Redistribution with Concrete Compressive Strength (l/d = 15 and ε_{su} = 0.05)